











TECH BRIEFS

NATIONAL AERONAUTICS AND SPACE ADMINISTRATION

-  **Technology Focus**
-  **Electronics/Computers**
-  **Software**
-  **Materials**
-  **Mechanics/Machinery**
-  **Manufacturing**
-  **Bio-Medical**
-  **Physical Sciences**
-  **Information Sciences**
-  **Books and Reports**

INTRODUCTION

Tech Briefs are short announcements of innovations originating from research and development activities of the National Aeronautics and Space Administration. They emphasize information considered likely to be transferable across industrial, regional, or disciplinary lines and are issued to encourage commercial application.

Availability of NASA Tech Briefs and TSPs

Requests for individual Tech Briefs or for Technical Support Packages (TSPs) announced herein should be addressed to

National Technology Transfer Center

Telephone No. (800) 678-6882 or via World Wide Web at www2.nttc.edu/leads/

Please reference the control numbers appearing at the end of each Tech Brief. Information on NASA's Innovative Partnerships Program (IPP), its documents, and services is also available at the same facility or on the World Wide Web at <http://ipp.nasa.gov>.

Innovative Partnerships Offices are located at NASA field centers to provide technology-transfer access to industrial users. Inquiries can be made by contacting NASA field centers listed below.

NASA Field Centers and Program Offices

Ames Research Center

Lisa L. Lockyer
(650) 604-1754
lisa.l.lockyer@nasa.gov

Dryden Flight Research Center

Gregory Poteat
(661) 276-3872
greg.poteat@dfrc.nasa.gov

Glenn Research Center

Kathy Needham
(216) 433-2802
kathleen.k.needham@nasa.gov

Goddard Space Flight Center

Nona Cheeks
(301) 286-5810
nona.k.cheeks@nasa.gov

Jet Propulsion Laboratory

Andrew Gray
(818) 354-3821
gray@jpl.nasa.gov

Johnson Space Center

information
(281) 483-3809
jsc.techtran@mail.nasa.gov

Kennedy Space Center

David R. Makufka
(321) 867-6227
david.r.makufka@nasa.gov

Langley Research Center

Brian Beaton
(757) 864-2192
brian.f.beaton@nasa.gov

Marshall Space Flight Center

Jim Dowdy
(256) 544-7604
jim.dowdy@msfc.nasa.gov

Stennis Space Center

Ramona Travis
(228) 688-3832
ramona.e.travis@nasa.gov

Carl Ray, Program Executive

Small Business Innovation
Research (SBIR) & Small
Business Technology
Transfer (STTR) Programs
(202) 358-4652
carl.g.ray@nasa.gov

Doug Comstock, Director

Innovative Partnerships
Program Office
(202) 358-2560
doug.comstock@nasa.gov



TECH BRIEFS

NATIONAL AERONAUTICS AND SPACE ADMINISTRATION



5 Technology Focus: Nano Materials & Manufacturing

- 5 Filtering Water by Use of Ultrasonically Vibrated Nanotubes
- 6 Computer Code for Nanostructure Simulation
- 6 Functionalizing CNTs for Making Epoxy/CNT Composites
- 6 Improvements in Production of Single-Walled Carbon Nanotubes
- 7 Progress Toward Sequestering Carbon Nanotubes in PmPV



9 Electronics/Computers

- 9 Two-Stage Variable Sample-Rate Conversion System
- 9 Estimating Transmitted-Signal Phase Variations for Uplink Array Antennas
- 10 Board Saver for Use With Developmental FPGAs
- 11 Circuit for Driving Piezoelectric Transducers
- 12 Digital Synchronizer Without Metastability
- 13 Compact, Low-Overhead, MIL-STD-1553B Controller
- 13 Parallel-Processing CMOS Circuitry for M-QAM and 8PSK TCM
- 13 Differential InP HEMT MMIC Amplifiers Embedded in Waveguides



15 Materials

- 15 Improved Aerogel Vacuum Thermal Insulation
- 15 Fluoroester Co-Solvents for Low-Temperature Li⁺ Cells
- 16 Using Volcanic Ash To Remove Dissolved Uranium and Lead



17 Manufacturing & Prototyping

- 17 High-Efficiency Artificial Photosynthesis Using a Novel Alkaline Membrane Cell
- 18 Silicon Wafer-Scale Substrate for Microshutters and Detector Arrays



19 Mechanics/Machinery

- 19 Micro-Horn Arrays for Ultrasonic Impedance Matching

- 20 Improved Controller for a Three-Axis Piezoelectric Stage



21 Bio-Medical

- 21 Nano-Pervaporation Membrane With Heat Exchanger Generates Medical-Grade Water
- 21 Micro-Organ Devices



23 Physical Sciences

- 23 Nonlinear Thermal Compensators for WGM Resonators
- 24 Dynamic Self-Locking of an OEO Containing a VCSEL
- 25 Internal Water Vapor Photoacoustic Calibration
- 25 Mid-Infrared Reflectance Imaging of Thermal-Barrier Coatings
- 26 Improving the Visible and Infrared Contrast Ratio of Microshutter Arrays
- 27 Improved Scanners for Microscopic Hyperspectral Imaging



29 Information Sciences

- 29 Rate-Compatible LDPC Codes With Linear Minimum Distance
- 30 PrimeSupplier Cross-Program Impact Analysis and Supplier Stability Indicator Simulation Model
- 30 Integrated Planning for Telepresence With Time Delays
- 31 Minimizing Input-to-Output Latency in Virtual Environment



33 Books & Reports

- 33 Battery Cell Voltage Sensing and Balancing Using Addressable Transformers
- 33 Gaussian and Lognormal Models of Hurricane Gust Factors



35 Software

- 35 Simulation of Attitude and Trajectory Dynamics and Control of Multiple Spacecraft
- 35 Integrated Modeling of Spacecraft Touch-And-Go Sampling
- 35 Spacecraft Station-Keeping Trajectory and Mission Design Tools

36	Efficient Model-Based Diagnosis Engine	53	Robot Vision Library
37	DSN Simulator	53	Mission Operations and Navigation Toolkit Environment
38	Proton Upset Monte Carlo Simulation	54	Extensible Infrastructure for Browsing and Searching Abstracted Spacecraft Data
38	FPGA Boot Loader and Scrubber	54	Lossless Compression of Data Into Fixed-Length Packets
38	Using Thermal Radiation in Detection of Negative Obstacles	54	Video-Game-Like Engine for Depicting Spacecraft Trajectories
39	Planning Flight Paths of Autonomous Aerobots	55	Alert Notification System Router
40	Cliffbot Maestro	55	Lossless Compression of Classification-Map Data
40	Tracking Debris Shed by a Space-Shuttle Launch Vehicle	56	Framework for ReSTful Web Services in OSGi
41	Estimating Thruster Impulses From IMU and Doppler Data	56	MAGIC: Model and Graphic Information Converter
41	Oxygen Generation System Laptop Bus Controller Flight Software	57	Data Management Applications for the Service Preparation Subsystem
41	Port-O-Sim Object Simulation Application	57	Policy-Based Management Natural Language Parser
42	Monitoring and Controlling an Underwater Robotic Arm		
42	Digital Camera Control for Faster Inspection		
42	Reaction Wheel Disturbance Model Extraction Software — RWDMEs		
43	Conical-Domain Model for Estimating GPS Ionospheric Delays		
44	Evolvable Neural Software System		
44	Prediction of Launch Vehicle Ignition Overpressure and Liftoff Acoustics		
45	Interactive, Automated Management of Icing Data		
45	LDPC-PPM Coding Scheme for Optical Communication		
46	Complex Event Recognition Architecture		
47	TurboTech Technical Evaluation Automated System		
47	Robot Vision Library		
47	Perl Modules for Constructing Iterators		
48	Tropical Cyclone Information System		
48	XML Translator for Interface Descriptions		
49	Group Capability Model		
49	Dynamic Hurricane Data Analysis Tool		
49	XVD Image Display Program		
50	Geospatial Authentication		
50	Mars Science Laboratory Workstation Test Set		
50	Computing Bounds on Resource Levels for Flexible Plans		
51	MSLICE Science Activity Planner for the Mars Science Laboratory Mission		
52	Telemetry-Enhancing Scripts		
52	Analog Input Data Acquisition Software		
52	Relay Sequence Generation Software		
53	GlastCam: A Telemetry-Driven Spacecraft Visualization Tool		

This document was prepared under the sponsorship of the National Aeronautics and Space Administration. Neither the United States Government nor any person acting on behalf of the United States Government assumes any liability resulting from the use of the information contained in this document, or warrants that such use will be free from privately owned rights.



Technology Focus: Nano Materials & Manufacturing

Filtering Water by Use of Ultrasonically Vibrated Nanotubes

Water molecules could flow through; larger molecules and other particles could not.

Lyndon B. Johnson Space Center, Houston, Texas

Devices that could be characterized as acoustically driven molecular sieves have been proposed for filtering water to remove all biological contaminants and all molecules larger than water molecules. Originally intended for purifying wastewater for reuse aboard spacecraft, these devices could also be attractive for use on Earth in numerous settings in which there are requirements to obtain potable, medical-grade, or otherwise pure water from contaminated water supplies. These devices could also serve as efficient means of removing some or all water from chemical products — for example, they might be useful as adjuncts or substitutes for stills in the removal of water from alcohols and alcoholic beverages. These devices may be constructed using various materials, such as ceramics, metallics, or polymers,

depending on end-use requirements.

A representative device of this type (see figure) would include a polymeric disk, about 1 mm in diameter and between 1 and 40 μm thick, within which would be embedded single-wall carbon nanotubes aligned along the thickness axis. The polymeric disk would be part of a unitary polymeric ring assembly. An acoustic transducer in the form of a piezoelectric-film-and-electrode sub-assembly — typically 9 μm thick and made of poly(vinylidene fluoride) coated with copper 150 nm thick — would be affixed to the outside of the outer polymeric ring by means of an electrically nonconductive epoxy.

The nanotubes would be chosen to have diameters between about 8 and about 13.5 \AA because water molecules could fit into the nanotubes, but larger

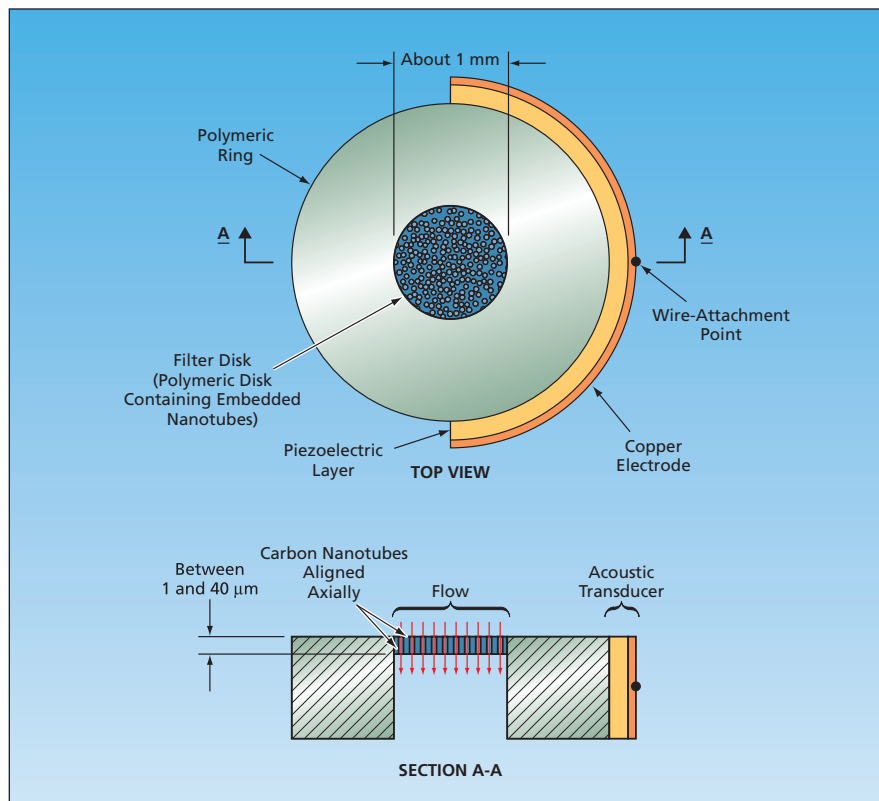
molecules could not. Water to be purified would be placed in contact with one face (typically, the upper face) of the filter disk. The surface tension of water is low enough that water molecules should enter and travel along the nanotubes, and computational simulations of molecular dynamics and experimental measurements have shown that the water molecules inside the nanotubes in this size range can be expected to become aligned into helical columns that exhibit properties of both hexagonal ice crystals and liquid water.

The acoustic transducer would be excited by means of an oscillator operating in the frequency range from 50 to 200 MHz. The assembly can feasibly be operated in the gigahertz range with a choice of a different oscillator. The frequency could be varied automatically over this range. The resulting acoustic waves would be coupled via the polymeric ring and disk to the nanotubes and water molecules. The acoustic energy transferred to the water molecules by the acoustic waves would, conservatively, equal or exceed the specific heat of fusion of ice — sufficient to cause the water molecules to become detached from each other, collectively behaving more like liquid water. Thus, the acoustic excitation would enable water to flow more freely along the nanotubes and to leave the filter disk on the lower face.

Devices of this type would be scalable to larger diameters and power levels and to multiple-filter assemblies. Although a quantitative estimate of power consumption was not available at the time of writing this article, it was reported that a single-filter device having the dimensions described above could be powered by a 9-volt battery. Larger assemblies could be powered from household and industrial power lines.

This work was done by Lillian Susan Gavalas of Johnson Space Center.

This invention is owned by NASA, and a patent application has been filed. Inquiries concerning nonexclusive or exclusive license for its commercial development should be addressed to the Patent Counsel, Johnson Space Center, (281) 483-1003. Refer to MSC-24180-1.



Aligned Carbon Nanotubes having diameters within a critical range would be embedded in a polymeric disk. The acoustic transducer would be used to excite vibrations at or near a resonance frequency of water molecules inside the nanotubes, thereby hastening the movement of the water molecules from the inlet to the outlet face of the disk.

Computer Code for Nanostructure Simulation

John H. Glenn Research Center, Cleveland, Ohio

Due to their small size, nanostructures can have stress and thermal gradients that are larger than any macroscopic analogue. These gradients can lead to specific regions that are susceptible to failure via processes such as plastic deformation by dislocation emission, chemical debonding, and interfacial alloying.

A program has been developed that rigorously simulates and predicts optoelectronic properties of nanostructures of virtually any geometrical complexity and material composition. It can be used in simulations of energy level structure, wave functions, density of states of spatially configured phonon-coupled electrons, excitons in quantum dots,

quantum rings, quantum ring complexes, and more. The code can be used to calculate stress distributions and thermal transport properties for a variety of nanostructures and interfaces, transport and scattering at nanoscale interfaces and surfaces under various stress states, and alloy compositional gradients.

The code allows users to perform modeling of charge transport processes through quantum-dot (QD) arrays as functions of inter-dot distance, array order versus disorder, QD orientation, shape, size, and chemical composition for applications in photovoltaics and physical properties of QD-based biochemical sensors. The code can be used to study the hot exciton formation/relation dynamics in ar-

rays of QDs of different shapes and sizes at different temperatures.

It also can be used to understand the relation among the deposition parameters and inherent stresses, strain deformation, heat flow, and failure of nanostructures.

This work was done by Igor Filikhin and Branislav Vlahovic of North Carolina Central University for Glenn Research Center. Further information is contained in a TSP (see page 1).

Inquiries concerning rights for the commercial use of this invention should be addressed to NASA Glenn Research Center, Innovative Partnerships Office, Attn: Steve Fedor, Mail Stop 4-8, 21000 Brookpark Road, Cleveland, Ohio 44135. Refer to LEW-18414-1.

Functionalizing CNTs for Making Epoxy/CNT Composites

Lyndon B. Johnson Space Center, Houston, Texas

Functionalization of carbon nanotubes (CNTs) with linear molecular side chains of polyphenylene ether (PPE) has been shown to be effective in solubilizing the CNTs in the solvent components of solutions that are cast to make epoxy/CNT composite films. (In the absence of solubilization, the CNTs tend to clump together instead of becoming dispersed in solution as needed to impart, to the films, the desired CNT properties of electrical conductivity and mechanical strength.) Because the PPE functionalizes the CNTs in a non-covalent manner, the functionalization does not damage the CNTs. The function-

alization can also be exploited to improve the interactions between CNTs and epoxy matrices to enhance the properties of the resulting composite films.

In addition to the CNTs, solvent, epoxy resin, epoxy hardener, and PPE, a properly formulated solution also includes a small amount of polycarbonate, which serves to fill voids that, if allowed to remain, would degrade the performance of the film. To form the film, the solution is drop-cast or spin-cast, then the solvent is allowed to evaporate.

This work was done by Jian Chen and Ramasubramaniam Rajagopal of Zyvex Corp.

for Johnson Space Center. For further information, contact the Johnson Commercial Technology Office at (281) 483-3809.

In accordance with Public Law 96-517, the contractor has elected to retain title to this invention. Inquiries concerning rights for its commercial use should be addressed to:

Zyvex Corp

1321 North Plano Rd.

Richardson TX 75081-2426

Web Address: <http://www.zyvex.com>

Refer to MSC-23719-1, volume and number of this NASA Tech Briefs issue, and the page number.

Improvements in Production of Single-Walled Carbon Nanotubes

Continuous mass production in fluidized-bed reactors now appears feasible.

Lyndon B. Johnson Space Center, Houston, Texas

A continuing program of research and development has been directed toward improvement of a prior batch process in which single-walled carbon nanotubes are formed by catalytic disproportionation of carbon monoxide in a fluidized-bed reactor. The overall effect of the improvements has been to make progress toward converting the

process from a batch mode to a continuous mode and to scaling of production to larger quantities. Efforts have also been made to optimize associated purification and dispersion post processes to make them effective at large scales and to investigate means of incorporating the purified products into composite materials. The ultimate purpose of the

program is to enable the production of high-quality single-walled carbon nanotubes in quantities large enough and at costs low enough to foster the further development of practical applications.

The fluidized bed used in this process contains mixed-metal catalyst particles. The choice of the catalyst and the operating conditions is such that the yield of

single-walled carbon nanotubes, relative to all forms of carbon (including carbon fibers, multi-walled carbon nanotubes, and graphite) produced in the disproportionation reaction is more than 90 weight percent. After the reaction, the nanotubes are dispersed in various solvents in preparation for end use, which typically involves blending into a plastic, ceramic, or other matrix to form a composite material.

Notwithstanding the batch nature of the unmodified prior fluidized-bed process, the fluidized-bed reactor operates in a continuous mode during the process. The operation is almost entirely automated, utilizing mass flow controllers, a control computer running software specific to the process, and other equipment. Moreover, an important inherent advantage of fluidized-bed reactors in general is that solid particles can be added to and re-

moved from fluidized beds during operation. For these reasons, the process and equipment were amenable to modification for conversion from batch to continuous production.

The improvements include the following:

- A provision has been made for continuous addition of catalyst particles by entraining them in a stream of helium that is fed into the reactor.
- Progress has been made toward implementation of a purification/suspension post-process.
- Progress has also been made toward implementation of an alternative purification process that involves the use of hydrofluoric acid.
- A post-purification drying method was invented. This method increases the probability of success of subsequent efforts to re-disperse lyophilized samples of purified product material.

- Techniques of *in-situ* polymerization were explored. The findings may lead to development of strong, lightweight carbon-nanotube/polymer composites.

This work was done by Leandro Balzano and Daniel E. Resasco of SouthWest Nano Technologies, Inc., for Johnson Space Center. For more information, see www.swnano.com.

In accordance with Public Law 96-517, the contractor has elected to retain title to this invention. Inquiries concerning rights for its commercial use should be addressed to:

Leandro Balzano, SWeNT Development Engineer

SouthWest NanoTechnologies Inc.

2501 Technology Place

Norman, OK 73071-1102

Phone No.: (405) 217-8388

E-mail: info@swntnano.com

Refer to MSC-23706-1, volume and number of this NASA Tech Briefs issue, and the page number.

Progress Toward Sequestering Carbon Nanotubes in PmPV

Lyndon B. Johnson Space Center, Houston, Texas

A report reopens the discussion of "Sequestration of Single-Walled Carbon Nanotubes in a Polymer" (MSC-23257), *NASA Tech Briefs*, Vol. 31, No. 12 (December 2007), page 38. To recapitulate: Sequestration of single-walled carbon nanotubes (SWNTs) in molecules of poly(*m*-phenylenevinylene-co-2,5-dioctyloxy-*p*-phenylenevinylene) [PmPV] is a candidate means of promoting dissolution of single-walled carbon nanotubes (SWNTs) into epoxies for making strong, lightweight epoxy-matrix/carbon-fiber composite materials. Bare SWNTs cannot be incorporated because they are not soluble in epoxies. One can render SWNTs soluble by chemically at-

taching various molecular chains to them, but such chemical attachments weaken them. In the present approach, one exploits the tendency of PmPV molecules to wrap themselves around SWNTs without chemically bonding to them. Attached to the backbones of the PmPV molecules are side chains that are soluble in, and chemically reactive with, epoxy precursors, and thus enable suspension of SWNTs in epoxy precursors. At time of the cited prior article, there had been only partial success in functionalizing the side chains to make them sufficiently soluble and reactive. The instant report states that a method of functionalization has been developed.

This work was done by Richard A. Bley of Eltron Research, Inc. for Johnson Space Center. Further information is contained in a TSP (see page 1).

In accordance with Public Law 96-517, the contractor has elected to retain title to this invention. Inquiries concerning rights for its commercial use should be addressed to:

Eltron Research Inc.

4600 Nautilus Court South

Boulder, Co 80301-3241

Phone No.: (303) 530-0263

E-mail: business@eltronresearch.com

Refer to MSC-23733-1, volume and number of this NASA Tech Briefs issue, and the page number.



Two-Stage Variable Sample-Rate Conversion System

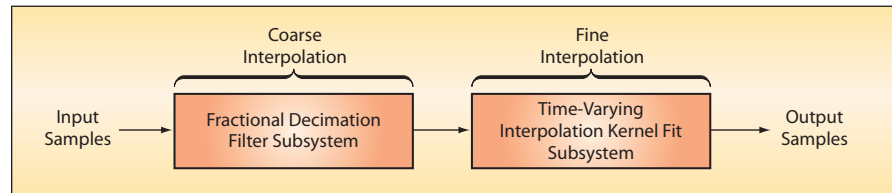
A filtering/coarse-interpolation process would precede a fine-interpolation process.

NASA's Jet Propulsion Laboratory, Pasadena, California

A two-stage variable sample-rate conversion (SRC) system has been proposed as part of a digital signal-processing system in a digital communication radio receiver that utilizes a variety of data rates. The proposed system would be used as an interface between (1) an analog-to-digital converter used in the front end of the receiver to sample an intermediate-frequency signal at a fixed input rate and (2) digitally implemented tracking loops in subsequent stages that operate at various sample rates that are generally lower than the input sample rate.

Traditional SRC systems are constructed from multirate building blocks that typically include integer/fractional decimation filter subsystems. Traditional SRC systems work well when SRC factors are fixed at rational values, but not when SRC factors vary or are irrational.

The input to the proposed two-stage SRC system would be the input sampled signal, $r[l] = r_d[l] + r_u[l]$, where $r_d[l]$ is the desired component (the signal of interest); $r_u[l]$ is the undesired component, which may include noise plus out-of-desired-frequency-band artifacts of the sampling process (alias components); and l is an integer denoting the



This **Two-Stage System** would be capable of converting from an input sample rate to a desired lower output sample rate that could be variable and not necessarily a rational fraction of the input rate.

current sample time index. In the proposed system (see figure), the first stage would be a fractional decimation filter subsystem that would suppress the alias components and would effect a coarse interpolation in the sense that it would convert to a sample rate approximating the desired value. The second stage would effect a fine interpolation from the approximate to the desired sample rate by means of a fit to a temporally varying interpolation kernel.

Several approaches to implementation of both the coarse- and the fine-interpolation stages have been studied theoretically and their strengths and weaknesses have been examined by analyzing results of computational simulations. For the coarse-interpolation stage, single and cascaded sets of filters and

decimation filter subsystems were considered, with emphasis on the cascaded subsystems because of their modularity. For the fine-interpolation stage, the computationally efficient Farrow structure (a multirate, continuously-variable-delay filter structure, a description of which would exceed the space available for this article) was used in conjunction with a variety of piecewise-polynomial interpolation kernels, with emphasis on the cubic B-spline kernel on account of its commendable performance.

This work was done by Andre Tkachenko of Caltech for NASA's Jet Propulsion Laboratory.

The software used in this innovation is available for commercial licensing. Please contact Karina Edmonds of the California Institute of Technology at (626) 395-2322. Refer to NPO-44539.

Estimating Transmitted-Signal Phase Variations for Uplink Array Antennas

Transmitted signals serve as their own phase references.

NASA's Jet Propulsion Laboratory, Pasadena, California

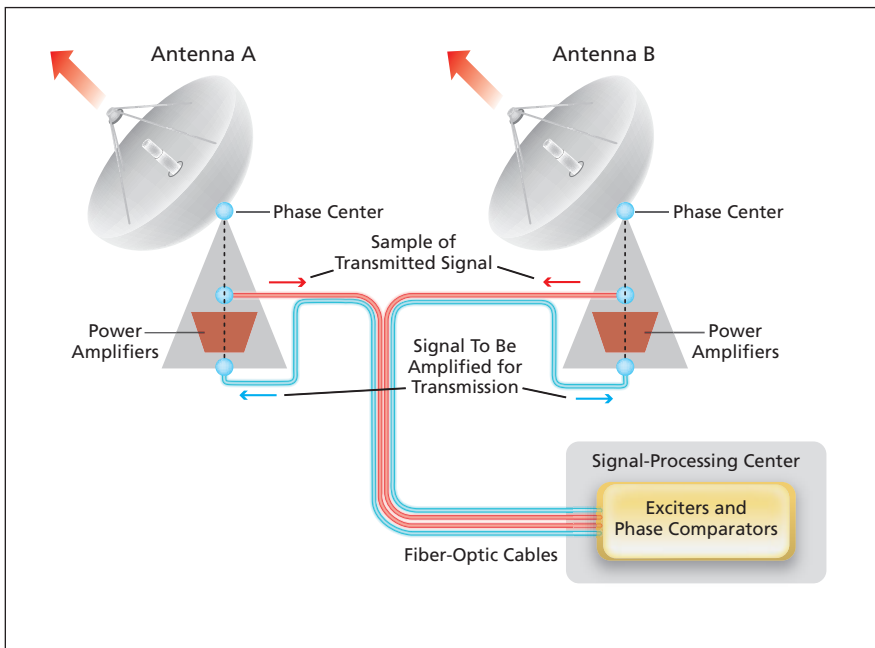
A method of estimating phase drifts of microwave signals distributed to, and transmitted by, antennas in an array involves the use of the signals themselves as phase references. The method was conceived as part of the solution of the problem of maintaining precise phase calibration required for proper operation of an array of Deep Space Network (DSN) antennas on Earth used for communicating with distant spacecraft at frequencies be-

tween 7 and 8 GHz. The method could also be applied to purely terrestrial phased-array radar and other radio antenna array systems.

In the DSN application, the electrical lengths (effective signal-propagation path lengths) of the various branches of the system for distributing the transmitted signals to the antennas are not precisely known, and they vary with time. The variations are attributable mostly to thermal expansion

and contraction of fiber-optic and electrical signal cables and to a variety of causes associated with aging of signal-handling components. The variations are large enough to introduce large phase drifts at the signal frequency. It is necessary to measure and correct for these phase drifts in order to maintain phase calibration of the antennas.

A prior method of measuring phase drifts involves the use of reference-frequency signals separate from the trans-



The **Signal-Distribution and Phase-Measurement Subsystems** for two antennas in an array are depicted here in greatly simplified form to illustrate the present phase-measurement method.

mitted signals. A major impediment to accurate measurement of phase drifts over time by the prior method is the fact that although DSN reference-frequency sources separate from the transmitting signal sources are stable and accurate enough for most DSN purposes, they are not stable enough for use in maintaining phase calibrations, as required, to within a few degrees over times as long as days or possibly even weeks. By eliminating reliance on the reference-frequency subsystem, the present method overcomes this impediment.

In a DSN array to which the present method applies (see figure), the microwave signals to be transmitted are generated by exciters in a signal-processing center, then distributed to the antennas via optical fibers. At each antenna, the signals are used to drive a microwave power-amplifier train, the output of

which is coupled to the antenna for transmission. A small fraction of the power-amplifier-train output is sent back to the signal-processing center along another optical fiber that is part of the same fiber-optic cable used to distribute the transmitted signal to the antenna. In the signal-processing center, the signal thus returned from each antenna is detected and its phase is compared with the phase of the signal sampled directly from the corresponding exciter. It is known, from other measurements, that the signal-propagation path length from the power-amplifier-train output port to the phase center of each antenna is sufficiently stable and, hence, that sampling the signal at the power-amplifier-train output port suffices for the purpose of characterizing the phase drift of the transmitted signal at the phase center of the antenna.

In this method, the phase comparison is performed continuously while the transmitting frequency is ramped as a known function of time. On the basis of the fundamental relationships among frequency, phase, and signal-propagation path length, it can be shown that if the sweep for a given antenna is started at frequency f and the phase-comparison measurement is found to change by an amount $\Delta\theta$ when the frequency has changed by an amount Δf , then

$$\Delta\theta = (2\pi/c)(f\Delta_d + d\Delta_f + \Delta_d\Delta_f),$$

where c is the speed of light in the fiber-optic cable or other signal-propagation medium and Δ_d is the change in the path length during the frequency-sweep interval. If the frequency is ramped over an interval just large enough to cause $\Delta\theta = 2\pi$ and the ramp is rapid enough that Δ_d is negligible during the measurement time interval, then after straightforward algebraic manipulation of the above equation for $\Delta\theta$, the electrical length can be estimated by the simple equation $d = c/\Delta_f$.

It must be recognized that the phase-comparison measurement used in this method is a round-trip phase-difference measurement: as such, it does not inherently distinguish between round-trip and one-way phase effects. Inasmuch as the primary goal of the measurement is to estimate the phase drift at the phase center of the antenna, it is important to distinguish between (1) round-trip phase accumulation, for which approximately half of the measured phase applies at the phase center, and (2) phase drifts in the power-amplifier train, which are one-way effects that contribute in their entirety to the phase drift at the phase center of the antenna.

This work was done by Leslie Paal, Ryan Mukai, Victor Vilnrotter, Timothy Cornish, and Dennis Lee of Caltech for NASA's Jet Propulsion Laboratory. Further information is contained in a TSP (see page 1). NPO-44611

Board Saver for Use With Developmental FPGAs

A printed-circuit board is protected against repeated soldering and unsoldering.

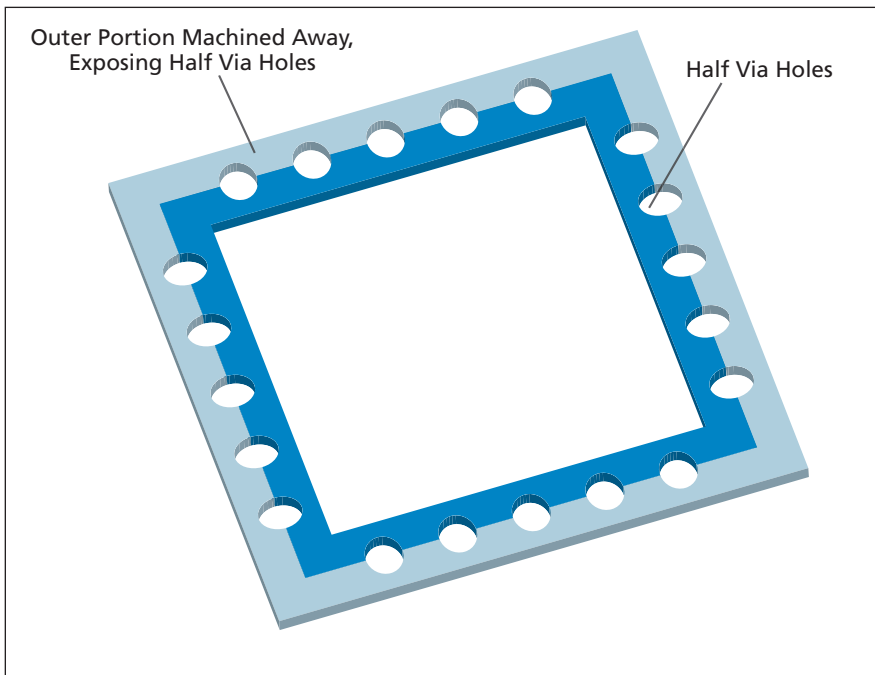
NASA's Jet Propulsion Laboratory, Pasadena, California

A device denoted a board saver has been developed as a means of reducing wear and tear of a printed-circuit board onto which an antifuse field-programmable gate array (FPGA) is to be eventually soldered permanently after a number of design iterations.

The need for the board saver or a similar device arises because (1) antifuse-FPGA design iterations are common and (2) repeated soldering and unsoldering of FPGAs on the printed-circuit board to accommodate design iterations can wear out the printed-circuit

board. The board saver is basically a solderable/unsolderable FPGA receptacle that is installed temporarily on the printed-circuit board.

The board saver is, more specifically, a smaller, square-ring-shaped, printed-circuit board (see figure) that contains half



The **Board Saver** is shown here in a simplified plan view (greatly reduced number of via holes) and not to scale, to facilitate understanding of its basic layout.

via holes — one for each contact pad — along its periphery. As initially fabricated, the board saver is a wider ring containing full via holes, but then it is milled along its outer edges, cutting the

via holes in half and laterally exposing their interiors. The board saver is positioned in registration with the designated FPGA footprint and each via hole is soldered to the outer portion of the

corresponding FPGA contact pad on the first-mentioned printed-circuit board. The via-hole/contact joints can be inspected visually and can be easily unsoldered later.

The square hole in the middle of the board saver is sized to accommodate the FPGA, and the thickness of the board saver is the same as that of the FPGA. Hence, when a non-final FPGA is placed in the square hole, the combination of the non-final FPGA and the board saver occupy no more area and thickness than would a final FPGA soldered directly into its designated position on the first-mentioned circuit board. The contact leads of a non-final FPGA are not bent and are soldered, at the top of the board saver, to the corresponding via holes. A non-final FPGA can readily be unsoldered from the board saver and replaced by another one. Once the final FPGA design has been determined, the board saver can be unsoldered from the contact pads on the first-mentioned printed-circuit board and replaced by the final FPGA.

This work was done by Andrew Berkun of Caltech for NASA's Jet Propulsion Laboratory. Further information is contained in a TSP (see page 1). NPO-44745

Circuit for Driving Piezoelectric Transducers

Circuits similar to this one could be useful in ultrasonic cleaners.

NASA's Jet Propulsion Laboratory, Pasadena, California

The figure schematically depicts an oscillator circuit for driving a piezoelectric transducer to excite vibrations in a mechanical structure. The circuit was designed and built to satisfy application-specific requirements to drive a selected one of 16 such transducers at a regulated amplitude and frequency chosen to optimize the amount of work performed by the transducer and to compensate for both (1) temporal variations of the resonance frequency and damping time of each transducer and (2) initially unknown differences among the resonance frequencies and damping times of different transducers. In other words, the circuit is designed to adjust itself to optimize the performance of whichever transducer is selected at any given time. The basic design concept may be adaptable to other applications that involve the use of piezoelectric transducers in ultrasonic cleaners and

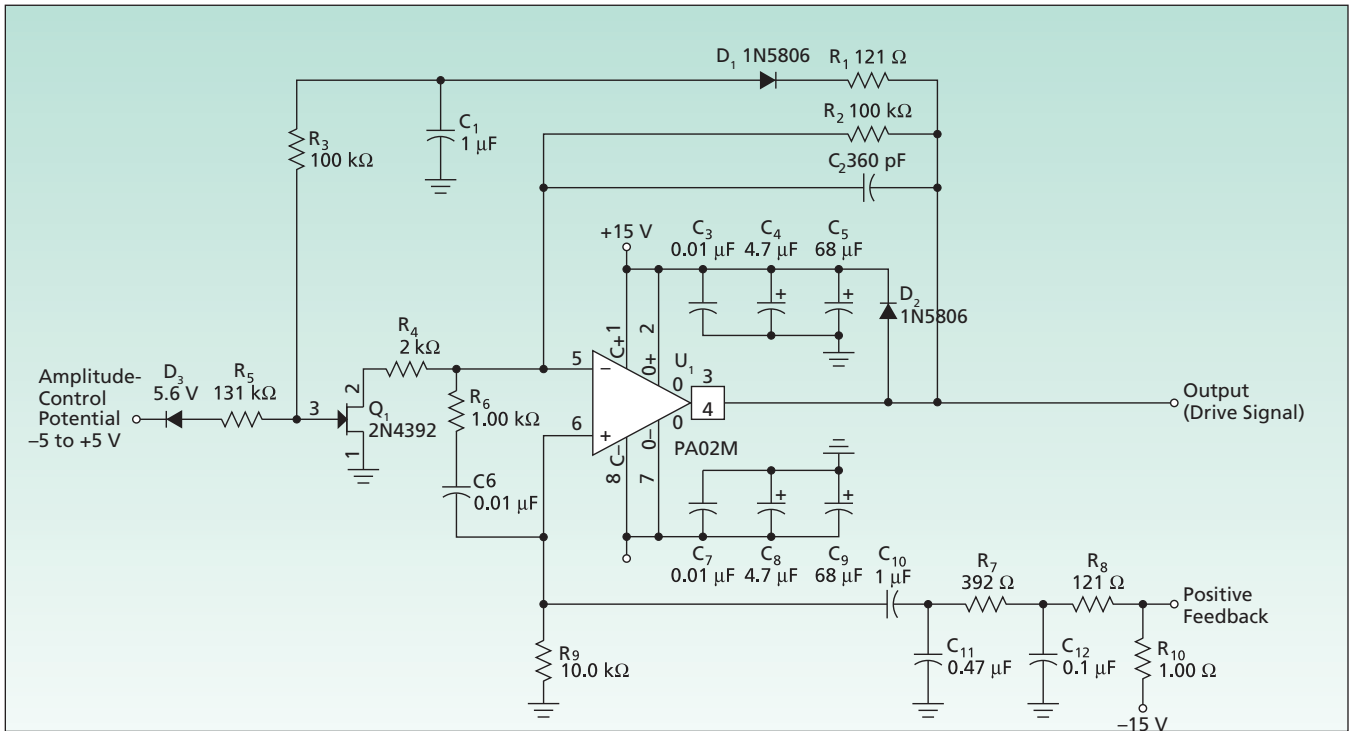
other apparatuses in which high-frequency mechanical drives are utilized.

This circuit includes three resistor-capacitor networks that, together with the selected piezoelectric transducer, constitute a band-pass filter having a peak response at a frequency of about 2 kHz, which is approximately the resonance frequency of the piezoelectric transducers. Gain for generating oscillations is provided by a power hybrid operational amplifier (U_1). A junction field-effect transistor (Q_1) in combination with a resistor (R_4) is used as a voltage-variable resistor to control the magnitude of the oscillation. The voltage-variable resistor is part of a feedback control loop: Part of the output of the oscillator is rectified and filtered for use as a slow negative feedback to the gate of Q_1 to keep the output amplitude constant. The response of this control loop is much slower than 2 kHz and, therefore, does

not introduce significant distortion of the oscillator output, which is a fairly clean sine wave.

The positive AC feedback needed to sustain oscillations is derived from sampling the current through the piezoelectric transducer. This positive AC feedback, in combination with the slow feedback to the voltage-variable resistors, causes the overall loop gain to be just large enough to keep the oscillator running.

The positive feedback loop includes two 16-channel multiplexers, which are not shown in the figure. One multiplexer is used to select the desired piezoelectric transducer. The other multiplexer, which is provided for use in the event that there are significant differences among the damping times of the 16 piezoelectric transducers, facilitates changing the value of one of the resistors in the positive-feedback loop to accommodate the damping time of the selected transducer.



This Oscillator Circuit generates a nearly optimum, nearly sinusoidal output for driving a vibrational piezoelectric transducer.

The amplitude of the oscillator output is controlled by use of an externally generated potential, between -5 and +5 VDC, applied via Zener diode D_3 and resistor R_5 to the gate of Q_1 : +5 VDC corresponds to an output amplitude of 25 V peak to peak; -5 VDC corresponds to an output amplitude of 9 V peak to peak.

Prior to the development of this circuit, it was common practice to excite vibrational piezoelectric transducers by use of

“bang-bang” oscillators, the outputs of which contain significant proportions of harmonics. The harmonics contribute to stress and waste of power in heating the transducers. The near-sine-wave output of this circuit has much lower harmonic content and, therefore, imposes less stress on the transducers and enables them to operate at lower temperature.

Previously, it was also common practice to control the drive amplitude of oscillation

by using an additional regulator circuit to control the supply potential. In this circuit, the supply potential is not varied and the amplitude of oscillation is controlled by use of a DC control potential as described above, eliminating the need for the additional regulator circuit.

This work was done by David P. Randall and Jacob Chapsky of Caltech for NASA's Jet Propulsion Laboratory. For more information, contact iaoffice@jpl.nasa.gov. NPO-45529

Digital Synchronizer Without Metastability

Lyndon B. Johnson Space Center, Houston, Texas

A proposed design for a digital synchronizing circuit would eliminate metastability that plagues flip-flop circuits in digital input/output interfaces. This metastability is associated with sampling, by use of flip-flops, of an external signal that is asynchronous with a clock signal that drives the flip-flops: it is a temporary flip-flop failure that can occur when a rising or falling edge of an asynchronous signal occurs during the setup and/or hold time of a flip-flop.

The proposed design calls for (1) use of a clock frequency greater than the frequency of the asynchronous signal, (2) use of flip-flop asynchronous

preset or clear signals for the asynchronous input, (3) use of a clock asynchronous recovery delay with pulse width discriminator, and (4) tying the data inputs to constant logic levels to obtain (5) two half-rate synchronous partial signals — one for the falling and one for the rising edge. Inasmuch as the flip-flop data inputs would be permanently tied to constant logic levels, setup and hold times would not be violated. The half-rate partial signals would be recombined to construct a signal that would replicate the original asynchronous signal at its original rate but would be synchronous with the clock signal.

This work was done by Robert M. Simle and Jose A. Cavazos of Lockheed Martin Corp. for Johnson Space Center.

Title to this invention, covered by U.S. Patent No. 6,771,099 B2, has been waived under the provisions of the National Aeronautics and Space Act [42 U.S.C. 2457 (f)]. Inquiries concerning licenses for its commercial development should be addressed to:

*Lockheed Martin General Counsel
Lockheed Martin
2400 NASA Road 1
Houston, TX 77258*

Refer to MSC-23220-1, volume and number of this NASA Tech Briefs issue, and the page number.

Compact, Low-Overhead, MIL-STD-1553B Controller

Goddard Space Flight Center, Greenbelt, Maryland

A compact and flexible controller has been developed to provide MIL-STD-1553B Remote Terminal (RT) communications and supporting and related functions with minimal demand on the resources of the system in which the controller is to be installed. (MIL-STD-1553B is a military standard that encompasses a method of communication and electrical-interface requirements for digital electronic subsystems connected to a

data bus. MIL-STD-1553B is commonly used in defense and space applications.) Many other MIL-STD-1553B RT controllers are complicated, and to enable them to function, it is necessary to provide software and to use such ancillary separate hardware devices as microprocessors and dual-port memories.

The present controller functions without need for software and any ancillary hardware. In addition, it contains a flexi-

ble system interface and extensive support hardware while including on-chip error-checking and diagnostic support circuitry. This controller is implemented within part of a modern field-programmable gate array.

This work was done by Richard Katz and Rod Barto of Goddard Space Flight Center. For further information, contact the Goddard Innovative Partnerships Office at (301) 286-5810. GSC-15491-1

Parallel-Processing CMOS Circuitry for M-QAM and 8PSK TCM

NASA's Jet Propulsion Laboratory, Pasadena, California

There has been some additional development of parts reported in "Multi-Modulator for Bandwidth-Efficient Communication" (NPO-40807), *NASA Tech Briefs*, Vol. 32, No. 6 (June 2009), page 34. The focus was on

- The generation of M-order quadrature amplitude modulation (M-QAM) and octonary-phase-shift-keying, trellis-

coded modulation (8PSK TCM),

- The use of square-root raised-cosine pulse-shaping filters,
- A parallel-processing architecture that enables low-speed [complementary metal oxide/semiconductor (CMOS)] circuitry to perform the coding, modulation, and pulse-shaping computations at a high rate; and

- Implementation of the architecture in a CMOS field-programmable gate array.

This work was done by Andrew Gray and Dennis Lee of Caltech; Scott Hoy of Lockheed-Martin; Dave Fisher of SGT Inc.; Wai Fong and Parminder Ghuman of GSFC for NASA's Jet Propulsion Laboratory. For more information, contact iaoffice@jpl.nasa.gov. NPO-40809

Differential InP HEMT MMIC Amplifiers Embedded in Waveguides

The differential configuration confers advantages over the single-ended configuration.

NASA's Jet Propulsion Laboratory, Pasadena, California

Monolithic microwave integrated-circuit (MMIC) amplifiers of a type now being developed for operation at frequencies of hundreds of gigahertz contain InP high-electron-mobility transistors (HEMTs) in a differential configuration. The differential configuration makes it possible to obtain gains greater than those of amplifiers having the single-ended configuration. To reduce losses associated with packaging, the MMIC chips are designed integrally with, and embedded in, waveguide packages, with the additional benefit that the packages are compact enough to fit into phased transmitting and/or receiving antenna arrays.

Differential configurations (which are inherently balanced) have been used to extend the upper limits of oper-

ating frequencies of complementary metal oxide/semiconductor (CMOS) amplifiers to the microwave range but, until now, have not been applied in millimeter-wave amplifier circuits. Baluns have traditionally been used to transform from single-ended to balanced configurations, but baluns tend to be lossy. Instead of baluns, finlines are used to effect this transformation in the present line of development. Finlines have been used extensively to drive millimeter-wave mixers in balanced configurations. In the present extension of the finline balancing concept, finline transitions are integrated onto the affected MMICs (see figure).

The differential configuration creates a virtual ground within each pair of InP HEMT gate fingers, eliminating the

need for inductive vias to ground. Elimination of these vias greatly reduces parasitic components of current and the associated losses within an amplifier, thereby enabling more nearly complete utilization of the full performance of each transistor. The differential configuration offers the additional benefit of multiplying (relative to the single-ended configuration) the input and output impedances of each transistor by a factor of four, so that it is possible to use large transistors that would otherwise have prohibitively low impedances.

Yet another advantage afforded by the virtual ground of the differential configuration is elimination of the need for a ground plane and, hence, elimination of the need for back-side metallization of the MMIC chip. In turn, elimination of

the back-side metallization simplifies fabrication, reduces parasitic capacitances, and enables mounting of the MMIC in the electric-field plane (“E-plane”) of a waveguide. E-plane mounting is consistent with (and essential for the utility of) the finline configuration, in which transmission lines lie on a dielectric sheet in the middle of a broad side of the waveguide.

E-plane mounting offers a combination of low loss and ease of assembly because no millimeter-wave wire bonds or transition substrates are required. More-

over, because there is no ground plane behind the MMIC, the impedance for the detrimental even (single-ended) mode is high, suppressing coupling to that mode. Still another advantage of E-plane mounting is that the fundamental waveguide mode is inherently differential, eliminating the need for a balun to excite the differential mode.

This work was done by Pekka Kangaslahti, Erich Schlecht, and Lorene Samoska of Caltech for NASA’s Jet Propulsion Laboratory. Further information is contained in a TSP (see page 1).

In accordance with Public Law 96-517, the contractor has elected to retain title to this invention. Inquiries concerning rights for its commercial use should be addressed to:

*Innovative Technology Assets Management
JPL*

Mail Stop 202-233

4800 Oak Grove Drive

Pasadena, CA 91109-8099

(818) 354-2240

E-mail: iaoffice@jpl.nasa.gov

Refer to NPO-42857, volume and number of this NASA Tech Briefs issue, and the page number.



Improved Aerogel Vacuum Thermal Insulation

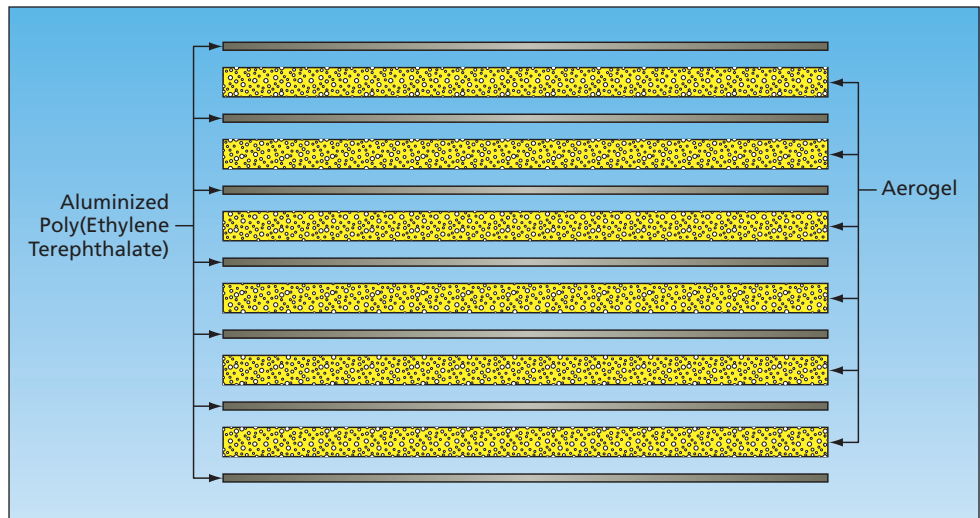
Multilayer structures offer reduced effective thermal conductivity.

Lyndon B. Johnson Space Center, Houston, Texas

An improved design concept for aerogel vacuum thermal-insulation panels calls for multiple layers of aerogel sandwiched between layers of aluminized Mylar (or equivalent) poly(ethylene terephthalate), as depicted in the figure. This concept is applicable to both the rigid (brick) form and the flexible (blanket) form of aerogel vacuum thermal-insulation panels.

Heretofore, the fabrication of a typical aerogel vacuum insulating panel has involved encapsulation of a single layer of aerogel in poly(ethylene terephthalate) and pumping of gases out of the aerogel-filled volume. A multilayer panel according to the improved design concept is fabricated in basically the same way: Multiple alternating layers of aerogel and aluminized poly(ethylene terephthalate) are assembled, then encapsulated in an outer layer of poly(ethylene terephthalate), and then the volume containing the multilayer structure is evacuated as in the single-layer case.

The multilayer concept makes it possible to reduce effective thermal conductivity of a panel below that of a compar-



An Improved Aerogel Vacuum Insulation Panel contains multiple layers of aerogel interspersed with layers of aluminized poly(ethylene terephthalate). The panel is shown here in the uncompressed form at an intermediate stage of fabrication. Once the interior of the panel is evacuated, exterior atmospheric pressure squeezes the layers together.

able single-layer panel, without adding weight or incurring other performance penalties. Implementation of the multilayer concept is simple and relatively inexpensive, involving only a few additional fabrication steps to assemble the multiple layers prior to evacuation. For a

panel of the blanket type, the multilayer concept, affords the additional advantage of reduced stiffness.

This work was done by Warren P. Ruemele and Grant C. Bue of Johnson Space Center. Further information is contained in a TSP (see page 1). MSC-24351-1

Fluoroester Co-Solvents for Low-Temperature Li⁺ Cells

Both low-temperature performance and high-temperature resilience are improved.

NASA's Jet Propulsion Laboratory, Pasadena, California

Electrolytes comprising LiPF₆ dissolved in alkyl carbonate/fluoroester mixtures have been found to afford improved low-temperature performance and greater high-temperature resilience in rechargeable lithium-ion electrochemical cells. These and other electrolytes comprising lithium salts dissolved mixtures of esters have been studied in continuing research directed toward extending the lower limit of operating temperatures of such cells. This research at earlier stages, and the un-

derlying physical and chemical principles, were reported in numerous previous *NASA Tech Briefs* articles.

The purpose of the present focus on high-temperature resilience in addition to low-temperature performance is to address issues posed by the flammability of the esters and, at temperatures near the upper end (about 55 °C) of their intended operating temperature range, by their high chemical reactivity. As used here, "high-temperature resilience" signifies, loosely, a desired combination of

low flammability of an electrolyte mixture and the ability of a cell that contains the mixture to sustain a relatively small loss of reversible charge/discharge capacity during storage in the fully charged condition at high temperature. The selection of fluoroesters for study as candidate electrolyte solvent components to increase high-temperature resilience was prompted in part by the observation that like other halogenated compounds, fluoroesters have low flammability.

The fluoroesters investigated in this study include trifluoroethyl butyrate (TFEB), ethyl trifluoroacetate (ETFA), trifluoroethyl acetate (TFEA), and methyl pentafluoropropionate (MPFP). Solvent mixtures were prepared by mixing these fluoroesters with two other esters: ethylene carbonate (EC) and ethyl methyl carbonate (EMC). The specific solvent mixtures were the following:

- IEC + 3EMC + 1TFEB
- IEC + 2EMC + 2TFEB
- IEC + 1EMC + 3TFEB
- IEC + 3EMC + 1ETFA
- IEC + 2EMC + 2TFEA
- IEC + 3EMC + 1TFEA
- IEC + 3EMC + 1MPFP

where the numbers indicate the relative volume proportions of the constituents.

Electrolytes were prepared by dissolving LiPF_6 at a concentration of 1.0 M in these solvents. In addition, baseline (non-fluoroester-containing) electrolytes were prepared by dissolving LiPF_6 at a concentration of 1.0 M in the following solvent mixtures:

- IEC + 1DEC + 1DMC
- IEC + 4EMC

where "DEC" signifies diethyl carbonate and "DMC" signifies dimethyl carbonate.

Rechargeable carbonanode/ $\text{LiNi}_{0.8}\text{Co}_{0.2}\text{O}_2$ -cathode cells containing these electrolytes were assembled and subjected to charge-discharge cycling tests at various temperatures from room temperature (23 °C) down to -60 °C. The cells were also evaluated with respect to high-temperature re-

silience by measuring the fractions of initial reversible capacity retained after storage for 10 days at a temperature of 55 °C. In these tests, the cell containing the electrolyte 1.0 M LiPF_6 in (1EC + 3EMC + 1TFEB) exhibited the greatest overall improvements in both low-temperature performance (see figure) and high-temperature resilience over the cells containing the baseline electrolytes.

This work was done by Marshall Smart, and Ratnakumar Bugga of Caltech and G. K. Surya Prakash, Kiah Smith, and Pooja Bhalla of the University of Southern California for NASA's Jet Propulsion Labo-

ratory. Further information is contained in a TSP (see page 1).

In accordance with Public Law 96-517, the contractor has elected to retain title to this invention. Inquiries concerning rights for its commercial use should be addressed to:

*Innovative Technology Assets Management
JPL*

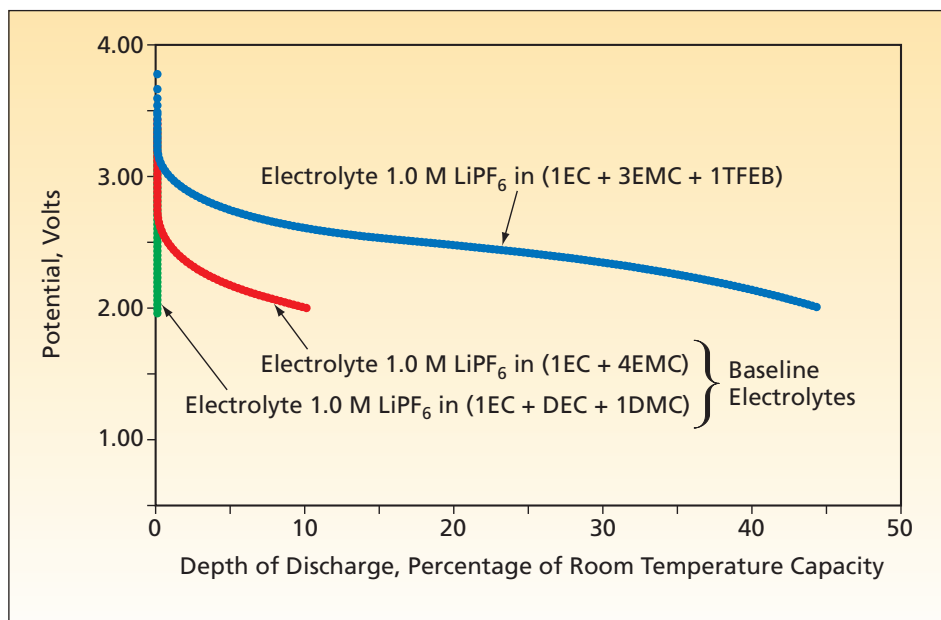
Mail Stop 202-233

4800 Oak Grove Drive

Pasadena, CA 91109-8099

E-mail: iaoffice@jpl.nasa.gov

Refer to NPO-44626, volume and number of this NASA Tech Briefs issue, and the page number.



Potentials of Cells containing various electrolytes were measured at a temperature of -60 °C during discharge at a current of 10 mA to a final potential of 2.0 V.

Using Volcanic Ash To Remove Dissolved Uranium and Lead

Lyndon B. Johnson Space Center, Houston, Texas

Experiments have shown that significant fractions of uranium, lead, and possibly other toxic and/or radioactive substances can be removed from an aqueous solution by simply exposing the solution, at ambient temperature, to a treatment medium that includes weathered volcanic ash from Pu'u Nene, which is a cinder cone on the Island of Hawaii. Heretofore, this specific volcanic ash has been used for an entirely different purpose: simulating the spectral properties of Martian soil.

The treatment medium can consist of the volcanic ash alone or in combination

with chitosan, which is a natural polymer that can be produced from seafood waste or easily extracted from fungi, some bacteria, and some algae. The medium is harmless to plants and animals and, because of the abundance and natural origin of its ingredient(s), is inexpensive. The medium can be used in a variety of ways and settings: it can be incorporated into water-filtration systems; placed in contact or mixed with water-containing solids (e.g., soils and sludges); immersed in bodies of water (e.g., reservoirs, lakes, rivers, or wells); or placed in and around nuclear power plants, mines, and farm fields.

This work was done by David S. McKay of Johnson Space Center and Raul G. Cuero of Prairie View A&M University. For further information, contact the JSC Innovation Partnerships Office at (281) 483-3809.

In accordance with Public Law 96-517, the contractor has elected to retain title to this invention. Inquiries concerning rights for its commercial use should be addressed to:

Prairie View A&M University

P.O. Box 685

Prairie View, TX 77446

Refer to MSC-23545-1, volume and number of this NASA Tech Briefs issue, and the page number.



High-Efficiency Artificial Photosynthesis Using a Novel Alkaline Membrane Cell

Successful artificial photosynthesis is significant for future human/robotic exploration and terrestrial carbon emissions control.

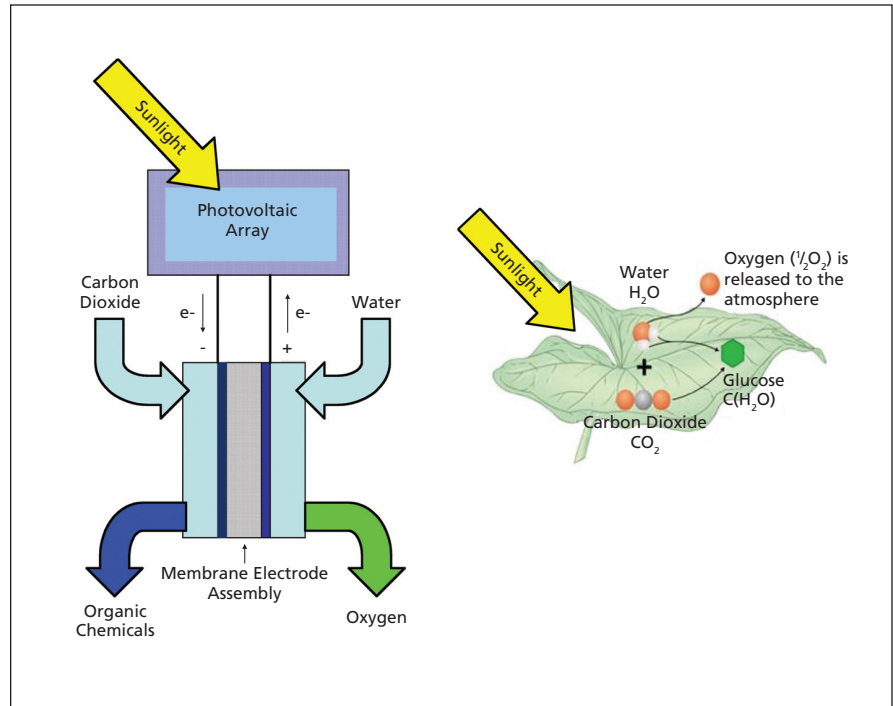
NASA's Jet Propulsion Laboratory, Pasadena, California

A new cell designed to mimic the photosynthetic processes of plants to convert carbon dioxide into carbonaceous products and oxygen at high efficiency, has an improved configuration using a polymer membrane electrolyte and an alkaline medium. This increases efficiency of the artificial photosynthetic process, achieves high conversion rates, permits the use of inexpensive catalysts, and widens the range of products generated by this type of process.

The alkaline membrane electrolyte allows for the continuous generation of sodium formate without the need for any additional separation system. The electrolyte type, pH, electrocatalyst type, and cell voltage were found to have a strong effect on the efficiency of conversion of carbon dioxide to formate. Indium electrodes were found to have higher conversion efficiency compared to lead. Bicarbonate electrolyte offers higher conversion efficiency and higher rates than water solutions saturated with carbon dioxide. pH values between 8 and 9 lead to the maximum values of efficiency. The operating cell voltage of 2.5 V, or higher, ensures conversion of the carbon dioxide to formate, although the hydrogen evolution reaction begins to compete strongly with the formate production reaction at higher cell voltages.

Formate is produced at indium and lead electrodes at a conversion efficiency of 48 mg of CO₂/kilojoule of energy input. This efficiency is about eight times that of natural photosynthesis in green plants. The electrochemical method of artificial photosynthesis is a promising approach for the conversion, separation and sequestration of carbon dioxide for confined environments as in space habitats, and also for carbon dioxide management in the terrestrial context.

The heart of the reactor is a membrane cell fabricated from an alkaline polymer electrolyte membrane and cat-



The **Artificial Photosynthesis Process** and its similarity to natural photosynthesis. The reduction of carbon dioxide to organic chemicals in an electrochemical cell is a viable approach to achieving artificial photosynthesis.

alyst-coated electrodes. This cell is assembled and held in compression in gold-plated hardware. The cathode side of the cell is supplied with carbon dioxide-saturated water or bicarbonate solution. The anode side of the cell is supplied with sodium hydroxide solution. The solutions are circulated past the electrodes in the electrochemical cell using pumps. A regulated power supply provides the electrical energy required for the reactions. Photovoltaic cells can be used to better mimic the photosynthetic reaction. The current flowing through the electrochemical cell, and the cell voltage, are monitored during experimentation. The products of the electrochemical reduction of carbon dioxide are allowed to accumulate in the cathode reservoir. Samples of the cathode solution are withdrawn for

product analysis. Oxygen is generated on the anode side and is allowed to vent out of the reservoir.

This work was done by Sri Narayan, Brennan Haines, Julian Blosiu, and Neville Marzwell of Caltech for NASA's Jet Propulsion Laboratory. Further information is contained in a TSP (see page 1).

In accordance with Public Law 96-517, the contractor has elected to retain title to this invention. Inquiries concerning rights for its commercial use should be addressed to:

*Innovative Technology Assets Management
JPL*

*Mail Stop 202-233
4800 Oak Grove Drive
Pasadena, CA 91109-8099*

E-mail: iaoffice@jpl.nasa.gov

Refer to NPO-45777, volume and number of this NASA Tech Briefs issue, and the page number.

Silicon Wafer-Scale Substrate for Microshutters and Detector Arrays

These substrates can be used in photomask generation and stepper equipment used to make ICs and MEMS devices.

Goddard Space Flight Center, Greenbelt, Maryland

The silicon substrate carrier was created so that a large-area array (in this case 62,000+ elements of a microshutter array) and a variety of discrete passive and active devices could be mounted on a single board, similar to a printed circuit board. However, the density and number of interconnects far exceeds the capabilities of printed circuit board technology. To overcome this hurdle, a method was developed to fabricate this carrier out of silicon and implement silicon integrated circuit (IC) technology. This method achieves a large number of high-density metal interconnects; a 100-percent yield over a 6-in. (≈ 15 -cm) diameter wafer (one unit per wafer); a rigid, thermally compatible structure (all components and operating conditions) to cryogenic temperatures; re-workability and component replaceability, if required; and the ability to precisely cut large-area holes through the substrate.

A method that would employ indium bump technology along with wafer-scale integration onto a silicon carrier was also developed. By establishing a silicon-based version of a printed circuit board, the objectives could be met with one solution. The silicon substrate would be 2 mm thick to survive the environmental loads of a launch. More than 2,300 metal traces and over 1,500 individual wire bonds are required. To mate the microshutter array to the silicon substrate, more than 10,000 indium bumps are required. A window was cut in the substrate to allow the light signal to pass through the substrate and reach the microshutter array. The substrate was also the receptacle for multiple unpackaged IC die wire-bonded directly to the substrate (thus conserving space over conventionally packaged die).

Unique features of this technology include the implementation of a 2-mm-

thick silicon wafer to withstand extreme mechanical loads (from a rocket launch); integrated polysilicon resistor heaters directly on the substrate; the precise formation of an open aperture ($\approx 3 \times 3$ cm) without any crack propagation; implementation of IR transmission blocking techniques; and compatibility with indium bump bonding. Although designed for the microshutter arrays for the NIRSpec instrument on the James Webb Space Telescope, these substrates can be linked to microshutter applications in the photomask generation and stepper equipment used to make ICs and microelectromechanical system (MEMS) devices.

This work was done by Murzy Jhabvala, David E. Franz, Audrey J. Ewin, Christine Jhabvala, and Sachi Babu of Goddard Space Flight Center and Larry Hess, Stephen Snodgrass, Nicholas Costen, and Christian Zincke of MEI. Further information is contained in a TSP (see page 1). GSC-15665-1



Micro-Horn Arrays for Ultrasonic Impedance Matching

Horn impedance matching is extended from lower frequencies into the ultrasonic range.

NASA's Jet Propulsion Laboratory, Pasadena, California

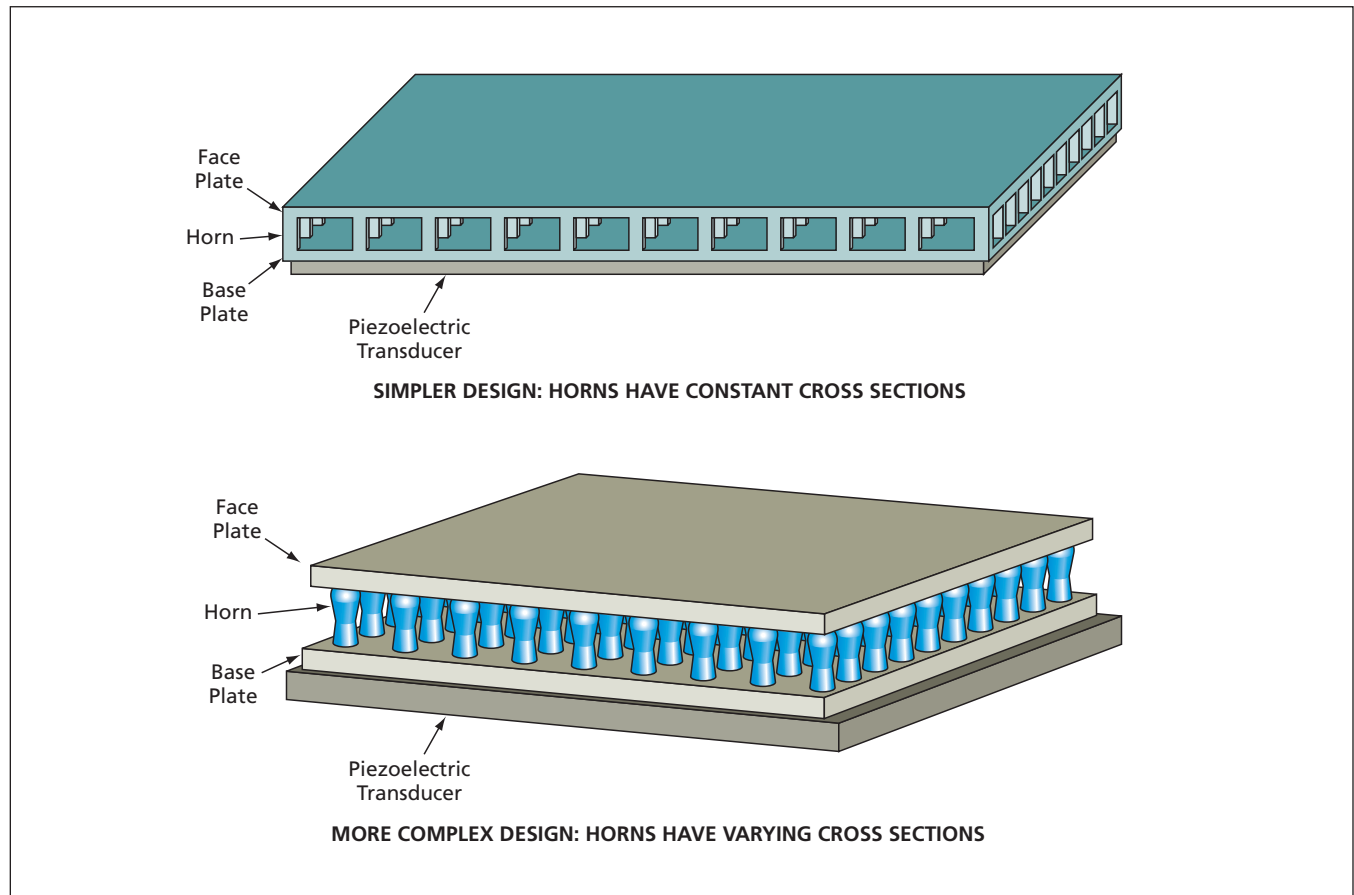
Thin-layered structures containing arrays of micromachined horns, denoted solid micro-horn arrays (SMIHAs), have been conceived as improved means of matching acoustic impedances between ultrasonic transducers and the media with which the transducers are required to exchange acoustic energy. Typically, ultrasonic transducers (e.g., those used in medical imaging) are piezoelectric or similar devices, which produce small displacements at large stresses. However, larger displacements at smaller stresses are required in the target media (e.g., human tissues) with which acoustic energy is to be exchanged. Heretofore, efficiencies in transmission of acoustic energy between ultrasonic transducers and target media have been severely limited

because substantial mismatches of acoustic impedances have remained, even when coupling material layers have been interposed between the transducers and the target media. In contrast, SMIHAs can, in principle, be designed to effect more nearly complete acoustic impedance matching, leading to power-transmission efficiencies of 90 percent or even greater.

The SMiHA concept is based on extension, into the higher-frequency/lower-wavelength ultrasonic range, of the use of horns to match acoustic impedances in the audible and lower-frequency ultrasonic ranges. In matching acoustic impedance in transmission from a higher-impedance acoustic source (e.g., a piezoelectric transducer) and a lower-

impedance target medium (e.g., air or human tissue), a horn acts as a mechanical amplifier. The shape and size of the horn can be optimized for matching acoustic impedance in a specified frequency range.

A typical SMiHA would consist of a base plate, a face plate, and an array of horns that would constitute pillars that connect the two plates (see figure). In use, the base plate would be connected to an ultrasonic transducer and the face plate would be placed in contact with the target medium. As at lower frequencies, the sizes and shapes of the pillars could be tailored for impedance matching in a specified ultrasonic frequency range. In a design that would be simplest to implement by micromachining, the



Small Horns in a Planar Array would be sized and shaped for matching acoustic impedance between an ultrasonic transducer and a medium in contact with the face plate. The horns could be fabricated by micromachining.

horns would have constant cross-sectional areas as shown in the upper part of the figure. In this case, the dimensions of the horns could be chosen on the basis of a Mason equivalent-circuit model (a simplified model, well-known in the piezoelectric-transducer art, in which the electrical and mechanical dy-

namics, including electromechanical couplings, are expressed as electrical circuit elements that can include inductors, capacitors, and lumped-parameter complex impedances.) In a more complex, more nearly optimum design, the cross-sectional area of each horn would be either stepped or made to vary as a

continuous function of through-the-thickness position, as shown in the lower part of the figure.

This work was done by Stewart Sherrit, Xiaoli Bao, and Yoseph Bar-Cohen of Caltech for NASA's Jet Propulsion Laboratory. For more information contact iaoffice@jpl.nasa.gov. NPO-43907

⚙ Improved Controller for a Three-Axis Piezoelectric Stage

Advantages over a prior controller include compactness, greater adaptability, and higher resolution.

NASA's Jet Propulsion Laboratory, Pasadena, California

An improved closed-loop controller has been built for a three-axis piezoelectric positioning stage. The stage can be any of a number of commercially available or custom-made units that are used for precise three-axis positioning of optics in astronomical instruments and could be used for precise positioning in diverse fields of endeavor that include adaptive optics, fabrication of semiconductor, and nanotechnology.

In a typical application, the stage is used to move an optic through a small distance with a required resolution of the order of a nanometer or a fraction of a nanometer. Typically, the piezoelectric actuator for each axis can be made to expand through a maximum stroke $\leq 12 \mu\text{m}$ by applying a potential $\leq 120 \text{ V}$ to it. To provide position feedback for closed-loop control of the potential applied to the piezoelectric actuator for each axis, the expansion of the actuator is sensed by means of a strain gauge bonded to the side of the actuator. The resistance of the strain gauge changes from about 700 to 701 Ω as the actuator expands through its maximum stroke. The strain gauge is part of a Wheatstone bridge, so that the small change in resistance from a nominal value can be converted to a Wheatstone-bridge output voltage. To close the control loop, the Wheatstone-bridge output voltage is amplified and compared with a voltage representing an actuator set point specified by an external control computer or other external source. The difference between these voltages constitutes a servo error signal, which is amplified for application to the affected piezoelectric actuator.

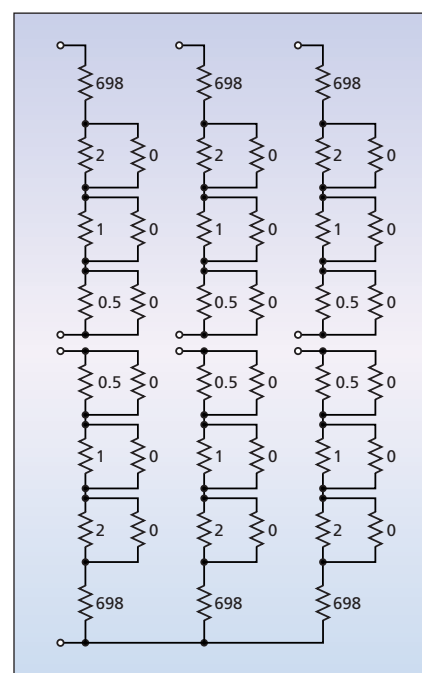
The improved controller supplants a prior controller that resided in a 19-in. ($\approx 48\text{-cm}$) rack. The most expensive part of the improved controller consists of servocontroller circuitry on a 4.25-by-7.5-in. ($\approx 11\text{-by-19-cm}$) printed-circuit

board, denoted the main board. The strain gauges are connected into Wheatstone-bridge circuits that include relatively inexpensive, interchangeable resistor bridge circuits (see figure) on a 2.5-by-3.5-in. (approximately 6-by-9-cm) satellite printed-circuit board. The satellite board can readily be replaced by another with different circuitry tailored for a different actuator/strain-gauge combination.

The three Wheatstone bridges are driven by a precision voltage reference on the satellite board, powered by a cable from the main board. The voltages representing the actuator set points are generated by three 18-bit, self-calibrating, digital-to-analog converters on the main board. The amplification of the Wheatstone-bridge output voltages is effected by two-stage, low-noise instrumentation amplifiers on the main board.

The servo error signal for each axis is further amplified and filtered. The filter circuitry can be built to have either 2-Hz bandwidth (resulting in spatial resolution of 0.1 nm) or 200-Hz bandwidth (resulting in spatial resolution of 1 nm). The amplified, filtered signal is fed to a final high-voltage amplifier, the output of which is applied to the piezoelectric actuator. By means of a CMOS input on a control connector, some of the servo-controller circuitry can be bypassed, causing the actuators to operate in a rapid-motion, open-loop control mode.

One of the greatest advantages of improved controller over the prior controller arises from a low-noise design. The dominant component of noise is now Johnson noise from the strain gauges; the input-referred noise from all other components is lower by design. The lower-noise design makes it possible to refine spatial resolution from a prior limit of 1 nm to the present limit of 0.1 nm.



These Resistor Bridge Circuits are parts of Wheatstone bridges that include strain gauges. Resistance values are in ohms. The zero-ohm resistors are jumpers that can be removed to trim the bridges.

This work was done by Shanti Rao and Dean Palmer of Caltech for NASA's Jet Propulsion Laboratory. Further information is contained in a TSP (see page 1).

In accordance with Public Law 96-517, the contractor has elected to retain title to this invention. Inquiries concerning rights for its commercial use should be addressed to:

*Innovative Technology Assets Management
JPL*

*Mail Stop 202-233
4800 Oak Grove Drive
Pasadena, CA 91109-8099*

E-mail: iaoffice@jpl.nasa.gov

Refer to NPO-44806, volume and number of this NASA Tech Briefs issue, and the page number.



Nano-Pervaporation Membrane With Heat Exchanger Generates Medical-Grade Water

A small system produces high-quality water using a heat exchanger that meets requirements for evaporation of substances such as pharmaceuticals and vitamins.

Lyndon B. Johnson Space Center, Houston, Texas

A nanoporous membrane is used for the pervaporation process in which potable water is maintained, at atmospheric pressure, on the feed side of the membrane. The water enters the non-pervaporation (NPV) membrane device where it is separated into two streams — retentate water and permeated water. The permeated pure water is removed by applying low vapor pressure on the permeate side to create water vapor before condensation. This permeated water vapor is subsequently condensed by coming in contact with the cool surface of a heat exchanger with heat being recovered through transfer to the feed water stream.

A thermoelectric heat exchanger is used here to pump heat from the condensing surface to the feed water stream. Because the temperature differential across this heat exchanger is relatively small, the thermoelectric process is highly energy efficient. This new heat exchanger provides high surface area for vapor condensation with controllable temperature on the hot and cold sides to meet the operating temperature requirements for the evaporation of solvent-containing, heat-sensitive sub-

stances, such as pharmacological substances, vitamins, etc.

The heat exchanger is a sandwich, with the copper interface plates on both sides of the heat pumps interfacing with the radiators. The outside of the radiators is insulated with two cover plates bolted together to hold the entire heat exchange unit together. Four heat-pump units are connected in series and are controlled by one circuit. The control electronics are built around a standard commercial voltage regulator. This was chosen in part because it has a 6.2-volt reference output that is needed for the bridge circuit. The radiator on the incoming potable-water side is heating, and the vapor side is cooling.

The NPV process can be operated at close to room temperature, and is driven by the space vacuum (provided by a secondary loop controlled by a secondary vacuum valve with built-in redundancy for safety) applied on the permeate side with minimal energy consumption. A primary valve controls the inlet space vacuum. The nanoporous membrane serves as a barrier, not only between liquid and water vapor phases, but also be-

tween pure water and dissolved solids to be removed. The nanopore selectively adsorbs liquid water and excludes undesirable constituents such as particles, microbes (e.g., bacteria), viruses, and volatile organic compounds.

The system only requires a low-pressure gradient across the membrane [<25 psi (≈ 172 kPa)] as compared to a high-pressure gradient required for reverse osmosis (RO) (>150 psi (≈ 1.03 MPa)], to achieve high water-flow rate. As a result, the novel membrane will not be prone to the fouling issues that are commonly seen in the RO system. The cross-flow design can also allow the concentration stream to sweep away retained molecules and prevent the membrane surface from clogging or fouling, making the system able to deliver medical-grade water to point of use. The overall process has no moving parts and has low maintenance requirements.

This work was done by Chung-Yi Tsai and Jerry Alexander of T3 Scientific Limited Liability for Johnson Space Center. For further information, contact the Johnson Commercial Technology Office at (281) 483-3809. MSC-24264-1/6-1

Micro-Organ Devices

Effects of drugs can be tested realistically, without experimentation on animals.

Lyndon B. Johnson Space Center, Houston, Texas

Micro-organ devices (MODs) are being developed to satisfy an emerging need for small, lightweight, reproducible, biological-experimentation apparatuses that are amenable to automated operation and that impose minimal demands for resources (principally, power and fluids). MODs are intended to overcome major disadvantages of conventional *in vitro* and conventional *in vivo* experimentation for purposes of investigating effects of

medicines, toxins, and possibly other foreign substances.

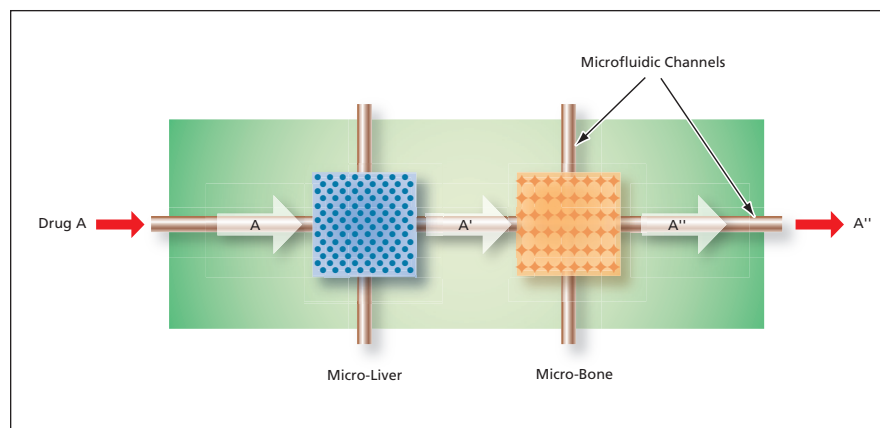
Conventional *in vitro* cell cultures do not mimic the complex environments to which toxins and medicines are subjected in living organisms. Conventional *in vivo* studies in non-human animals can account for complex intercellular and inter-tissue effects not observable in *in vitro* tests, but experimentation on animals is expensive, labor intensive, time-consuming, and unpopular. Moreover, cross-

species extrapolation of toxicity and pharmacokinetic characteristics is problematic. In contrast, because MODs could host life-like miniature assemblies of human cells, the effects observed in tests performed in MODs could be extrapolated more readily to humans than could effects observed in conventional *in vitro* cell cultures, making it possible to reduce or eliminate experimentation on animals.

In simplest terms, a MOD is a microfluidic device containing a variety of

microstructures and assemblies of cells (see figure), all designed to mimic a complex *in vivo* microenvironment by replicating one or more *in vivo* micro-organ structures, the architectures and composition of the extracellular matrices in the organs of interest, and the *in vivo* fluid flows. In addition to microscopic flow channels, a MOD contains one or more micro-organ wells containing cells residing in microscopic extracellular matrices and/or scaffolds, the shapes and compositions of which enable replication of the corresponding *in vivo* cell assemblies and flows.

Once the basic microfluidic device infrastructure of a MOD containing micro-organ wells and flow channels has been fabricated, single cells or multiple cells of the same type or different types needed for a given micro-organ are encapsulated or suspended in a solution that may contain micro-organ-specific extracellular matrix molecules and scaffolding. The suspension or solution is placed in a syringe that is part of a computer-controlled apparatus; under computer control, cells and any extracellular matrix material are dispensed as the syringe is moved, thereby effectively printing a unitary three-dimensional assem-



This **Simple Example MOD** is designed for use in monitoring (1) conversion of a drug from inactive form A to active form A' in the liver and (2) indirectly monitoring the effect of A' on a bone by monitoring the concentration of A'', which is a tertiary metabolite form of the drug.

bly of cells and extracellular matrix material into a micro-organ well. The dimensions of each printed micro-organ are chosen so as not to exceed optimum dimensions for perfusion of cells with nutrient fluid, exchange of gases between the cells and the nutrient fluid, and removal of non-gaseous cell wastes in the nutrient flow.

This work was done by Steven R. Gonda and Julia Leslie of Johnson Space Center; Robert C. Chang, Binil Starly, and Wei Sun

of Drexel University; Christopher Culbertson of Kansas State University; and Heidi Holtorf of USRA. For further information, contact the JSC Innovation Partnerships Office at (281) 483-3809.

This invention is owned by NASA, and a patent application has been filed. Inquiries concerning nonexclusive or exclusive license for its commercial development should be addressed to the Patent Counsel, Johnson Space Center, (281) 483-1003. Refer to MSC-23988-1.



Nonlinear Thermal Compensators for WGM Resonators

At one target temperature, thermal frequency fluctuations would vanish to first order.

NASA's Jet Propulsion Laboratory, Pasadena, California

In an alternative version of a proposed bimaterial thermal compensator for a whispering-gallery-mode (WGM) optical resonator, a mechanical element having nonlinear stiffness would be added to enable stabilization of a desired resonance frequency at a suitable fixed working temperature. The previous version was described in "Bimaterial Thermal Compensators for WGM Resonators" (NPO-44441), *NASA Tech Briefs*, Vol. 32, No. 10 (October 2008), page 96. Both versions are intended to serve as inexpensive

means of preventing (to first order) or reducing temperature-related changes in resonance frequencies.

A bimaterial compensator would apply, to a WGM resonator, a force that would slightly change the shape of the resonator and thereby change its resonance frequencies. Through suitable choice of the design of the compensator, it should be possible to make the temperature dependence of the force-induced frequency shift equal in magnitude and opposite in sign to the

temperature dependence of the frequency shift of the uncompensated resonator so that, to first order, a change in temperature would cause zero net change in frequency.

Because the version now proposed is similar to the previous version in most respects, it is necessary to recapitulate most of the description from the cited prior article, with appropriate modifications. In both the previous and present versions (see figure), a compensator as proposed would include (1) a frame made of one material having a thermal-expansion coefficient α_1 and (2) a spacer made of another material having a thermal-expansion coefficient α_2 . The WGM resonator would be sandwiched between disks, and the resulting sandwich would be squeezed between the frame and the spacer. Assuming that the cross-sectional area of the frame greatly exceeded the cross-sectional area of the spacer and that the thickness of the sandwich was small relative to the length of the spacer, the net rate of change of a resonance frequency with changing temperature would be given by

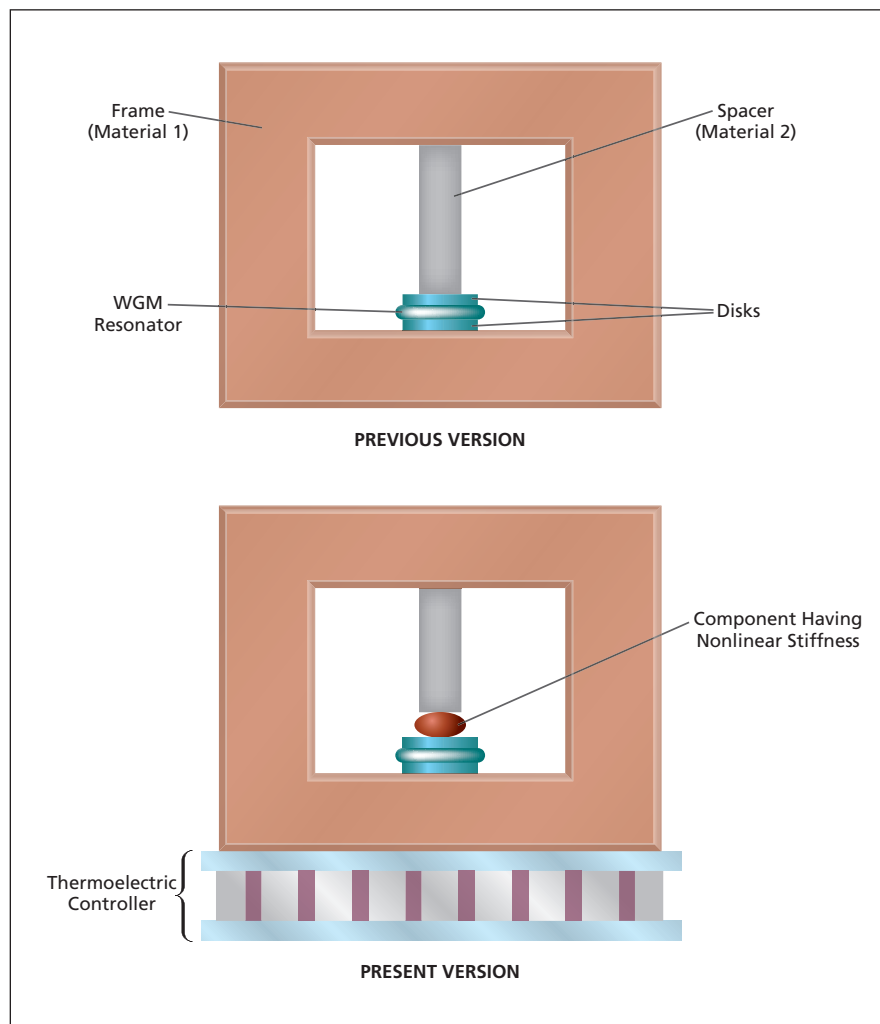
$$df/dT \approx \partial f/\partial T + (\partial f/\partial F)S_2E_2(\alpha_2 - \alpha_1)$$

where f is the resonance frequency, T is temperature, $\partial f/\partial T$ is the rate of change of resonance frequency as a function of temperature of the uncompensated resonator, $\partial f/\partial F$ is the rate of change of frequency as a function of applied force F at constant temperature, S_2 is the effective cross-sectional area of the spacer, and E_2 is the modulus of elasticity of the spacer.

In principle, through appropriate choice of materials and geometry, one could obtain temperature compensation — that is, one could make $df/dT \approx 0$. For example, the effective spacer cross-sectional area for temperature compensation is given by

$$S_2 \approx (\partial f/\partial T) / [(\partial f/\partial F)E_2(\alpha_1 - \alpha_2)].$$

In practice, because of inevitable manufacturing errors and imprecise knowledge of thermomechanical responses of



A Component Having Nonlinear Stiffness and a means of temperature control would be added to a previous, basic version of a bimaterial compensator for a WGM resonator. In both versions, a temperature-dependent stress would be applied to counteract the temperature dependence of the spectrum of the uncompensated resonator.

structural components, it is difficult or impossible to obtain exact temperature compensation of frequency through selection of S_2 .

According to the present proposal, to make it possible to obtain exact temperature compensation, one would add a component having a nonlinear stiffness to the mechanical load path and would place the entire resonator-and-compensator assembly on a thermoelectric controller, in an oven, or both. Then the temperature dependence of frequency would be approximately quadratic and the net derivative of frequency with respect to temperature would be given by

$$df/dT \approx \partial f/\partial T + (\partial f/\partial F)S_2E_2(\alpha_2 - \alpha_1) + \Delta T$$

where A is a parameter that characterizes the nonlinearity to lowest order in

temperature and ΔT is the difference between the present temperature and some other temperature, which could be a target temperature. To find the target temperature that gives exact temperature compensation, one sets the derivative equal to zero and solves for ΔT :

$$\Delta T \approx -A^{-1}[\partial f/\partial T + (\partial f/\partial F)S_2E_2(\alpha_2 - \alpha_1)]$$

The oven and/or the thermoelectric controller could be used to set the temperature to the exact compensation temperature. Even if the exact values of A , $\partial f/\partial T$, $\partial f/\partial F$, S_2 , E_2 , α_1 , and α_2 were not known in advance, one could still determine the exact compensation temperature by measuring frequency as a function of temperature and finding the lowest point on the approxi-

mately quadratic frequency-versus-temperature curve.

This work was done by Anatoliy Savchenkov, Andrey Matsko, Dmitry Strelkov, Lute Maleki, Nan Yu, and Vladimir Iltchenko of Caltech for NASA's Jet Propulsion Laboratory.

In accordance with Public Law 96-517, the contractor has elected to retain title to this invention. Inquiries concerning rights for its commercial use should be addressed to:

*Innovative Technology Assets Management
JPL*

*Mail Stop 202-233
4800 Oak Grove Drive*

Pasadena, CA 91109-8099

E-mail: iaoffice@jpl.nasa.gov

Refer to NPO-44567, volume and number of this NASA Tech Briefs issue, and the page number.

Dynamic Self-Locking of an OEO Containing a VCSEL

This is an alternative scheme for developing small, low-power atomic clocks.

NASA's Jet Propulsion Laboratory, Pasadena, California

A method of dynamic self-locking has been demonstrated to be effective as a means of stabilizing the wavelength of light emitted by a vertical-cavity surface-emitting laser (VCSEL) that is an active element in the frequency-control loop of an optoelectronic oscillator (OEO) designed to implement an atomic clock based on an electromagnetically-induced-transparency (EIT) resonance. This scheme can be considered an alternative to the one described in "Optical Injection Locking of a VCSEL in an OEO" (NPO-43454), *NASA Tech Briefs*, Vol. 33, No. 7 (July 2009), page 33. Both schemes are expected to enable the development of small, low-power, high-stability atomic clocks that would be suitable for use in

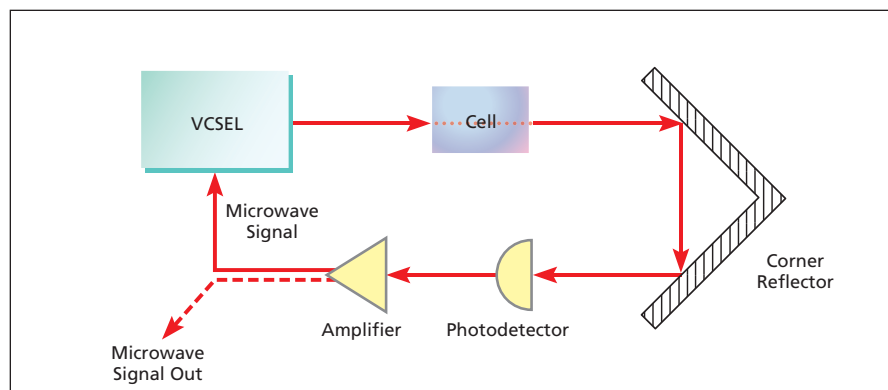
applications involving precise navigation and/or communication.

To recapitulate from the cited prior article: In one essential aspect of operation of an OEO of the type described above, a microwave modulation signal is coupled into the VCSEL. Heretofore, it has been well known that the wavelength of light emitted by a VCSEL depends on its temperature and drive current, necessitating thorough stabilization of these operational parameters. Recently, it was discovered that the wavelength also depends on the microwave power coupled into the VCSEL. This concludes the background information.

From the perspective that led to the conception of the optical injection-

locking scheme described in the cited prior article, the variation of the VCSEL wavelength with the microwave power circulating in the frequency-control loop is regarded as a disadvantage and optical injection locking is a solution of the problem of stabilizing the wavelength in the presence of uncontrolled fluctuations in the microwave power. The present scheme for dynamic self-locking emerges from a different perspective, in which the dependence of VCSEL wavelength on microwave power is regarded as an advantageous phenomenon that can be exploited as a means of controlling the wavelength.

The figure schematically depicts an atomic-clock OEO of the type in question, wherein (1) the light from the VCSEL is used to excite an EIT resonance in selected atoms in a gas cell (e.g., ^{87}Rb atoms in a low-pressure mixture of Ar and Ne) and (2) the power supplied to the VCSEL is modulated by a microwave signal that includes components at beat frequencies among the VCSEL wavelength and modulation sidebands. As the VCSEL wavelength changes, it moves closer to or farther from a nearby absorption spectral line, and the optical power transmitted through the cell (and thus the loop gain) changes accordingly. A change in the loop gain causes a change in the



This **Optoelectronic Oscillator** is a compact, relatively simple implementation of an atomic clock. The cell contains the optically absorbing atoms upon which the clock is based.

microwave power and, thus, in the VCSEL wavelength. It is possible to choose a set of design and operational parameters (most importantly, the electronic part of the loop gain) such that the OEO stabilizes itself in the sense that an increase in circulating microwave power causes the VCSEL wavelength to change in a direction that results in an increase in optical absorption and thus a decrease in circulating microwave power. Typically, such an appropriate choice of opera-

tional parameters involves setting the nominal VCSEL wavelength to a point on the shorter-wavelength wing of an absorption spectral line.

This work was done by Dmitry Strelakov, Andrey Matsko, Nan Yu, Anatoliy Savchenkov, and Lute Maleki of Caltech for NASA's Jet Propulsion Laboratory. Further information is contained in a TSP (see page 1). Further information is contained in a TSP (see page 1).

In accordance with Public Law 96-517, the contractor has elected to retain title to

this invention. Inquiries concerning rights for its commercial use should be addressed to:

*Innovative Technology Assets Management
JPL*

*Mail Stop 202-233
4800 Oak Grove Drive
Pasadena, CA 91109-8099
(818) 354-2240*

E-mail: iaoffice@jpl.nasa.gov

Refer to NPO-43751, volume and number of this NASA Tech Briefs issue, and the page number.

Internal Water Vapor Photoacoustic Calibration

John H. Glenn Research Center, Cleveland, Ohio

Water vapor absorption is ubiquitous in the infrared wavelength range where photoacoustic trace gas detectors operate. This technique allows for discontinuous wavelength tuning by temperature-jumping a laser diode from one range to another within a time span suitable for photoacoustic

calibration. The use of an internal calibration eliminates the need for external calibrated reference gases. Commercial applications include an improvement of photoacoustic spectrometers in all fields of use.

This work was done by Jeffrey S. Pilgrim of Vista Photonics, Inc. for Glenn Research Cen-

ter. Further information is contained in a TSP (see page 1).

Inquiries concerning rights for the commercial use of this invention should be addressed to NASA Glenn Research Center, Innovative Partnerships Office, Attn: Steve Fedor, Mail Stop 4-8, 21000 Brookpark Road, Cleveland, Ohio 44135. Refer to LEW-18417-1

Mid-Infrared Reflectance Imaging of Thermal-Barrier Coatings Apparatus successfully monitors extent of hidden subsurface delamination.

John H. Glenn Research Center, Cleveland, Ohio

An apparatus for mid-infrared reflectance imaging has been developed as means of inspecting for subsurface damage in thermal-barrier coatings (TBCs). The apparatus is designed, more specifically, for imaging the progression of buried delamination cracks in plasma-sprayed yttria-stabilized zirconia coatings on turbine-engine components. Progression of TBC delamination occurs by the formation of buried cracks that grow and then link together to produce eventual TBC spallation. The mid-infrared reflectance imaging system described here makes it possible to see delamination progression that is invisible to the unaided eye, and therefore give sufficiently advanced warning before delamination progression adversely affects engine performance and safety.

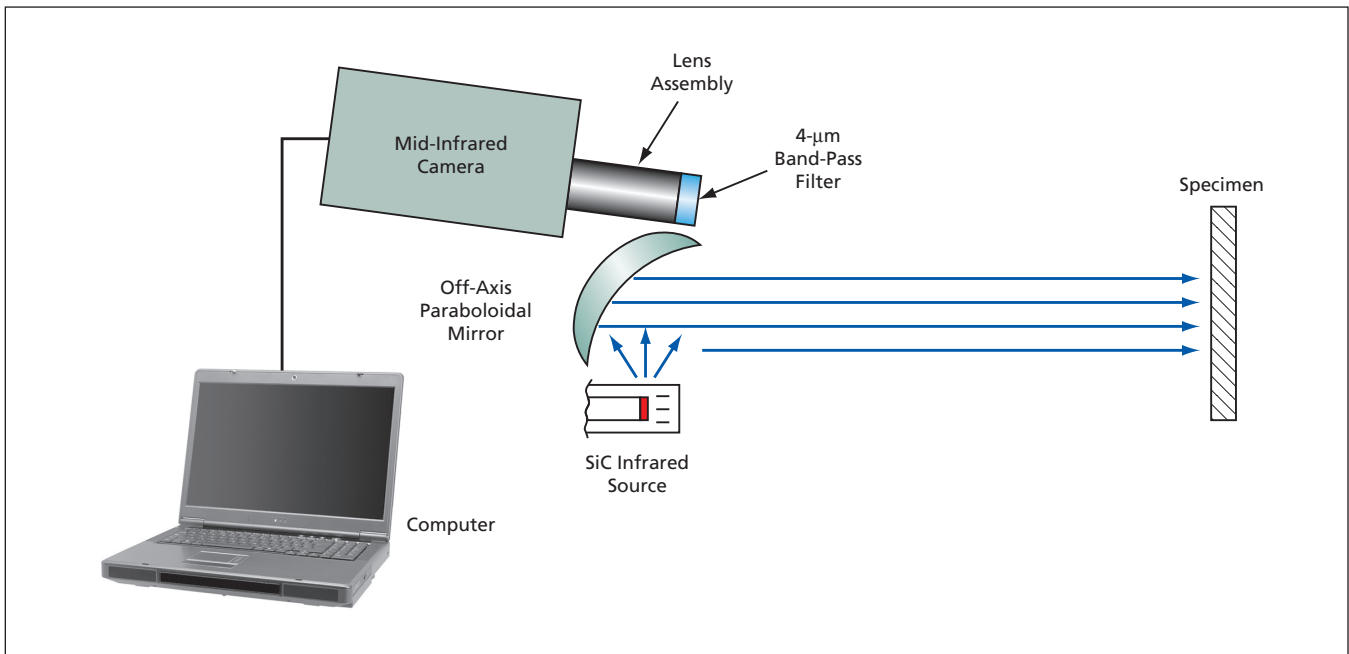
The apparatus (see figure) includes a commercial mid-infrared camera that contains a liquid-nitrogen-cooled focal-plane indium antimonide photodetector array, and imaging is restricted by a nar-

row bandpass centered at wavelength of 4 μm . This narrow wavelength range centered at 4 μm was chosen because (1) it enables avoidance of interfering absorptions by atmospheric OH and CO₂ at 3 and 4.25 μm , respectively; and (2) the coating material exhibits maximum transparency in this wavelength range. Delamination contrast is produced in the mid-infrared reflectance images because the introduction of cracks into the TBC creates an internal TBC/air-gap interface with a high diffuse reflectivity of 0.81, resulting in substantially higher reflectance of mid-infrared radiation in regions that contain buried delamination cracks.

The camera is positioned a short distance (≈ 12 cm) from the specimen. The mid-infrared illumination is generated by a 50-watt silicon carbide source positioned to the side of the mid-infrared camera, and the illumination is collimated and reflected onto the specimen by a 6.35-cm-diameter off-axis paraboloidal mirror. Because the collected images are of a steady-state reflected inten-

sity (in contrast to the transient thermal response observed in infrared thermography), collection times can be lengthened to whatever extent needed to achieve desired signal-to-noise ratios.

Each image is digitized, and the resulting data are processed in several steps to obtain a true mid-infrared reflectance image. The raw image includes thermal radiation emitted by the specimen in addition to the desired reflected radiation. The thermal-radiation contribution is eliminated by subtracting the image obtained with the illumination off from the image obtained with the illumination on. A flat-field correction is then made to remove the effects of non-uniformities in the illumination level and pixel-to-pixel variations in sensitivity. This correction is performed by normalizing to an image of a standard object that has a known reflectance at a wavelength of 4 μm . After correction, each pixel value is proportional to the reflectance (at a wavelength of 4- μm) at the corresponding location on the specimen.



A TBC-Coated Specimen Is Imaged using reflected mid-infrared radiation at a wavelength of 4 μm . At this wavelength, subsurface delamination progression in the TBC that is invisible to the unaided eye becomes visible in the mid-infrared reflectance image.

Mid-infrared reflectance imaging of specimens that were thermally cycled for different numbers of cycles was performed and demonstrated that mid-infrared reflectance imaging was able to monitor the gradual delamination progression that occurs with continued thermal cycling. Reproducible values

were obtained for the reflectance associated with an attached and fully delaminated TBC, so that intermediate reflectance values could be interpreted to successfully predict the number of thermal cycles to failure.

This work was done by Jeffrey I. Eldridge of Glenn Research Center and Richard E. Mar-

tin of Cleveland State University. Further information is contained in a TSP (see page 1).

Inquiries concerning rights for the commercial use of this invention should be addressed to NASA Glenn Research Center, Innovative Partnerships Office, Attn: Steve Fedor, Mail Stop 4-8, 21000 Brookpark Road, Cleveland, Ohio 44135. Refer to LEW-17950-1.

Improving the Visible and Infrared Contrast Ratio of Microshutter Arrays

Microshutters are used in the fabrication of integrated circuits and MEMS devices.

Goddard Space Flight Center, Greenbelt, Maryland

Three device improvements have been developed that dramatically enhance the contrast ratio of microshutters. The goal of a microshutter is to allow as much light through as possible when the shutters are in the open configuration, and preventing any light from passing through when they are in the closed position. The ratio of the transmitted light that is blocked is defined here as the contrast ratio.

Three major components contribute to the improved performance of these microshutters:

1. The precise implementation of light shields, which protect the gap around the shutters so no light can leak through. It has been ascertained that without the light shield there would be

a gap on the order of 1 percent of the shutter area, limiting the contrast to a maximum of 100.

2. The precise coating of the interior wall of each microshutter was improved with an insulator and metal using an angle deposition technique. The coating prevents any infrared light that finds an entrance on the surface of the microshutter cell from being emitted from a sidewall. Since silicon is in effect transparent to any light with a wavelength longer than ≈ 1 micrometer, these coatings are essential to blocking any stray signals when the shutters are closed.

3. A thin film of molybdenum nitride (MoN) was integrated onto the surface of the microshutter blade. This film

provides the majority of light blockage over the microshutter and also ensures that the shutter can be operated over a wide temperature range by maintaining its flatness.

These improvements were motivated by the requirements dictated by the James Webb Space Telescope NIRSpec instrument. The science goals of the NIRSpec require observing some of the very faintest objects in a given field of view that also may contain some very bright objects. To observe the faint objects, the light from the bright objects — which could be thousands of times brighter — must be completely blocked. If a closed microshutter is even slightly transmissive, a very bright object will still transmit a small signal,

which can be larger than a signal from a very faint object transmitted through an open shutter. Since this situation can completely corrupt the results, it was necessary that the closed shutters be able to attenuate light by at least a factor of 2,000.

There currently exist four flight-quality microshutter arrays that have been fully or are currently undergoing testing and

the results support that the three improvements described above have successfully led to contrast levels >50,000 in over 99 percent of the microshutters at an operating temperature of 35 K. Applications for these high-contrast microshutters are in the photomask generation and stepper equipment used to make integrated circuits and microelectromechanical (MEMS) devices. Since microshutters are

a reconfigurable optical element, their versatility in these industries provides an improvement over printed masks and fixed projection alignment systems.

This work was done Murzy Jhabwala, Mary Li, Harvey Moseley, Dave Franz, Yun Zheng, and Alexander Kuttyrev of Goddard Space Flight Center. For further information, contact the Goddard Innovative Partnerships Office at (301) 286-5810. GSC-15609-1

Improved Scanners for Microscopic Hyperspectral Imaging

Neither specimens nor entire optical assemblies would be moved.

Stennis Space Center, Mississippi

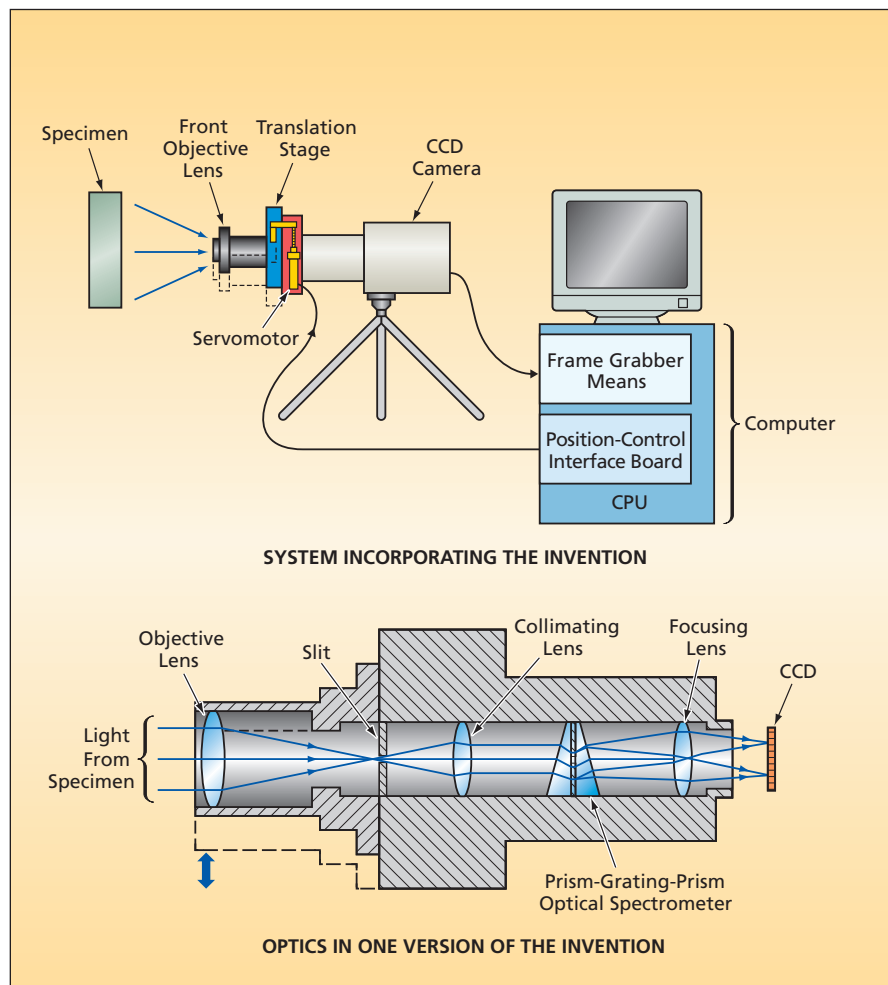
Improved scanners to be incorporated into hyperspectral microscope-based imaging systems have been invented. Heretofore, in microscopic imaging, including spectral imaging, it has been customary to either move the specimen relative to the optical assembly that includes the microscope or else

move the entire assembly relative to the specimen. It becomes extremely difficult to control such scanning when submicron translation increments are required, because the high magnification of the microscope enlarges all movements in the specimen image on the focal plane. To overcome this difficulty,

in a system based on this invention, no attempt would be made to move either the specimen or the optical assembly. Instead, an objective lens would be moved within the assembly so as to cause translation of the image at the focal plane: the effect would be equivalent to scanning in the focal plane.

The upper part of the figure depicts a generic proposed microscope-based hyperspectral imaging system incorporating the invention. The optical assembly of this system would include an objective lens (normally, a microscope objective lens) and a charge-coupled-device (CCD) camera. The objective lens would be mounted on a servomotor-driven translation stage, which would be capable of moving the lens in precisely controlled increments, relative to the camera, parallel to the focal-plane scan axis. The output of the CCD camera would be digitized and fed to a frame grabber in a computer. The computer would store the frame-grabber output for subsequent viewing and/or processing of images. The computer would contain a position-control interface board, through which it would control the servomotor.

There are several versions of the invention. An essential feature common to all versions is that the stationary optical subassembly containing the camera would also contain a spatial window, at the focal plane of the objective lens, that would pass only a selected portion of the image. In one version, the window would be a slit, the CCD would contain a one-dimensional array of pixels, and the objective lens would be moved along an axis perpendicular to the slit to spatially scan the image of the specimen in "pushbroom" fashion. The image built up by scanning in this case would be an ordinary (non-spectral) image.



The **Objective Lens Would Be Moved**, relative to the rest of the optical assembly, to scan the image in the focal plane.

In another version, the optics of which are depicted in the lower part of the figure, the spatial window would be a slit, the CCD would contain a two-dimensional array of pixels, the slit image would be refocused onto the CCD by a relay-lens pair consisting of a collimating and a focusing lens, and a prism-grating-prism optical spectrometer would be placed between the collimating and focusing lenses. Consequently, the image

on the CCD would be spatially resolved along the slit axis and spectrally resolved along the axis perpendicular to the slit. As in the first-mentioned version, the objective lens would be moved along an axis perpendicular to the slit to spatially scan the image of the specimen in "pushbroom" fashion.

This work was done by Chengye Mao of the Institute for Technology Development for Stennis Space Center.

Inquiries concerning this technology should be addressed to:

Chengye Mao

Institute for Technology Development

Building 1103, Suite 118

Stennis Space Center, MS 39529

Phone No.: (510) 353-9881

E-mail: chengye.geo@yahoo.com

Refer to SSC-00280-1, volume and number of this NASA Tech Briefs issue, and the page number.



Rate-Compatible LDPC Codes With Linear Minimum Distance

These protograph-based codes can have fixed input or output block sizes.

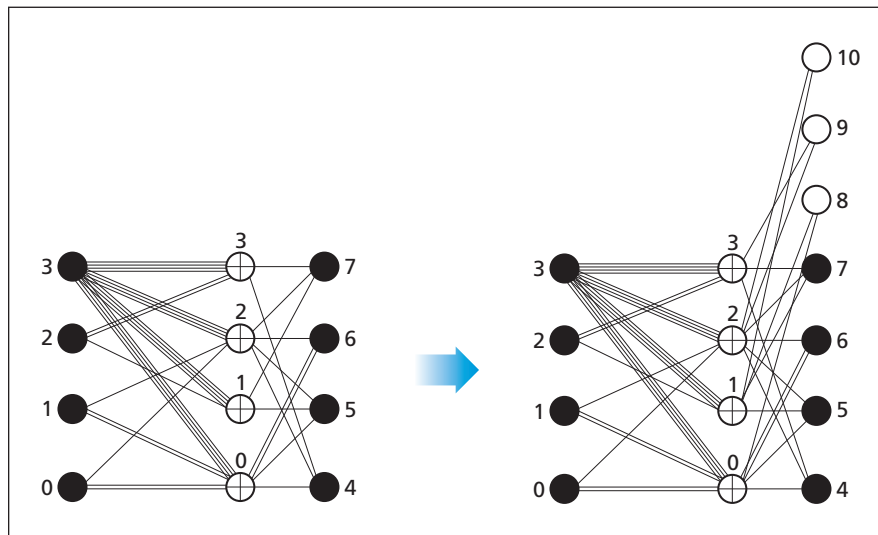
NASA's Jet Propulsion Laboratory, Pasadena, California

A recently developed method of constructing protograph-based low-density parity-check (LDPC) codes provides for low iterative decoding thresholds and minimum distances proportional to block sizes, and can be used for various code rates. A code constructed by this method can have either fixed input block size or fixed output block size and, in either case, provides rate compatibility.

The method comprises two submethods: one for fixed input block size and one for fixed output block size. The first-mentioned submethod is useful for applications in which there are requirements for rate-compatible codes that have fixed input block sizes. These are codes in which only the numbers of parity bits are allowed to vary. The fixed-output-block-size submethod is useful for applications in which framing constraints are imposed on the physical layers of affected communication systems. An example of such a system is one that conforms to one of many new wireless-communication standards that involve the use of orthogonal frequency-division modulation.

Construction of a fixed-input-block-length code according to this method begins with selection of a high-rate protograph LDPC code having variable node degrees of at least 3. Lower-rate codes are obtained by splitting check nodes in the protograph and connecting them with degree-2 variable nodes. Iterative decoding thresholds are calculated for each protograph by using the reciprocal channel approximation. Thresholds are lowered by use of either precoding or one very-high-degree node in the base protograph.

It has been proven that this construction guarantees that the linear-minimum-distance property (the proportionality of minimum distance to block size) is preserved for the lower-rate codes. It has been further proven that a sufficient condition for a protograph LDPC code having only transmitted variable nodes of degree-2 and higher to have linear minimum distance is that, in each connected subgraph of degree-2 variable nodes and their attached edges and check nodes, the number of check



Starting From an Eight-Node Protograph of rate 1/2 that contains seven nodes of degree 3 and one node of degree 16, one can construct codes having rates of 5/8, 3/4, and 7/8.

nodes strictly exceeds the number of variable nodes.

To construct fixed-output-block-length codes, one uses degree-2 punctured nodes to merge pairs of check nodes in a low-rate base protograph, and thereby form higher-rate codes. The linear-minimum-distance property is preserved for higher code rates, provided that the base protograph has variable node degrees of at least 3.

The figure presents an example of such a construction, starting with a rate-1/2 base protograph and inserting three punctured degree-2 variables nodes to merge three different pairs of check nodes. The protograph resulting from these three check node mergers has rate 7/8. To achieve rate 3/4, simply force one of the inserted variable nodes (#10 in the figure) to bit value 0. To achieve rate 5/8, force two of the new variable nodes (#9, #10) to bit value 0. For rate 1/2, force all three of the new variable nodes to bit value 0. The decoder assigns (infinitely) high reliability to those punctured nodes forced to bit value 0, and zero reliability to the punctured nodes not forced to bit value 0

Iterative decoding thresholds for the rate-compatible family of codes in the figure exceed the corresponding rate-

dependent capacity limits by only 0.43 dB, 0.48 dB, 0.30 dB, and 0.21 dB, for rates 1/2, 5/8, 3/4, 7/8, respectively. Additional rate-1/2 base protographs with variable node degrees at least 3 have been designed with iterative decoding thresholds within 0.36 dB of the capacity limit, about 0.2 dB better than the thresholds achieved by the best-known unstructured irregular LDPC codes satisfying the same constraint. Rate-compatible families constructed by this method from any such base protograph will preserve the linear minimum distance property.

This work was done by Dariush Divsalar, Christopher Jones, and Samuel Dolinar of Caltech for NASA's Jet Propulsion Laboratory.

In accordance with Public Law 96-517, the contractor has elected to retain title to this invention. Inquiries concerning rights for its commercial use should be addressed to:

Innovative Technology Assets Management
JPL

Mail Stop 202-233
4800 Oak Grove Drive
Pasadena, CA 91109-8099
(818) 354-2240

E-mail: iaoffice@jpl.nasa.gov

Refer to NPO-43949, volume and number of this NASA Tech Briefs issue, and the page number.

② PrimeSupplier Cross-Program Impact Analysis and Supplier Stability Indicator Simulation Model

This application has potential uses in supply-chain and enterprise-resource planning software.

John F. Kennedy Space Center, Florida

PrimeSupplier, a supplier cross-program and element-impact simulation model, with supplier solvency indicator (SSI), has been developed so that the shuttle program can see early indicators of supplier and product line stability, while identifying the various elements and/or programs that have a particular supplier or product designed into the system. The model calculates two categories of benchmarks to determine the SSI, with one category focusing on agency programmatic data and the other focusing on a supplier's financial liquidity.

To expand further on programmatic data, excessive time gaps between manufacturing, repair, and/or failure analysis requirements [and subsequent purchase orders supporting the logistics purchase requests, established by the project elements through Logistics Supportability Analysis (LSA), which are for flight hardware (personal property) only] focus on hardware mean-time-between failure, manufacturing lead time, quantity per assembly, and system effectiveness. Procurement minimum buy quantities, Federal Acquisition Regulations (FARs), and International Traffic and Arms Regulation (ITAR) also influence, and sometimes extend, this time-gap exposure for manufacturing product, thus leaving the supplier and subse-

quent second- and third-tier suppliers vulnerable to financial instability. This results in either poor product quality, or in a supplier-induced product discontinuance.

To understand this time-gap exposure, the last supplier product or service requirement need date, and first expected need dates, are documented in number of days for all three supplier offerings of manufacturing, repair, or failure analysis. Each functional capability of manufacturing, repair, and failure analysis is weighted slightly differently, with manufacturing having a heavier weight than repair, and repair would have a heavier weight than failure analysis.

The programmatic data feeding into the weighting calculations are collected from internal logistics support analysis data, like Line Replaceable Unit Probability of Sufficiency (LRUPOS), mean-time-between-failure, and repair generation rate forecasts, as well as last supplier capability need dates and first capability need dates that are all reported from the NASA project elements to the Program Office. Supplier capabilities include: manufacturing, repair and sustaining engineering, failure analysis and tear-down, and test and evaluation. Other programmatic weighting factors include: procurement data, contract value, a supplier's percentage distribution of NASA business, and procurement-order

time-gap exposure. The financial benchmarks include liquidity performance measures, such as net profit margin, current ratio (current assets over current liabilities), and price earnings ratio. These financial indicators are all compared against industry standards with various business-centric weighting factors, and could be automated with a real-time data feed.

PrimeSupplier was developed to help NASA smoothly transition design, manufacturing, and repair operations from the Shuttle program to the Constellation program, without disruption in the industrial supply base. Complicating this effort are today's economic conditions that have created unprecedented volatility within the country's industrial supply base, negatively affecting quality and ability to deliver. PrimeSupplier helps organizations identify at-risk suppliers by providing a holistic assessment of suppliers' total economic stability accounting for programmatic and enterprise-wide demands and general economic conditions.

This work was done by Michael Galluzzi of Kennedy Space Center. Learn more about PrimeSupplier at <http://www.fuentek.com/technologies/Primesupplier.htm>. For more information, please contact Karen Hiser at (919) 622-9995 (ksc13185@fuentek.com) or Pasquale Ferrari at (321) 867-4322. KSC-13185

② Integrated Planning for Telepresence With Time Delays

An artificial-intelligence assistant helps a human supervisor control a distant robot.

NASA's Jet Propulsion Laboratory, Pasadena, California

A conceptual "intelligent assistant" and an artificial-intelligence computer program that implements the intelligent assistant have been developed to improve control exerted by a human supervisor over a robot that is so distant that communication between the human and the robot involves significant signal-propagation delays. The goal of the effort is not only to help the human supervisor monitor and control the state of the robot, but also to improve the efficiency

of the robot by allowing the supervisor to "work ahead." The intelligent assistant is an integrated combination of an artificial-intelligence planner and a monitor of states of both the human supervisor and the remote robot. The novelty of the system lies in the way it uses the planner to reason about the states at both ends of the time delay.

To enable the human supervisor to work ahead of the robot, the planner and executive parts of the artificial-intelli-

gence system must comprehend that execution of a task becomes split into two stages: that of the "leader" (the human supervisor) and that of the "follower" (the robot). Although a task is not truly complete until done by both the leader and the follower, it is nevertheless essential for the planner and executive parts of the artificial-intelligence system to work on the assumption that the follower will indeed follow, until this assumption is violated. Violations can occur (1) when the human

supervisor intentionally or unintentionally deviates from activities previously planned in coordination with robot activities directed toward a goal, (2) the robot fails to execute a command as directed or fails to do anything else required of it within a maximum allowable time, or (3) the robot environment changes or is progressively revealed to be significantly different from what was previously assumed.

The planner part of the intelligent assistant must respond gracefully to such violations and notify the human supervisor. Graceful response must include re-planning, for which it is necessary to cause the state model to revert to the

most recent known state of the robot. In re-planning, it is also necessary to recognize which goals have been reached so as not to again expand and schedule the constituent tasks involved in reaching those goals.

The purpose served by the assistant is to provide advice to the human supervisor about current and future activities, derived from a sequence of high-level goals to be achieved. To do this, the assistant must simultaneously monitor and react to various data sources, including (1) actions taken by the supervisor, including commands being issued by the supervisor to the robot; (2) actions

taken by the robot as reported with delay; (3) the environment of the robot as currently perceived with time delay; and (4) the current sequence of goals. As any of these change, the assistant must respond appropriately, detecting both normal completion of tasks and exceptional conditions.

This work was done by Mark Johnston and Kenneth Rabe of Caltech for NASA's Jet Propulsion Laboratory.

The software used in this innovation is available for commercial licensing. Please contact Kavina Edmonds of the California Institute of Technology at (626) 395-2322. Refer to NPO-43520.

Σ Minimizing Input-to-Output Latency in Virtual Environment

Ames Research Center, Moffett Field, California

A method and apparatus were developed to minimize latency (time delay) in virtual environment (VE) and other discrete-time computer-based systems that require real-time display in response to sensor inputs. Latency in such systems is due to the sum of the finite time required for information processing and communication within and between sensors, software, and displays. Even though the latencies intrinsic to each individual hardware, software, and communication component can be minimized (or theoretically eliminated) by speeding up internal computation and transmission

speeds, time delays due to the integration of the overall system will persist. These "integration" delays arise when data produced or processed by earlier components or stages in a system pathway sit idle, waiting to be accessed by subsequent components. Such idle times can be sizeable when compared with latency of individual system components and can also be variable in duration because of insufficient synchrony between events in the data path. This development is intended specifically to reduce the magnitude and variability of idle-time type delays and thus enable the

minimization and stabilization of overall latency in the complete VE (or other computer) system.

This work was done by Bernard D. Adelstein and Stephen R. Ellis of Ames Research Center and Michael I. Hill of San Jose State University Foundation. Further information is contained in a TSP (see page 1).

This invention is owned by NASA and a patent application has been filed. Inquiries concerning rights for the commercial use of this invention should be addressed to the Ames Technology Partnerships Division at (650) 604-5761. Refer to ARC-15102-1.



Books & Reports

Battery Cell Voltage Sensing and Balancing Using Addressable Transformers

A document discusses the use of saturating transformers in a matrix arrangement to address individual cells in a high-voltage battery. This arrangement is able to monitor and charge individual cells while limiting the complexity of circuitry in the battery. The arrangement has inherent galvanic isolation, low cell leakage currents, and allows a single bad cell in a battery of several hundred cells to be easily spotted.

The system is divided up into the battery cell array, the monitoring array, and the battery voltage sensing and balancing system. The battery cell array is the parallel/series connection of cells that store electrical energy. The monitoring array is the set of diodes, transformer cores, and interconnecting wires that allow the voltages of individual cells to be measured, and for the small amounts of charge to be put in individual cells as desired. In the battery voltage sensing and balancing system, the circuitry connects to the monitoring array and provides the pulses to do sensing and charging. It is separate from any main charge system. Electrical isolation is intrinsic to the design and there is no fusing necessary on sense wires.

Maximum array size is set by wire resistance and parasitic inductances in the sense winding loop that would cause

waveform degradation. In practice, an array of several hundred cells could be monitored. Charge current is limited to a few hundred milliamperes, suitable for balancing cells after a main charge system is complete. Measurement accuracy is limited by leakage inductance in the cell/diode/core loop as well as in the sense winding loop. The length of the cable between the battery and the control electronics is limited by series resistance in the cable as well as inductance that degrades the shape of the measurement pulses.

This work was done by Francis Davies of Johnson Space Center. Further information is contained in a TSP (see page 1).

This invention is owned by NASA, and a patent application has been filed. Inquiries concerning nonexclusive or exclusive license for its commercial development should be addressed to the Patent Counsel, Johnson Space Center, (281) 483-1003. Refer to MSC-24466-1.

Gaussian and Lognormal Models of Hurricane Gust Factors

A document describes a tool that predicts the likelihood of land-falling tropical storms and hurricanes exceeding specified peak speeds, given the mean wind speed at various heights of up to 500 feet (150 meters) above ground level. Empirical models to calculate mean and standard deviation of the gust

factor as a function of height and mean wind speed were developed in Excel based on data from previous hurricanes. Separate models were developed for Gaussian and offset lognormal distributions for the gust factor. Rather than forecasting a single, specific peak wind speed, this tool provides a probability of exceeding a specified value. This probability is provided as a function of height, allowing it to be applied at a height appropriate for tall structures.

The user inputs the mean wind speed, height, and operational threshold. The tool produces the probability from each model that the given threshold will be exceeded. This application does have its limits. They were tested only in tropical storm conditions associated with the periphery of hurricanes. Winds of similar speed produced by non-tropical system may have different turbulence dynamics and stability, which may change those winds' statistical characteristics.

These models were developed along the Central Florida seacoast, and their results may not accurately extrapolate to inland areas, or even to coastal sites that are different from those used to build the models. Although this tool cannot be generalized for use in different environments, its methodology could be applied to those locations to develop a similar tool tuned to local conditions.

This work was done by Frank Merceret of Kennedy Space Center. Further information is contained in a TSP (see page 1).KSC-13347



▶ Simulation of Attitude and Trajectory Dynamics and Control of Multiple Spacecraft

Goddard Space Flight Center, Greenbelt, Maryland

Agora software is a simulation of spacecraft attitude and orbit dynamics. It supports spacecraft models composed of multiple rigid bodies or flexible structural models. Agora simulates multiple spacecraft simultaneously, supporting rendezvous, proximity operations, and precision formation flying studies. The Agora environment includes ephemerides for all planets and major moons in the solar system, supporting design studies for deep space as well as geocentric missions. The environment also contains standard models for gravity, atmospheric density, and magnetic fields. Disturbance force and torque models include aerodynamic, gravity-gradient, solar radiation pressure, and “third-body” gravitation. In addition

to the dynamic and environmental models, Agora supports geometrical visualization through an OpenGL interface.

Prototype models are provided for common sensors, actuators, and control laws. A clean interface accommodates linking in actual flight code in place of the prototype control laws. The same simulation may be used for rapid feasibility studies, and then used for flight software validation as the design matures.

Agora is open-source and portable across computing platforms, making it customizable and extensible. It is written to support the entire GNC (guidance, navigation, and control) design cycle, from rapid prototyping and design analysis, to high-fidelity flight code verification.

As a top-down design, Agora is intended to accommodate a large range of missions, anywhere in the solar system. Both “two-body” and “three-body” flight regimes are supported, as well as seamless transition between them. Multiple spacecraft may be simultaneously simulated, enabling simulation of rendezvous scenarios, as well as formation flying. Built-in reference frames and orbit perturbation dynamics provide accurate modeling of precision formation control.

This work was done by Eric T. Stoneking of Goddard Space Flight Center. For further information, contact the Goddard Innovative Partnerships Office at (301) 286-5810. GSC-15737-1

▶ Integrated Modeling of Spacecraft Touch-And-Go Sampling

NASA’s Jet Propulsion Laboratory, Pasadena, California

An integrated modeling tool has been developed to include multi-body dynamics, orbital dynamics, and touch-and-go dynamics for spacecraft covering three types of end-effectors: a sticky pad, a brush-wheel sampler, and a pellet gun.

Several multi-body models of a free-flying spacecraft with a multi-link manipulator driving these end-effectors have been tested with typical contact conditions arising when the manipulator arm is to sample the surface of an asteroidal body. The test data have been infused directly into the dynamics formulation including such information as the mass collected as a

function of end-effector longitudinal speed for the brush-wheel and sticky-pad samplers, and the mass collected as a function of projectile speed for the pellet gun sampler. These data represent the realistic behavior of the end effector while in contact with a surface, and represent a low-order model of more complex contact conditions that otherwise would have to be simulated. Numerical results demonstrate the adequacy of these multi-body models for spacecraft and manipulator-arm control design.

The work contributes to the development of a touch-and-go testbed for small-

body exploration, denoted as the GREX Testbed (GN&C for Rendezvous-based EXploration). The GREX testbed addresses the key issues involved in landing on an asteroidal body or comet; namely, a complex, low-gravity field; partially known terrain properties; possible comet outgassing; dust ejection; and navigating to a safe and scientifically desirable zone.

This program was written by Marco Quadrelli of Caltech for NASA’s Jet Propulsion Laboratory.

This software is available for commercial licensing. Please contact Karina Edmonds of the California Institute of Technology at (626) 395-2322. Refer to NPO-44371.

▶ Spacecraft Station-Keeping Trajectory and Mission Design Tools

NASA’s Jet Propulsion Laboratory, Pasadena, California

Two tools were developed for designing station-keeping trajectories and estimating delta-v requirements for designing missions to a small body such as a comet or asteroid. This innovation uses NPOPT, a non-sparse, general-purpose sequential

quadratic programming (SQP) optimizer and the Two-Level Differential Corrector (TLDC) in LTool (Libration point mission design Tool) to design three kinds of station-keeping scripts: vertical hovering, horizontal hovering, and orbiting.

The TLDC is used to differentially correct several trajectory legs that join hovering points. In a vertical hovering, the maximum and minimum range points must be connected smoothly while maintaining the spacecraft’s range from a

small body, all within the law of gravity and the solar radiation pressure. The same is true for a horizontal hover. A PatchPoint is an LTool class that denotes a space-time event with some extra information for differential correction, including a set of constraints to be satisfied by TLDC. Given a set of PatchPoints, each with its own constraint, the TLDC differentially corrects the entire trajectory by connecting each trajectory leg joined by PatchPoints while satisfying all specified constraints at the same time.

Vertical and horizontal hover both are needed to minimize delta-v spent

for station keeping. A Python I/F to NPOPT has been written to be used from an LTool script. In vertical hovering, the spacecraft stays along the line joining the Sun and a small body. An instantaneous delta-v toward the anti-Sun direction is applied at the closest approach to the small body for station keeping. For example, the spacecraft hovers between the minimum range (2 km) point and the maximum range (2.5 km) point from the asteroid 1989ML. Horizontal hovering buys more time for a spacecraft to recover if, for any reason, a planned thrust fails,

by returning almost to the initial position after some time later via a near elliptical orbit around the small body. The mapping or staging orbit may be similarly generated using TLDC with a set of constraints. Some delta-v tables are generated for several different asteroid masses.

This work was done by Min-Kun J. Chung of Caltech for NASA's Jet Propulsion Laboratory.

This software is available for commercial licensing. Please contact Karina Edmonds of the California Institute of Technology at (626) 395-2322. Refer to NPO-44452.

Efficient Model-Based Diagnosis Engine

A system as large as several thousand components can be diagnosed efficiently.

NASA's Jet Propulsion Laboratory, Pasadena, California

An efficient diagnosis engine — a combination of mathematical models and algorithms — has been developed for identifying faulty components in a possibly complex engineering system. This model-based diagnosis engine embodies a twofold approach to reducing, relative to prior model-based diagnosis engines, the amount of computation needed to perform a thorough, accurate diagnosis. The first part of the approach involves a reconstruction of the general diagnostic engine to reduce the complexity of the mathematical-model calculations and of the software needed to perform them. The second part of the approach involves algorithms for computing a minimal diagnosis (the term “minimal diagnosis” is defined below).

A somewhat lengthy background discussion is prerequisite to a meaningful summary of the innovative aspects of the present efficient model-based diagnosis engine. In model-based diagnosis, the function of each component and the relationships among all the components of the engineering system to be diagnosed are represented as a logical system denoted the system description (SD). Hence, the expected normal behavior of the engineering system is the set of logical consequences of the SD. Faulty components lead to inconsistencies between the observed behaviors of the system and the SD (see figure). Diagnosis — the task of finding faulty components — is reduced to finding those components, the abnormalities of which could explain all the inconsistencies. The solution of the diagnosis problem should be

a minimal diagnosis, which is a minimal set of faulty components. A minimal diagnosis stands in contradistinction to the trivial solution, in which all components are deemed to be faulty, and which, therefore, always explains all inconsistencies.

The general diagnosis engine (GDE) is widely used in the discipline of automated diagnosis. The GDE combines a model of each component of an engineering system with observations of the actual behavior of the component to detect discrepancies and diagnose root causes. The GDE uses an inference engine to compute the consequences of observations and uses an assumption-based truth maintenance system (ATMS) to manage the assumptions underlying each computation. One of the side effects of managing the assumptions is the detection of inconsistent sets of assumptions, which leads to conflict sets used in calculating minimal diagnoses. Unfortunately the GDE has two major limitations:

- The combination of the inference engine and ATMS must be represented by software that is so complex that the use of the GDE is too difficult and impractical for many complex engineering systems.
- The calculation of a minimal diagnosis is inherently a hard problem. Using typical prior algorithms, the conversion from conflict sets to a minimal diagnosis requires amounts of computation time and memory that increase exponentially with the number of components of the engineering system.

This concludes the background discussion.

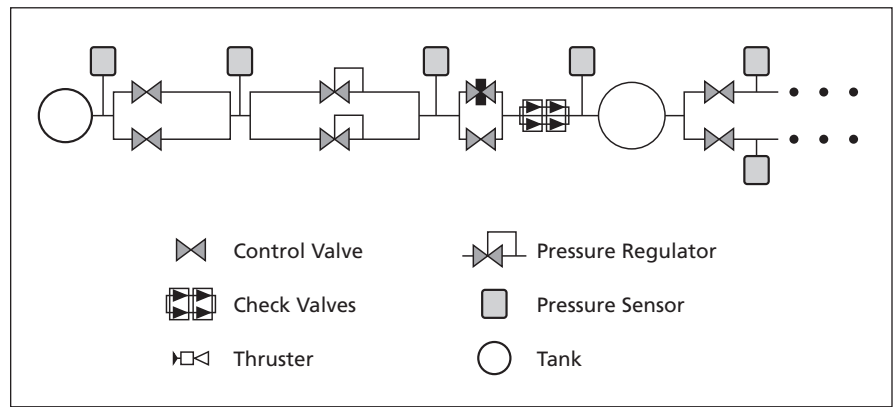
In the present efficient model-based diagnosis engine, the first-mentioned limitation of the GDE is overcome by the reconstructed general diagnostic engine (RGDE). Like the GDE, the RGDE combines a model of each component of an engineering system (represented graphically as a network) with observations of the actual behavior of the component to detect discrepancies and diagnose root causes. Also like the GDE, the RGDE performs a causal simulation by taking variable observations and using rules to compute the values of other variables in the network.

Although assumptions underly the computations in the RGDE as in the GDE, the RGDE does not include an ATMS. Instead, taking advantage of the discovery that the ATMS and the inference engine have many similarities, the RGDE combines the ATMS with the inference engine to simplify the diagnosis-engine algorithm and the software that implements it. In this approach, the value of each variable is tagged with the set of assumptions that contribute to its computation. This set of tags comprises the collective union of the tags of values that feed into the computation with a tag representing the computation itself. A discrepancy arises when two incompatible values are assigned to the same variable. In general, whenever the RGDE computes two incompatible values for the same variable, the union of the two supporting assumption sets is incompatible; that is, it is a conflict set. Typically in the course of causal simulation, no discrep-

ancies are found, but when failures occur, multiple incompatible assumption sets appear. This process continues to determine new incompatible sets until the causal simulation is completed.

The second-mentioned limitation of the GDE is overcome by a combination of two methods, embodied in algorithms that, relative to prior algorithms used for the same purpose, require less computation to arrive at a minimal diagnosis. These methods and algorithms were described in “Fast Algorithms for Model-Based Diagnosis” (NPO-30582) and “Two Methods of Efficient Solution of the Hitting-Set Problem” (NPO-30584), both published in *NASA Tech Briefs*, Vol. 29, No. 3, March 2005, pages 69 and 74, respectively. To recapitulate: One of the two improved methods is based on mapping of the diagnosis problem onto the Boolean satisfiability problem. This mapping makes it possible to utilize Boolean function theory to reduce the diagnosis problem to the prime-implicant problem (one of the problems in the theory). This, in turn, makes it possible to utilize very efficient algorithms, developed previously for the satisfiability problem, to compute the minimal diagnosis. The algorithm thus developed to solve the diagnosis problem requires an amount of computation proportional to a superpolynomial function of n (meaning that the computation time is proportional to $n^{ln(n)}$), where n is the number of components of the engineering system.

The other improved method is based on the mapping of the diagnosis prob-



A Relatively Simple Engineering System of tanks, valves, pipes, and pressure sensors serves to illustrate the basic diagnostic principle. This system would be diagnosed by comparing actual and expected values of pressure-sensor readings as correlated with commanded openings and closings of the valves.

lem onto the integer-programming problem. This mapping makes it possible to utilize a variety of algorithms developed previously for integer programming to solve the diagnosis problem. In the integer-programming approach, the diagnosis problem can be formulated as a linear integer optimization problem, which can be solved by use of well-developed integer-programming algorithms. Some of these algorithms, modified to make them suitable for solving the diagnosis problem, can efficiently diagnose a system that contains as many as several thousand components.

The development of this efficient model-based diagnosis engine has been accompanied by the derivation of a deep matrix analysis of the integer programming problem that makes it possible to extract bounds for the sizes of the solutions of the optimization problem, without solving the problem explicitly. This

analysis could be helpful in the development of algorithms that would be much more efficient for solving specific problems.

This work was done by Amir Fijany, Farrokh Vatan, Anthony Barrett, Mark James, Ryan Mackey, and Colin Williams of Caltech for NASA's Jet Propulsion Laboratory. Further information is contained in a TSP (see page 1).

In accordance with Public Law 96-517, the contractor has elected to retain title to this invention. Inquiries concerning rights for its commercial use should be addressed to:

*Innovative Technology Assets Management
JPL*

*Mail Stop 202-233
4800 Oak Grove Drive
Pasadena, CA 91109-8099*

E-mail: iaoffice@jpl.nasa.gov

Refer to NPO-40544, volume and number of this NASA Tech Briefs issue, and the page number.

DSN Simulator

NASA's Jet Propulsion Laboratory, Pasadena, California

The DSN Simulator (wherein “DSN” signifies NASA’s Deep Space Network) is an updated version of the software described in “DSN Array Simulator” (NPO-44506), *Software Tech Briefs* (Special supplement to *NASA Tech Briefs*), Vol. 32, No. 9 (September 2008), page 26. To recapitulate: This software is used for computational modeling of proposed DSN facilities comprising arrays of antennas and transmitting and receiving equipment for microwave communication with spacecraft on interplanetary missions. Such modeling is performed to estimate facility performance, evaluate require-

ments that govern facility design, and evaluate proposed improvements in hardware and/or software. The software includes a Monte Carlo simulation component that enables rapid generation of key mission-set metrics (e.g., numbers of links, data rates, and data volumes), and statistical distributions thereof as functions of time.

The prior version of the software could model only one DSN facility at a time and included hard-coded, unconfigurable metrics. The present updated version is capable of modeling the entire DSN and provides for configurable met-

rics, making it possible to perform loading analyses for alternative future DSN architectures and mission-set scenarios. The present version also features an improved user interface and interfaces for exchange of data with other DSN software and with a DSN mission model database.

This program was written by Ryan M. Mackey and Raffi P. Tikidjian of Caltech for NASA's Jet Propulsion Laboratory.

This software is available for commercial licensing. Please contact Karina Edmonds of the California Institute of Technology at (626) 395-2322. Refer to NPO-45513.

Proton Upset Monte Carlo Simulation

Lyndon B. Johnson Space Center, Houston, Texas

The Proton Upset Monte Carlo Simulation (PROPSET) program calculates the frequency of on-orbit upsets in computer chips (for given orbits such as Low Earth Orbit, Lunar Orbit, and the like) from proton bombardment based on the results of heavy ion testing alone. The software simulates the bombardment of modern microelectronic components (computer chips) with high-energy (≈ 200 MeV) protons. The nuclear interaction of the proton with the silicon of the chip is modeled and nuclear fragments from this interaction are tracked using Monte Carlo techniques to produce statistically accurate predictions.

Following the bombardment with high-energy heavy ions (such as carbon,

gold, and the like), the upset rate dependency on each of the ion species is known. This precisely defines the amount of energy an ion must deposit within the “sensitive volume” of the chip in order to cause an upset. These data are put through PROPSET, which repeatedly models the proton/silicon collision process and tracks each of these fragments from each collision and the energy that each imparts into the “sensitive volume” of the chip. PROPSET then counts the number of upsets produced by a given number of incident protons.

This innovation allows for the code to be easily modified so that the effect of input parameters, such as the thickness

and shape of a computer chip’s sensitive volume, can be assessed. Heavy ion data are easily entered in terms of only four Weibull parameters rather than a data file of 50 to 100 data pairs. In order to determine how to track ions through a chip’s sensitive volume while accounting for the variability of that sensitivity, a grid is defined and works outward where each shell has a different sensitivity. PROPSET executes rapidly on a personal computer.

This program was written by Patrick M. O’Neill and Coy K. Kouba of Johnson Space Center and Charles C. Foster of Foster Consulting Services. Further information is contained in a TSP (see page 1). MSC-24274-1

FPGA Boot Loader and Scrubber

Lyndon B. Johnson Space Center, Houston, Texas

A computer program loads configuration code into a Xilinx field-programmable gate array (FPGA), reads back and verifies that code, reloads the code if an error is detected, and monitors the performance of the FPGA for errors in the presence of radiation. The program consists mainly of a set of VHDL files (wherein “VHDL” signifies “VHSIC Hardware Description Language” and “VHSIC” signifies “very-high-speed integrated circuit”).

The first of three parts of the program loads the configuration code from a flash memory device by means of an industry-standard interface. The second part continuously reads back the configuration data stream through the interface, calculates a cyclic redundancy code (CRC) on the data, and compares the calculated CRC values with values stored in the flash memory device. If the calculated CRC values do not match the stored values, the configuration data memory is cleared and

the configuration data are reloaded. The third part of the program implements a watchdog register, to which the FPGA is required to write at regular intervals. If the FPGA fails to write to the register within a required time, the configuration memory is cleared and the configuration data are reloaded.

This program was written by Randall S. Wade of Johnson Space Center and Bailey Jones of Jacobs Sverdrup. Further information is contained in a TSP (see page 1). MSC-24124-1

Using Thermal Radiation in Detection of Negative Obstacles

At night, negative obstacles usually appear bright in infrared images.

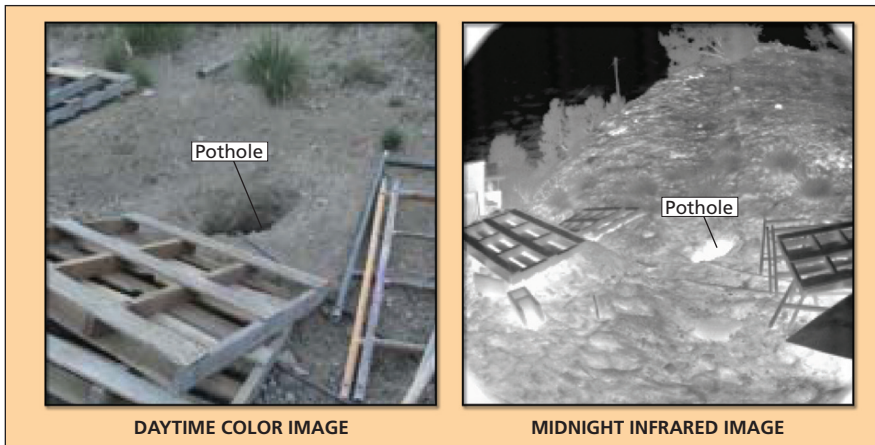
NASA’s Jet Propulsion Laboratory, Pasadena, California

A method of automated detection of negative obstacles (potholes, ditches, and the like) ahead of ground vehicles at night involves processing of imagery from thermal-infrared cameras aimed at the terrain ahead of the vehicles. The method is being developed as part of an overall obstacle-avoidance scheme for autonomous and semi-autonomous off-road robotic vehicles. The method could also be applied to help human drivers of cars and trucks avoid negative obstacles — a development that may entail only modest additional cost inas-

much as some commercially available passenger cars are already equipped with infrared cameras as aids for nighttime operation.

The need for this or an alternative method arises because the geometric nature of negative obstacles makes it difficult to detect them by processing of geometric information extracted from ordinary images: As drivers of ground vehicles know from common experience, it is difficult to visually detect negative obstacles in sufficient time to avoid them, making it necessary

to drive slowly enough to be able to stop or swerve within the limited safe look-ahead/stopping distance. In robotic vehicles equipped with stereoscopic machine vision or lidar systems that yield range and elevation data, obstacles are detected through analysis of those data, and essentially the same difficulty arises. The source of the difficulty is the fact that whereas the angle subtended by a positive obstacle is approximately inversely proportional to the horizontal distance, the angle subtended by a negative obstacle is ap-



A **Pothole Dug at a Construction Site** looks dark in a daytime image in visible light but looks bright in an infrared image acquired at midnight.

proximately inversely proportional to the square of the horizontal distance.

The method involves exploitation of the fact that throughout the night, negative obstacles are usually warmer than the surrounding terrain. Therefore, in in-

frared terrain images acquired at night, negative obstacles usually appear brighter than the surrounding terrain (see figure). (During the day, the negative obstacles can be warmer or cooler than their surroundings, depending on sky condi-

tions and the apparent position of the Sun.) At the present state of development, the method is embodied in a rudimentary algorithm that processes a combination of infrared imagery and range-versus-elevation data. The algorithm identifies candidate negative obstacles in the form of infrared bright spots on the terrain, then performs simple geometric tests to confirm or reject the candidate negative obstacles. The algorithm has been shown to be sufficient for initial proof-of-concept demonstrations. Further development of this or an improved algorithm will be necessary to enable reliable detection of negative obstacles under a variety of conditions.

This work was done by Arturo L. Rankin and Larry H. Matthies of Caltech for NASA's Jet Propulsion Laboratory.

The software used in this innovation is available for commercial licensing. Please contact Karina Edmonds of the California Institute of Technology at (626) 395-2322. Refer to NPO-40368.

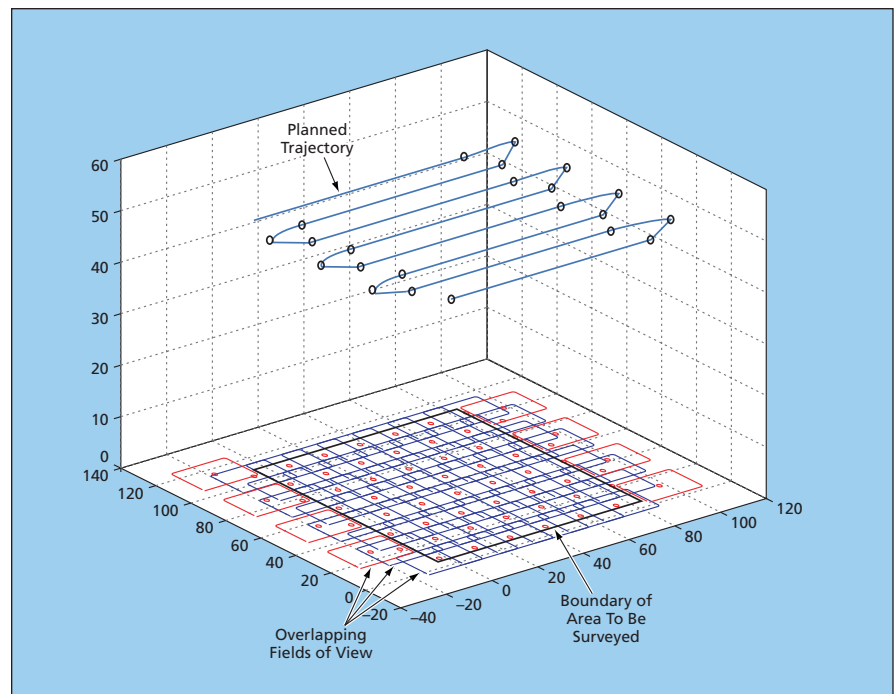
⚙️ Planning Flight Paths of Autonomous Aerobots

Trajectories are planned to satisfy survey coverage requirements without violating dynamical constraints.

NASA's Jet Propulsion Laboratory, Pasadena, California

Algorithms for planning flight paths of autonomous aerobots (robotic blimps) to be deployed in scientific exploration of remote planets are undergoing development. These algorithms are also adaptable to terrestrial applications involving robotic submarines as well as aerobots and other autonomous aircraft used to acquire scientific data or to perform surveying or monitoring functions.

These algorithms are built on a number of previously developed algorithms for planning optimal trajectories in two- and three-dimensional spaces. As used here, "optimal" could have any of a variety of different meanings. For example, "optimal" could be used to characterize a trajectory that passes through a set of waypoints specified by a user and that satisfies a minimum-length or a minimum-time criterion while also remaining within limits posed by dynamical and resource constraints. The present algorithms can also satisfy a requirement that the trajectory suffice to enable the field of view of camera aboard an aerobot to sweep all of a specified ground area to be surveyed (see figure).



This **Raster-Scan Trajectory** was calculated to enable surveying, from a fixed altitude, of a defined rectangular area by use of a camera having a rectangular field of view. First, the survey area was mapped using successive fields of view that were required to overlap by 35 percent in length and/or width. Then the centers of the successive fields of view were designated as waypoints. Finally, the waypoints were used to generate the trajectory.

A navigation software system that implements these algorithms generates a simple graphical user interface, through which the user can specify either waypoints in two or three dimensions or the ground area to be surveyed. Alternatively, the user can load a data file containing waypoint coordinates. The user can also specify other parameters that affect the planned trajectory, including the field of view of the camera and the dynamical parameters, the primary one being the minimum allowable turn radius of the aero-

bot. Then assuming constant airspeed, the algorithms compute a minimum-time or minimum-length trajectory that takes account of all of the aforementioned requirements and constraints. Notably, in one of the algorithms, the turning dynamics of the aerobot are represented by a cubic spline that is used to interpolate the trajectory between waypoints.

In some contemplated future versions, the need for intervention by human users would be reduced: Waypoints specified by users could be sup-

planted by data generated by onboard artificial-intelligence image-data-processing systems programmed to strive to satisfy mission specifications.

This work was done by Eric Kulczykcki and Alberto Elfes of Caltech and Shivanjli Sharma of University of California at Davis for NASA's Jet Propulsion Laboratory.

The software used in this innovation is available for commercial licensing. Please contact Karina Edmonds of the California Institute of Technology at (626) 395-2322. Refer to NPO-44395.

Cliffbot Maestro

NASA's Jet Propulsion Laboratory, Pasadena, California

Cliffbot Maestro (see figure) permits teleoperation of remote rovers for field testing in extreme environments. The application user interface provides two sets of tools for operations:

stereo image browsing and command generation.

The stereo image-browsing feature allows the operator to see images in either 2D or 3D views. This is useful in order to

develop a route for the rover to safely drive, as well as identify interesting objects for scientific exploration.

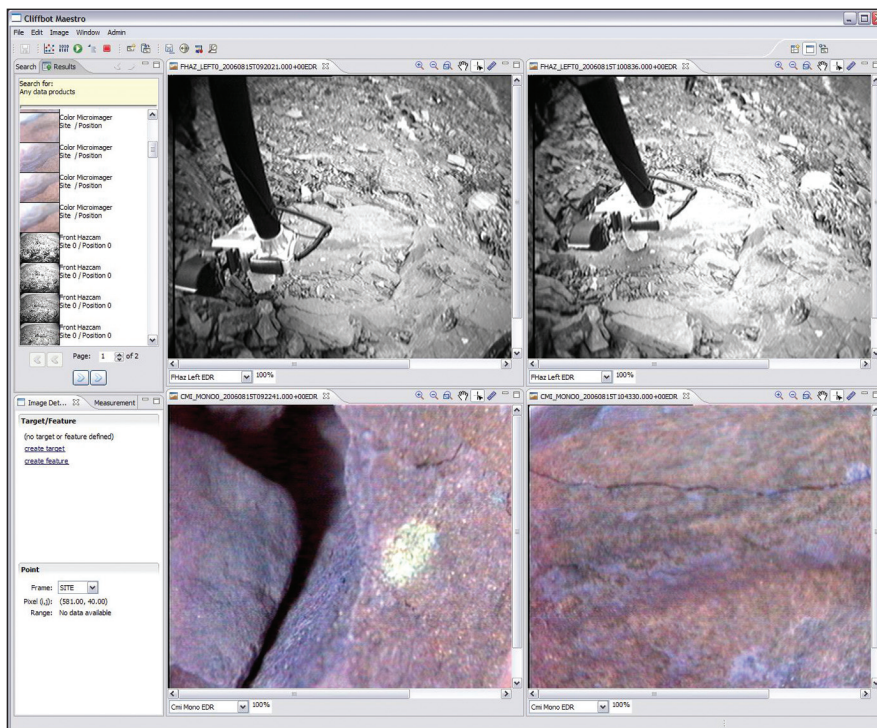
The command-generation tool is used to author a script (using either a drag & drop interface, or a textual command-line one) and send it to the rover. These scripts are not only for driving, but also for sample collection, reconnaissance, imaging, and science data acquisition.

The software runs on dedicated hardware that can withstand extremely cold temperatures. Its test bed is a Panasonic Toughbook (or equivalent) rugged laptop operating in the deep Arctic for extended periods. While the hardware doesn't have to be cutting-edge, it must withstand continued cold.

Cliffbot Maestro also provides engineering metrics about the state of the rover, in order to monitor its health, as well as the condition of the robotic arm. This allows for remote support while in the field.

This work was done by Jeffrey S. Norris, Mark W. Powell, Jason M. Fox, Thomas M. Crockett, and Joseph C. Joswig of Caltech for NASA's Jet Propulsion Laboratory.

This software is available for commercial licensing. Please contact Karina Edmonds of the California Institute of Technology at (626) 395-2322. Refer to NPO-46433.



Cliffbot Maestro User Interfaces.

Tracking Debris Shed by a Space-Shuttle Launch Vehicle

Lyndon B. Johnson Space Center, Houston, Texas

The DEBRIS software predicts the trajectories of debris particles shed by a space-shuttle launch vehicle during ascent, to aid in assessing potential harm to the space-shuttle orbiter and crew. The

user specifies the location of release and other initial conditions for a debris particle. DEBRIS tracks the particle within an overset grid system by means of a computational fluid dynamics (CFD) simulation

of the local flow field and a ballistic simulation that takes account of the mass of the particle and its aerodynamic properties in the flow field. The computed particle trajectory is stored in a file to be post-

processed by other software for viewing and analyzing the trajectory.

DEBRIS supplants a prior debris-tracking code that took ≈ 15 minutes to calculate a single particle trajectory: DEBRIS can calculate 1,000 trajectories in ≈ 20 seconds on a desktop computer.

Other improvements over the prior code include adaptive time-stepping to ensure accuracy, forcing at least one step per grid cell to ensure resolution of all CFD-resolved flow features, ability to simulate rebound of debris from surfaces, extensive error checking, a built-

in suite of test cases, and dynamic allocation of memory.

This program was written by Phillip C. Stuart of Johnson Space Center and Stuart E. Rogers of Ames Research Center. Further information is contained in a TSP (see page 1). MSC-23945-1

Estimating Thruster Impulses From IMU and Doppler Data

NASA's Jet Propulsion Laboratory, Pasadena, California

A computer program implements a thrust impulse measurement (TIM) filter, which processes data on changes in velocity and attitude of a spacecraft to estimate the small impulsive forces and torques exerted by the thrusters of the spacecraft reaction control system (RCS). The velocity-change data are obtained from line-of-sight-velocity data from Doppler measurements made from the Earth. The attitude-change data are telemetered from an inertial measurement unit (IMU) aboard the spacecraft.

The TIM filter estimates the three-axis thrust vector for each RCS thruster, thereby enabling reduction of cumulative navigation error attributable to inaccurate prediction of thrust vectors. The filter has been augmented with a simple mathematical model to compensate for large temperature fluctuations in the spacecraft thruster catalyst bed in order to estimate thrust more accurately at deadbanding "cold-firing" levels. Also, rigorous consider-covariance estimation is applied in the TIM to account for

the expected uncertainty in the moment of inertia and the location of the center of gravity of the spacecraft. The TIM filter was built with, and depends upon, a sigma-point consider-filter algorithm implemented in a Python-language computer program.

This program was written by Michael E. Lisano and Gerhard L. Kruijzinga of Caltech for NASA's Jet Propulsion Laboratory.

This software is available for commercial licensing. Please contact Karina Edmonds of the California Institute of Technology at (626) 395-2322. Refer to NPO-45825.

Oxygen Generation System Laptop Bus Controller Flight Software

Lyndon B. Johnson Space Center, Houston, Texas

The Oxygen Generation System Laptop Bus Controller Flight Software was developed to allow the International Space Station (ISS) program to activate specific components of the Oxygen Generation System (OGS) to perform a checkout of key hardware operation in a microgravity environment, as well as to perform preventative maintenance operations of system valves during a long period of what would otherwise be hardware dormancy. The software provides direct connectivity to the OGS

Firmware Controller with pre-programmed tasks operated by on-orbit astronauts to exercise OGS valves and motors. The software is used to manipulate the pump, separator, and valves to alleviate the concerns of hardware problems due to long-term inactivity and to allow for operational verification of microgravity-sensitive components early enough so that, if problems are found, they can be addressed before the hardware is required for operation on-orbit.

The decision was made to use existing on-orbit IBM ThinkPad A31p laptops and MIL-STD-1553B interface cards as the hardware configuration. The software at the time of this reporting was developed and tested for use under the Windows 2000 Professional operating system to ensure compatibility with the existing on-orbit computer systems.

This program was written by Chad Rowe and Donna Panter for Johnson Space Center. Further information is contained in a TSP (see page 1). MSC-24316-1

Port-O-Sim Object Simulation Application

Goddard Space Flight Center, Greenbelt, Maryland

Port-O-Sim is a software application that supports engineering modeling and simulation of launch-range systems and subsystems, as well as the vehicles that operate on them. It is flexible, distributed, object-oriented, and real-

time. A scripting language is used to configure an array of simulation objects and link them together. The script is contained in a text file, but executed and controlled using a graphical user interface.

A set of modules is defined, each with input variables, output variables, and settings. These engineering models can be either linked to each other or run as standalone. The settings can be modified during execution.

Since 2001, this application has been used for pre-mission failure mode training for many Range Safety Scenarios. It contains range asset link analysis, develops look-angle data, supports sky-screen site selection, drives GPS (Global Positioning System) and IMU (Inertial

Measurement Unit) simulators, and can support conceptual design efforts for multiple flight programs with its capacity for rapid six-degrees-of-freedom model development. Due to the assembly of various object types into one application, the application is applicable

across a wide variety of launch range problem domains.

This work was done by Raymond J. Lanzi of Goddard Space Flight Center. Further information is contained in a TSP (see page 1). GSC-15571-1

Monitoring and Controlling an Underwater Robotic Arm

Lyndon B. Johnson Space Center, Houston, Texas

The SSRMS Module 1 software is part of a system for monitoring an adaptive, closed-loop control of the motions of a robotic arm in NASA's Neutral Buoyancy Laboratory, where buoyancy in a pool of water is used to simulate the weightlessness of outer space. This software is so named because the robot arm is a replica of the Space Shuttle Remote Manipulator System (SSRMS).

This software is distributed, running on remote joint processors (RJPs), each of which is mounted in a hydraulic actu-

ator comprising the joint of the robotic arm and communicating with a pool-side processor denoted the Direct Control Rack (DCR). Each RJP executes the feedback joint-motion control algorithm for its joint and communicates with the DCR. The DCR receives joint-angular-velocity commands either locally from an operator or remotely from computers that simulate the flight like SSRMS and perform coordinated motion calculations based on hand-controller inputs. The received commands are checked for

validity before they are transmitted to the RJPs. The DCR software generates a display of the statuses of the RJPs for the DCR operator and can shut down the hydraulic pump when excessive joint-angle error or failure of a RJP is detected.

This work was done by John Haas and Brian Keith Todd of Johnson Space Center, Larry Woodcock and Fred M. Robinson of Oceaneering Space Systems, and Thomas (Jay) Costales of Raytheon Co. Further information is contained in a TSP (see page 1). MSC-24165-1

Digital Camera Control for Faster Inspection

Lyndon B. Johnson Space Center, Houston, Texas

Digital Camera Control Software (DCCS) is a computer program for controlling a boom and a boom-mounted camera used to inspect the external surface of a space shuttle in orbit around the Earth. Running in a laptop computer in the space-shuttle crew cabin, DCCS commands integrated displays and controls. By means of a simple one-button command, a crewmember can view low-resolution images to quickly spot problem areas and can then cause a rapid transition to high-resolution im-

ages. The crewmember can command that camera settings apply to a specific small area of interest within the field of view of the camera so as to maximize image quality within that area.

DCCS also provides critical high-resolution images to a ground screening team, which analyzes the images to assess damage (if any); in so doing, DCCS enables the team to clear initially suspect areas more quickly than would otherwise be possible and further saves time by minimizing the probability of re-im-

aging of areas already inspected. On the basis of experience with a previous version (2.0) of the software, the present version (3.0) incorporates a number of advanced imaging features that optimize crewmember capability and efficiency.

This program was written by Katharine Brown, James D. Siekierski, Mark L. Mangieri, Kent Dekome, John Cobarruvias, and Perry J. Piplani of Johnson Space Center and Joel Busa of the Draper Laboratory. Further information is contained in a TSP (see page 1). MSC-24319-1/168-1

Reaction Wheel Disturbance Model Extraction Software — RWDMES

Goddard Space Flight Center, Greenbelt, Maryland

The RMDMES is a tool for modeling the disturbances imparted on spacecraft by spinning reaction wheels. Reaction wheels are usually the largest disturbance source on a precision pointing spacecraft, and can be the dominating source of pointing error. Accurate knowledge of the disturbance

environment is critical to accurate prediction of the pointing performance. In the past, it has been difficult to extract an accurate wheel disturbance model since the forcing mechanisms are difficult to model physically, and the forcing amplitudes are filtered by the dynamics of the reaction wheel. RDMES

captures the wheel-induced disturbances using a hybrid physical/empirical model that is extracted directly from measured forcing data.

The empirical models capture the tonal forces that occur at harmonics of the spin rate, and the broadband forces that arise from random effects. The em-

pirical forcing functions are filtered by a physical model of the wheel structure that includes spin-rate-dependent moments (gyroscopic terms). The resulting hybrid model creates a highly accurate prediction of wheel-induced forces. It accounts for variation in disturbance frequency, as well as the shifts in structural amplification by the whirl modes, as the spin rate changes. This software provides a point-and-click environment for producing accurate models with minimal user effort. Where conventional approaches may take weeks to produce a model of variable quality, RWDMES can create a demonstrably high accuracy model in two hours.

The software consists of a graphical user interface (GUI) that enables the user to specify all analysis parameters, to evaluate analysis results and to iteratively refine the model. Underlying algorithms automatically extract disturbance harmonics, initialize and tune harmonic models, and initialize and tune broad-

band noise models. The component steps are described in the RWDMES user's guide and include: converting time domain data to waterfall PSDs (power spectral densities); converting PSDs to order analysis data; extracting harmonics; initializing and simultaneously tuning a harmonic model and a wheel structural model; initializing and tuning a broadband model; and verifying the harmonic/broadband/structural model against the measurement data.

Functional operation is through a MATLAB GUI that loads test data, performs the various analyses, plots evaluation data for assessment and refinement of analysis parameters, and exports the data to documentation or downstream analysis code. The harmonic models are defined as specified functions of frequency, typically speed-squared. The reaction wheel structural model is realized as mass, damping, and stiffness matrices (typically from a finite element analysis package) with the addition of a gyro-

scopic forcing matrix. The broadband noise model is realized as a set of speed-dependent filters. The tuning of the combined model is performed using nonlinear least squares techniques.

RWDMES is implemented as a MATLAB toolbox comprising the Fit Manager for performing the model extraction, Data Manager for managing input data and output models, the Gyro Manager for modifying wheel structural models, and the Harmonic Editor for evaluating and tuning harmonic models. This software was validated using data from Goodrich E wheels, and from GSFC Lunar Reconnaissance Orbiter (LRO) wheels. The validation testing proved that RWDMES has the capability to extract accurate disturbance models from flight reaction wheels with minimal user effort.

This work was done by Carl Blawrock of NightSky Systems, Inc. for Goddard Space Flight Center. Further information is contained in a TSP (see page 1). GSC15401-1

Conical-Domain Model for Estimating GPS Ionospheric Delays

Sources of error in a standard ionospheric delay model are eliminated.

NASA's Jet Propulsion Laboratory, Pasadena, California

The conical-domain model is a computational model, now undergoing development, for estimating ionospheric delays of Global Positioning System (GPS) signals. Relative to the standard ionospheric delay model described below, the conical-domain model offers improved accuracy.

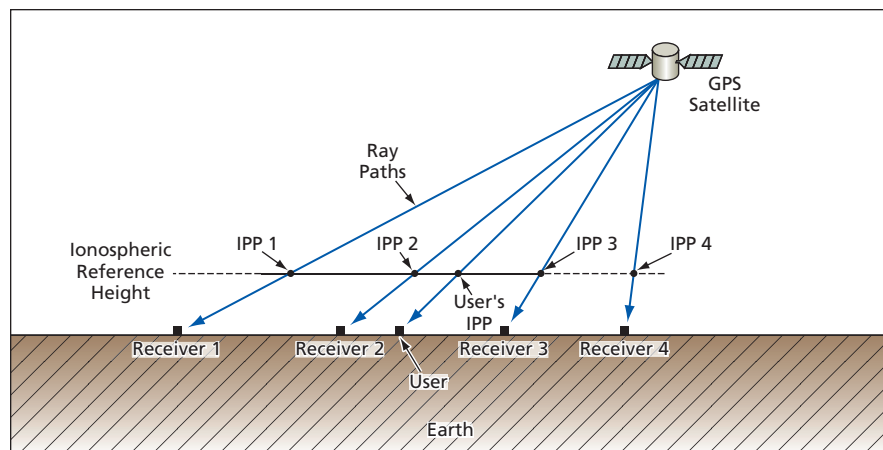
In the absence of selective availability, the ionosphere is the largest source of error for single-frequency users of GPS. Because ionospheric signal delays contribute to errors in GPS position and time measurements, satellite-based augmentation systems (SBASs) have been designed to estimate these delays and broadcast corrections. Several national and international SBASs are currently in various stages of development to enhance the integrity and accuracy of GPS measurements for airline navigation.

In the Wide Area Augmentation System (WAAS) of the United States, slant ionospheric delay errors and confidence bounds are derived from estimates of vertical ionospheric delay modeled on a grid at regularly spaced intervals of latitude and longitude. The estimate of vertical delay at each ionospheric grid point (IGP) is calculated

from a planar fit of neighboring slant delay measurements, projected to vertical using a standard, thin-shell model of the ionosphere. Interpolation on the WAAS grid enables estimation of the vertical delay at the ionospheric pierce point (IPP) corresponding to any arbitrary measurement of a user. (The IPP of a given user's measurement is the point where the GPS signal ray path intersects a reference ionospheric height.) The product of the interpo-

lated value and the user's thin-shell obliquity factor provides an estimate of the user's ionospheric slant delay.

Two types of error that restrict the accuracy of the thin-shell model are absent in the conical domain model: (1) error due to the implicit assumption that the electron density is independent of the azimuthal angle at the IPP and (2) error arising from the slant-to-vertical conversion. At low latitudes or at mid-latitudes under disturbed conditions, the accu-



Multiple GPS Receivers and a GPS Satellite define a conical domain. At locations between receivers, ionospheric slant delays are interpolated by a planar fit model at the ionospheric reference height.

racy of SBAS systems based upon the thin-shell model suffers due to the presence of complex ionospheric structure, high delay values, and large electron density gradients. Interpolation on the vertical delay grid serves as an additional source of delay error.

The conical-domain model permits direct computation of the user's slant delay estimate without the intervening use of a vertical delay grid. The key is to restrict each fit of GPS measurements to a spatial domain encompassing signals from only one satellite. The conical domain model is so named because each fit involves a group of GPS receivers that all receive signals from the same GPS satellite (see figure); the receiver and satellite positions define a cone, the satellite

position being the vertex. A user within a given cone evaluates the delay to the satellite directly, using (1) the IPP coordinates of the line of sight to the satellite and (2) broadcast fit parameters associated with the cone.

The conical-domain model partly resembles the thin-shell model in that both models reduce an inherently four-dimensional problem to two dimensions. However, unlike the thin-shell model, the conical domain model does not involve any potentially erroneous simplifying assumptions about the structure of the ionosphere. In the conical domain model, the initially four-dimensional problem becomes truly two-dimensional in the sense that once a satellite location has been specified, any

signal path emanating from a satellite can be identified by only two coordinates; for example, the IPP coordinates. As a consequence, a user's slant-delay estimate converges to the correct value in the limit that the receivers converge to the user's location (or, equivalently, in the limit that the measurement IPPs converge to the user's IPP).

This work was done by Lawrence Sparks, Attila Komjathy, and Anthony Mannucci of Caltech for NASA's Jet Propulsion Laboratory. Further information is contained in a TSP (see page 1).

The software used in this innovation is available for commercial licensing. Please contact Karina Edmonds of the California Institute of Technology at (626) 395-2322. Refer to NPO-40930.

Evolvable Neural Software System

Goddard Space Flight Center, Greenbelt, Maryland

The Evolvable Neural Software System (ENSS) is composed of sets of Neural Basis Functions (NBFs), which can be totally autonomously created and removed according to the changing needs and requirements of the software system. The resulting structure is both hierarchical and self-similar in that a given set of NBFs may have a ruler NBF, which in turn communicates with other sets of NBFs. These sets of NBFs may function as nodes to a ruler node, which are also NBF constructs. In this manner, the synthetic neural system can exhibit the complexity, three-dimensional connectivity, and adaptability of biological neural systems.

An added advantage of ENSS over a natural neural system is its ability to modify its core genetic code in response to environmental changes as reflected in needs and requirements. The neural system is fully adaptive and evolvable and is trainable before release. It continues to rewire itself while on the job. The NBF is a unique, bi-level intelligence neural system composed of a higher-level heuristic neural system (HNS) and a lower-level, autonomic neural system (ANS). Taken together, the HNS and the ANS give each NBF the complete capabilities of a biological neural system to match sensory inputs to actions.

Another feature of the NBF is the Evolvable Neural Interface (ENI), which

links the HNS and ANS. The ENI solves the interface problem between these two systems by actively adapting and evolving from a primitive initial state (a Neural Thread) to a complicated, operational ENI and successfully adapting to a training sequence of sensory input. This simulates the adaptation of a biological neural system in a developmental phase. Within the greater multi-NBF and multi-node ENSS, self-similar ENI's provide the basis for inter-NBF and inter-node connectivity.

This work was done by Steven A. Curtis of Goddard Space Flight Center. Further information is contained in a TSP (see page 1). GSC-14657-1

Prediction of Launch Vehicle Ignition Overpressure and Ltoff Acoustics

Marshall Space Flight Center, Alabama

The LAIOP (Launch Vehicle Ignition Overpressure and Ltoff Acoustic Environments) program predicts the external pressure environment generated during liftoff for a large variety of rocket types. These environments include ignition overpressure, produced by the rapid acceleration of exhaust gases during rocket-engine start transient, and launch acoustics, produced by turbulence in the rocket plume. The ignition overpressure predictions are time-based,

and the launch acoustic predictions are frequency-based. Additionally, the software can predict ignition overpressure mitigation, using water-spray injection into the rocket exhaust stream, for a limited number of configurations.

The framework developed for these predictions is extensive, though some options require additional relevant data and development time. Once these options are enabled, the already extensively capable code will be further enhanced.

The rockets, or launch vehicles, can either be elliptically or cylindrically shaped, and up to eight strap-on structures (boosters or tanks) are allowed. Up to four engines are allowed for the core launch vehicle, which can be of two different types. Also, two different sizes of strap-on structures can be used, and two different types of booster engines are allowed.

Both tabular and graphical presentations of the predicted environments at the selected locations can be reviewed

by the user. The output includes summaries of rocket-engine operation, ignition overpressure time histories, and one-third octave sound pressure spectra of the predicted launch acoustics.

Also, documentation is available to the user to help him or her understand the various aspects of the graphical user interface and the required input parameters.

This work was done by Matthew Casiano of Marshall Space Flight Center. For more information, contact Sammy Nabors, MSFC Commercialization Assistance Lead at sammy.a.nabors@nasa.gov. Refer to MFS-32579-1.

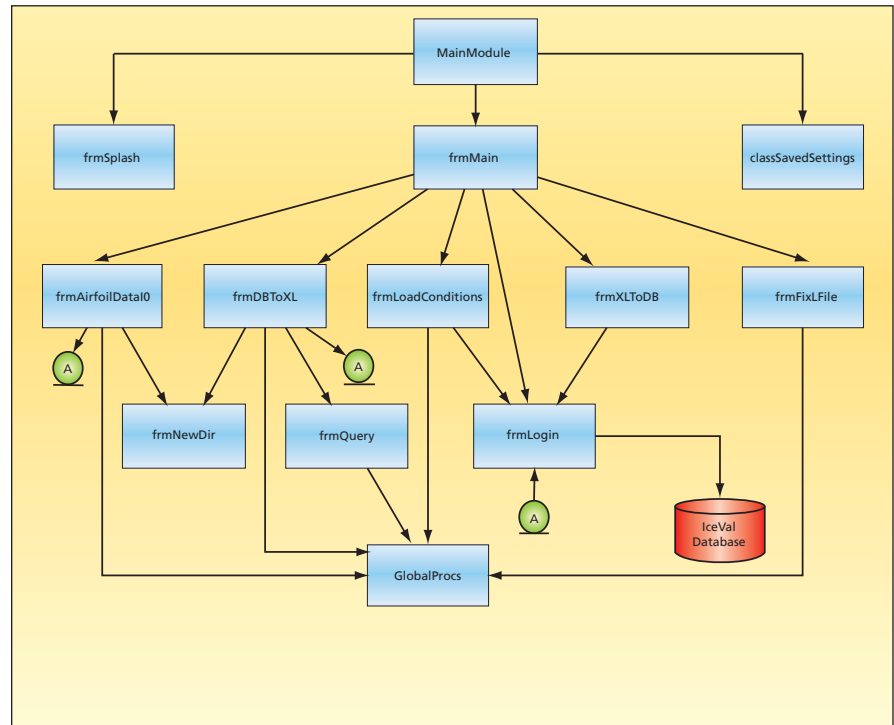
Interactive, Automated Management of Icing Data

John H. Glenn Research Center, Cleveland, Ohio

IceVal DatAssistant is software (see figure) that provides an automated, interactive solution for the management of data from research on aircraft icing. This software consists primarily of (1) a relational database component used to store ice shape and airfoil coordinates and associated data on operational and environmental test conditions and (2) a graphically oriented database access utility, used to upload, download, process, and/or display data selected by the user.

The relational database component consists of a Microsoft Access 2003 database file with nine tables containing data of different types. Included in the database are the data for all publicly releasable ice tracings with complete and verifiable test conditions from experiments conducted to date in the Glenn Research Center Icing Research Tunnel. Ice shapes from computational simulations with the corresponding conditions performed utilizing the latest version of the LEWICE ice shape prediction code are likewise included, and are linked to the equivalent experimental runs.

The database access component includes ten Microsoft Visual Basic 6.0 (VB) form modules and three VB support modules. Together, these modules enable uploading, downloading, processing, and display of all data contained in the database. This component also affords the capability to perform various



IceVal DatAssistant Software system structure.

database maintenance functions — for example, compacting the database or creating a new, fully initialized but empty database file.

This program was written by Laurie H. Levinson of Glenn Research Center. Further information is contained in a TSP (see page 1).

Inquiries concerning rights for the commercial use of this invention should be addressed to NASA Glenn Research Center, Innovative Partnerships Office, Attn: Steve Fedor, Mail Stop 4-8, 21000 Brookpark Road, Cleveland, Ohio 44135. Refer to LEW-18343-1.

LDPC-PPM Coding Scheme for Optical Communication

This scheme offers competitive performance and is suitable for parallel processing.

NASA's Jet Propulsion Laboratory, Pasadena, California

In a proposed coding-and-modulation/demodulation-and-decoding scheme for a free-space optical communication system, an error-correcting code of the low-density parity-check (LDPC) type would be concatenated with a modulation code that consists of a mapping of

bits to pulse-position-modulation (PPM) symbols. Hence, the scheme is denoted LDPC-PPM. This scheme could be considered a competitor of a related prior scheme in which an outer convolutional error-correcting code is concatenated with an interleaving operation, a bit-accu-

mulation operation, and a PPM inner code. Both the prior and present schemes can be characterized as serially concatenated pulse-position modulation (SCPPM) coding schemes.

Figure 1 represents a free-space optical communication system based on ei-

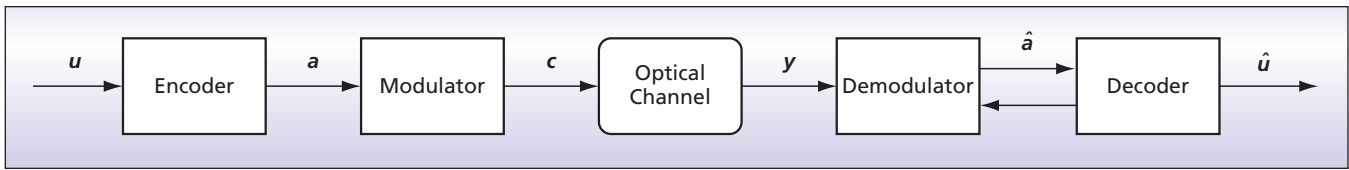


Figure 1. **Data Are Encoded**, then transmitted as a PPM optical signal. At the receiving end, the optical signal is demodulated and decoded in an iterative process.

ther the present LDPC-PPM scheme or the prior SCPPM scheme. At the transmitting terminal, the original data (u) are processed by an encoder into blocks of bits (a), and the encoded data are mapped to PPM of an optical signal (c). For the purpose of design and analysis, the optical channel in which the PPM signal propagates is modeled as a Poisson point process. At the receiving terminal, the arriving optical signal (y) is demodulated to obtain an estimate (\hat{a}) of the coded data, which is then processed by a decoder to obtain an estimate (\hat{u}) of the original data.

The demodulation and decoding sub-processes are iterated to improve the final estimates in an attempt to reconstruct the original data stream (u) exactly. The decoder implements a soft-input/soft-output (SISO) algorithm. This or any SISO decoder receives, as soft inputs, noisy versions (estimates and log-likelihoods of the estimates) of the input and output of the encoder and produces updated log-likelihoods of the estimates of the input, the output, or both. These estimates and their log-likelihoods may then be transmitted to other SISO modules in the receiver, where they are treated as noisy inputs.

In comparison with non-iterative alternatives, both the present LDPC-PPM scheme and the prior SCPPM scheme offer better performance. In comparison with iterative alternatives, both schemes afford better performance with less complexity. In comparison of these schemes with each other, each is partly advantageous and partly disadvantageous: For example, computational simulations have shown that for a block length of about 8Kb, the performance of the prior

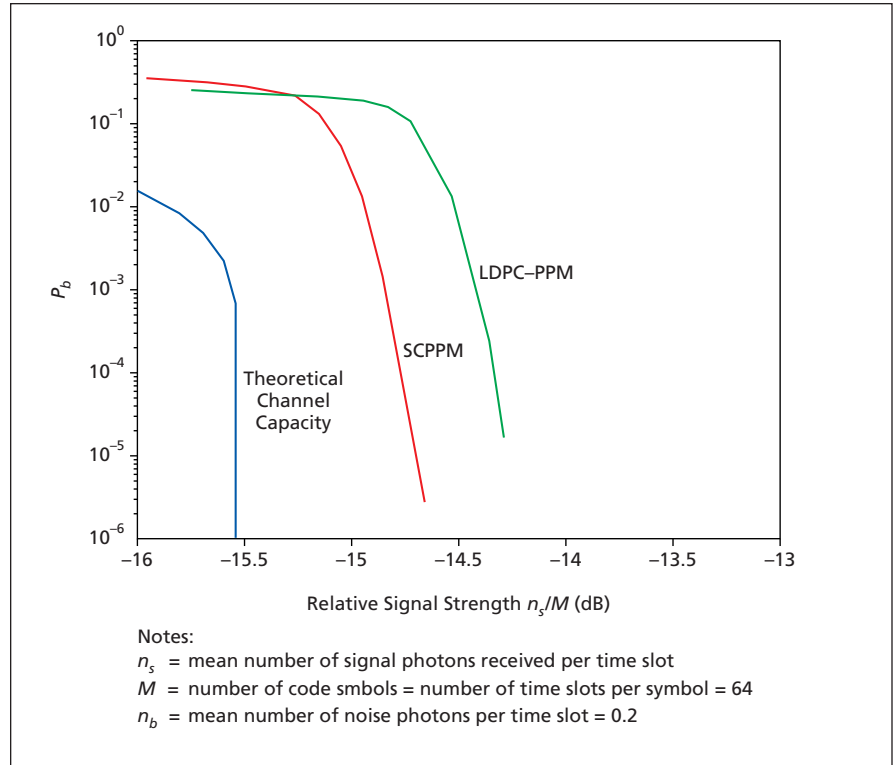


Figure 2. The **Bit-Error Rate (P_b)** was computed as a function of relative signal strength for two coding schemes and for the theoretical channel capacity for the special case of code blocks of ≈ 8 Kb length, $n_b = 0.2$, and $M = 64$.

SCPPM scheme is about 0.8 dB away from the theoretical channel capacity, while the performance of the LDPC-PPM scheme is expected to be about 1.2 dB away from the theoretical channel capacity at a bit-error rate of about 2×10^{-5} (see Figure 2); in other words, the performance of the LDPC-PPM scheme is expected to be about 0.4 dB below that of the prior SCPPM scheme. On the other hand, unlike the prior SCPPM scheme, the LDPC-PPM scheme lends itself very

well to low-latency parallel processing. Either scheme could serve as the basis of design of an optical communication system, depending on requirements pertaining to the PPM order, latency, and architecture of the system.

This work was done by Maged Barsoum, Bruce Moision, Dariush Divsalar, and Jon Hamkins of Caltech and Michael Fitz of UCLA for NASA's Jet Propulsion Laboratory. Further information is contained in a TSP (see page 1). NPO-44408

Complex Event Recognition Architecture

Lyndon B. Johnson Space Center, Houston, Texas

“Complex Event Recognition Architecture” (“CERA”) is the name of a computational architecture, and software that implements the architecture, for recognizing complex event patterns

that may be spread across multiple streams of input data. One of the main components of CERA is an intuitive event pattern language that simplifies what would otherwise be the complex,

difficult tasks of creating logical descriptions of combinations of temporal events and defining rules for combining information from different sources over time. In this language, recognition

patterns are defined in simple, declarative statements that combine point events from given input streams with those from other streams, using conjunction, disjunction, and negation. Patterns can be built on one another recursively to describe very rich, temporally extended combinations of events. Thereafter, a run-time matching algorithm in CERA efficiently matches these patterns against input data and signals when patterns are recognized.

CERA can be used to monitor complex systems and to signal operators or initiate corrective actions when anomalous conditions are recognized. CERA can be run as a stand-alone monitoring system, or it can be integrated into a larger system to automatically trigger responses to changing environments or problematic situations.

This program was written by William A. Fitzgerald and R. James Firby of I/NET, Inc. for Johnson Space Center. Further information is contained in a TSP (see page 1).

In accordance with Public Law 96;517, the contractor has elected to retain title to this invention. Inquiries concerning rights for its commercial use should be addressed to:

I/NET

P. O. Box 3338

Kalamazoo, MI 49003

Phone No.: (269) 978-6816

Fax No.: (800) 673-7352

Refer to MSC-23637-1, volume and number of this NASA Tech Briefs issue, and the page number.

▶ TurboTech Technical Evaluation Automated System

Goddard Space Flight Center, Greenbelt, Maryland

TurboTech software is a Web-based process that simplifies and semiautomates technical evaluation of NASA proposals for Contracting Officer's Technical Representatives (COTRs). At the time of this reporting, there have been no set standards or systems for training new COTRs in technical evaluations. This new process provides boilerplate text in response to "interview-style" questions. This text is collected into a Microsoft Word document that

can then be further edited to conform to specific cases.

By providing technical language and a structured format, TurboTech allows the COTRs to concentrate more on the actual evaluation, and less on deciding what language would be most appropriate. Since the actual word choice is one of the more time-consuming parts of a COTRs' job, this process should allow for an increase in quantity of proposals evaluated.

TurboTech is applicable to composing technical evaluations of contractor proposals, task and delivery orders, change order modifications, requests for proposals, new work modifications, task assignments, as well as any changes to existing contracts.

This work was done by Dorothy J. Tiffany of Goddard Space Flight Center. Further information is contained in a TSP (see page 1). GSC-15554-1

▶ Robot Vision Library

NASA's Jet Propulsion Laboratory, Pasadena, California

The JPL Robot Vision Library (JPLV) provides real-time robot vision algorithms for developers who are not vision specialists. The package includes algorithms for stereo ranging, visual odometry and unsurveyed camera calibration, and has unique support for very wide-angle lenses (as used on the Mars Exploration Rover HazCams). JPLV gathers these algorithms into one uniform, documented, and tested package with a consistent C API (application

programming interface). The software is designed for real-time execution (10–20 Hz) on COTS (commercial, off-the-shelf) workstations and embedded processors.

This package incorporates algorithms developed over more than ten years of research in ground and planetary robotics for NASA, DARPA (Defense Advanced Research Projects Agency) and the Army Research Labs, and is currently being used in applications as di-

verse as legged vehicle navigation and large-scale urban modeling.

This work was done by Andrew B. Howard, Adnan I. Ansar, and Todd E. Litwin of Caltech and Steven B. Goldberg of Indelible Systems for NASA's Jet Propulsion Laboratory.

This software is available for commercial licensing. Please contact Karina Edmonds of the California Institute of Technology at (626) 395-2322. Refer to NPO-46532.

▶ Perl Modules for Constructing Iterators

Goddard Space Flight Center, Greenbelt, Maryland

The *Iterator* Perl Module provides a general-purpose framework for constructing iterator objects within Perl, and a standard API for interacting with those objects. Iterators are an object-ori-

ented design pattern where a description of a series of values is used in a constructor. Subsequent queries can request values in that series. These Perl modules build on the standard *Iterator* framework

and provide iterators for some other types of values.

Iterator::DateTime constructs iterators from *DateTime* objects or *Date::Parse* descriptions and ICal/RFC 2445 style re-

currence descriptions. It supports a variety of input parameters, including a start to the sequence, an end to the sequence, an Ical/RFC 2445 recurrence describing the frequency of the values in the series, and a format description that can refine the presentation manner of the *DateTime*.

Iterator::String constructs iterators from string representations. This module is useful in contexts where the API consists of supplying a string and get-

ting back an iterator where the specific iteration desired is opaque to the caller. It is of particular value to the *Iterator::Hash* module which provides nested iterations.

Iterator::Hash constructs iterators from Perl hashes that can include multiple iterators. The constructed iterators will return all the permutations of the iterations of the hash by nested iteration of embedded iterators. A hash simply includes a set of keys mapped to values. It

is a very common data structure used throughout Perl programming. The *Iterator::Hash* module allows a hash to include strings defining iterators (parsed and dispatched with *Iterator::String*) that are used to construct an overall series of hash values.

This work was done by Curt Tilmes of Goddard Space Flight Center. For further information, contact the Goddard Innovative Partnerships Office at (301) 286-5810. GSC-15560-1/1-1/2-1

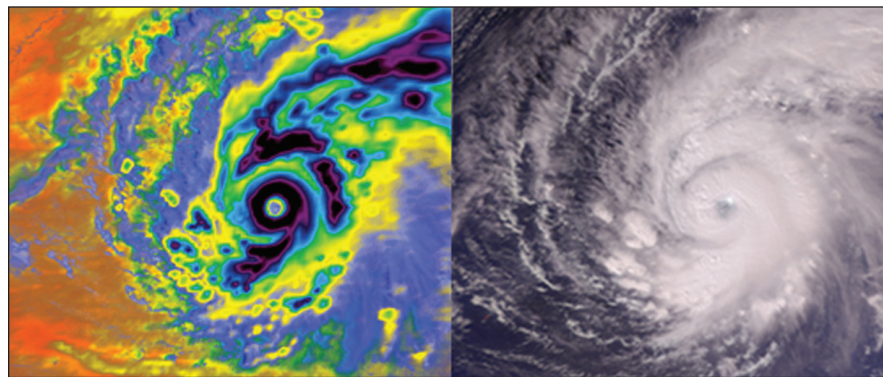
▶ Tropical Cyclone Information System

NASA's Jet Propulsion Laboratory, Pasadena, California

The JPL Tropical Cyclone Information System (TCIS) is a Web portal (<http://tropicalcyclone.jpl.nasa.gov>) that provides researchers with an extensive set of observed hurricane parameters together with large-scale and convection-resolving model outputs. It provides a comprehensive set of high-resolution satellite (see figure), airborne, and *in-situ* observations in both image and data formats. Large-scale datasets depict the surrounding environmental parameters such as SST (Sea Surface Temperature) and aerosol loading. Model outputs and analysis tools are provided to evaluate model performance and compare observations from different platforms.

The system pertains to the thermodynamic and microphysical structure of the storm, the air-sea interaction processes, and the larger-scale environment as depicted by ocean heat content and the aerosol loading of the environment.

Currently, the TCIS is populated with satellite observations of all tropical cy-



Images of Supertyphoon Pongsona that struck the U.S. island of Guam on December 8, 2002. The composite image on left was made by overlaying data from the infrared, microwave, and visible/near-infrared sensors. A standard image is on the right.

clones observed globally during 2005. There is a plan to extend the database both forward in time till present as well as backward to 1998. The portal is powered by a MySQL database and an Apache/Tomcat Web server on a Linux system. The interactive graphic user interface is provided by Google Map.

This work was done by P. Peggy Li, Brian W. Knosp, Quoc A. Vu, Yi Chao, and Svetla M. Hristova-Veleva of Caltech for NASA's Jet Propulsion Laboratory.

This software is available for commercial licensing. Please contact Karina Edmonds of the California Institute of Technology at (626) 395-2322. Refer to NPO-45748.

▶ XML Translator for Interface Descriptions

NASA's Jet Propulsion Laboratory, Pasadena, California

A computer program defines an XML schema for specifying the interface to a generic FPGA from the perspective of software that will interact with the device. This XML interface description is then translated into header files for C, Verilog, and VHDL. User interface definition input is checked via both the provided XML schema and the translator module to ensure consistency and accuracy.

Currently, programming used on both sides of an interface is inconsistent. This

makes it hard to find and fix errors. By using a common schema, both sides are forced to use the same structure by using the same framework and toolset. This makes for easy identification of problems, which leads to the ability to formulate a solution.

The toolset contains constants that allow a programmer to use each register, and to access each field in the register. Once programming is complete, the translator is run as part of the make

process, which ensures that whenever an interface is changed, all of the code that uses the header files describing it is recompiled.

This work was done by Elizabeth R. Borson of Caltech for NASA's Jet Propulsion Laboratory.

This software is available for commercial licensing. Please contact Karina Edmonds of the California Institute of Technology at (626) 395-2322. Refer to NPO-46447.

▶ Group Capability Model

John F. Kennedy Space Center, Florida

The Group Capability Model (GCM) is a software tool that allows an organization, from first line management to senior executive, to monitor and track the health (capability) of various groups in performing their contractual obligations. GCM calculates a Group Capability Index (GCI) by comparing actual head counts, certifications, and/or skills within a group. The model can also be used to simulate the effects of employee usage, training, and attrition on the GCI.

A universal tool and common method was required due to the high risk of losing skills necessary to complete the Space Shuttle Program and meet the needs of the Constellation Program. During this transition from one space vehicle to another, the uncertainty among the critical

skilled workforce is high and attrition has the potential to be unmanageable.

GCM allows managers to establish requirements for their group in the form of head counts, certification requirements, or skills requirements. GCM then calculates a Group Capability Index (GCI), where a score of 1 indicates that the group is at the appropriate level; anything less than 1 indicates a potential for improvement. This shows the “health” of a group, both currently and over time. GCM accepts as input head count, certification needs, critical needs, competency needs, and competency critical needs. In addition, team members are categorized by years of experience, percentage of contribution, ex-members and their skills, availability, function, and “in-work” requirements. Outputs are several re-

ports, including actual vs. required head count, actual vs. required certificates, CGI change over time (by month), and more. The program stores historical data for summary and historical reporting, which is done via an Excel spreadsheet that is color-coded to show health statistics at a glance.

GCM has provided the Shuttle Ground Processing team with a quantifiable, repeatable approach to assessing and managing the skills in their organization. They now have a common frame of reference across NASA/contractor lines to communicate and mitigate any critical skills concerns.

This work was done by Michael Olejarski, Amy Appleton, and Stephen Deltorchio of United Space Alliance for Kennedy Space Center. Further information is contained in a TSP (see page 1). KSC-13187

▶ Dynamic Hurricane Data Analysis Tool

NASA's Jet Propulsion Laboratory, Pasadena, California

A dynamic hurricane data analysis tool allows users of the JPL Tropical Cyclone Information System (TCIS) to analyze data over a Web medium. The TCIS software is described in the previous article, “Tropical Cyclone Information System (TCIS)” (NPO-45748).

This tool interfaces with the TCIS database to pull in data from several different atmospheric and oceanic data sets, both observed by instruments. Users can use this information to generate histograms, maps, and profile plots

for specific storms. The tool also displays statistical values for the user-selected parameter for the mean, standard deviation, median, minimum, and maximum values. There is little wait time, allowing for fast data plots over date and spatial ranges. Users may also “zoom-in” for a closer look at a particular spatial range.

This is version 1 of the software. Researchers will use the data and tools on the TCIS to understand hurricane processes, improve hurricane forecast

models and identify what types of measurements the next generation of instruments will need to collect.

This work was done by Brian W. Knosp, P. Peggy Li, and Quoc A. Vu of Caltech with student Michael J. Rosenman of the NASA USRP program for NASA's Jet Propulsion Laboratory. For more information, see <http://tropicalcyclone.jpl.nasa.gov>.

This software is available for commercial licensing. Please contact Karina Edmonds of the California Institute of Technology at (626) 395-2322. Refer to NPO-46417

▶ XVD Image Display Program

NASA's Jet Propulsion Laboratory, Pasadena, California

The XVD [X-Windows VICAR (video image communication and retrieval) Display] computer program offers an interactive display of VICAR and PDS (planetary data systems) images. It is designed to efficiently display multiple-GB images and runs on Solaris, Linux, or Mac OS X systems using X-Windows. XVD is the *de facto* standard image display program used within the Multimission Image Pro-

cessing Lab (MIPL) to process images from missions such as Voyager, Galileo, Cassini, MER, and Phoenix, among others.

XVD includes color, grayscale, or pseudocolor display; arbitrary zoom; the ability to display non-byte images; metadata (image label) display; full-screen displays; dither modes for 8-bit screens; 17 different stretch types; magnifying glass; and capabilities to rotate images

and display latitude and longitude for certain types of images.

This work was done by Robert G. Deen, Paul M. Andres, Helen B. Mortensen, Vadim Parizher, Myche McAuley, Paul Bartholomew, and Gloria Connor of Caltech for NASA's Jet Propulsion Laboratory.

This software is available for commercial licensing. Please contact Karina Edmonds of the California Institute of Technology at (626) 395-2322. Refer to NPO-46412.

Geospatial Authentication

Stennis Space Center, Mississippi

A software package that has been designed to allow authentication for determining if the rover(s) is/are within a set of boundaries or a specific area to access critical geospatial information by using GPS signal structures as a means to authenticate mobile devices into a network wirelessly and in real-time. The advantage lies in that the system only allows those with designated geospatial boundaries or areas into the server.

The Geospatial Authentication software has two parts — Server and Client. The server software is a virtual private

network (VPN) developed in Linux operating system using Perl programming language. The server can be a stand-alone VPN server or can be combined with other applications and services. The client software is a GUI Windows CE software, or Mobile Graphical Software, that allows users to authenticate into a network. The purpose of the client software is to pass the needed satellite information to the server for authentication.

This work was done by Stacey D. Lyle of Geospatial Research Innovation Design for

NASA's Stennis Space Center.

Inquiries concerning rights for its commercial use should be addressed to:

Dr. Stacey D. Lyle, RLPS

*Conrad Blucher Institute of Surveying and Science
6300 Ocean Drive*

Texas A&M University

Corpus Christi, TX 78412

Phone No. : (361) 825-3712

Fax: (361) 825-5848

E-mail: stacey.lyle@tamucc.edu

Refer to SSC-00282, volume and number of this NASA Tech Briefs issue, and the page number.

Mars Science Laboratory Workstation Test Set

NASA's Jet Propulsion Laboratory, Pasadena, California

The Mars Science Laboratory developed the Workstation TestSet (WSTS) is a computer program that enables flight software development on virtual MSL avionics. The WSTS is the non-real-time flight avionics simulator that is designed to be completely software-based and run on a workstation class Linux PC. This provides flight software developers with their own virtual avionics testbed and allows device-level and functional software testing. The WSTS has successfully off-loaded many flight software develop-

ment activities from the project testbeds. Flight software developers can now instantiate as many virtual testbeds as there are available computer resources and also enables device level fault injections that are difficult to achieve on real avionics testbeds.

The WSTS provides peripheral component interface (PCI)-card-level simulation of avionics hardware, enabling testing of all but the lowest layers of the flight software. The WSTS utilizes shared-memory and synchronization

provisions of POSIX in a Linux environment to provide high-resolution simulation with synchronization of the interaction between simulation and the flight software.

This program was written by David A. Henriquez, Timothy K. Canham, Johnny T. Chang, and Nathaniel J. Villavme of Caltech for NASA's Jet Propulsion Laboratory.

This software is available for commercial licensing. Please contact Karina Edmonds of the California Institute of Technology at (626) 395-2322. Refer to NPO-45690.

Computing Bounds on Resource Levels for Flexible Plans

New algorithm entails less computation than previous algorithms.

Ames Research Center, Moffett Field, California

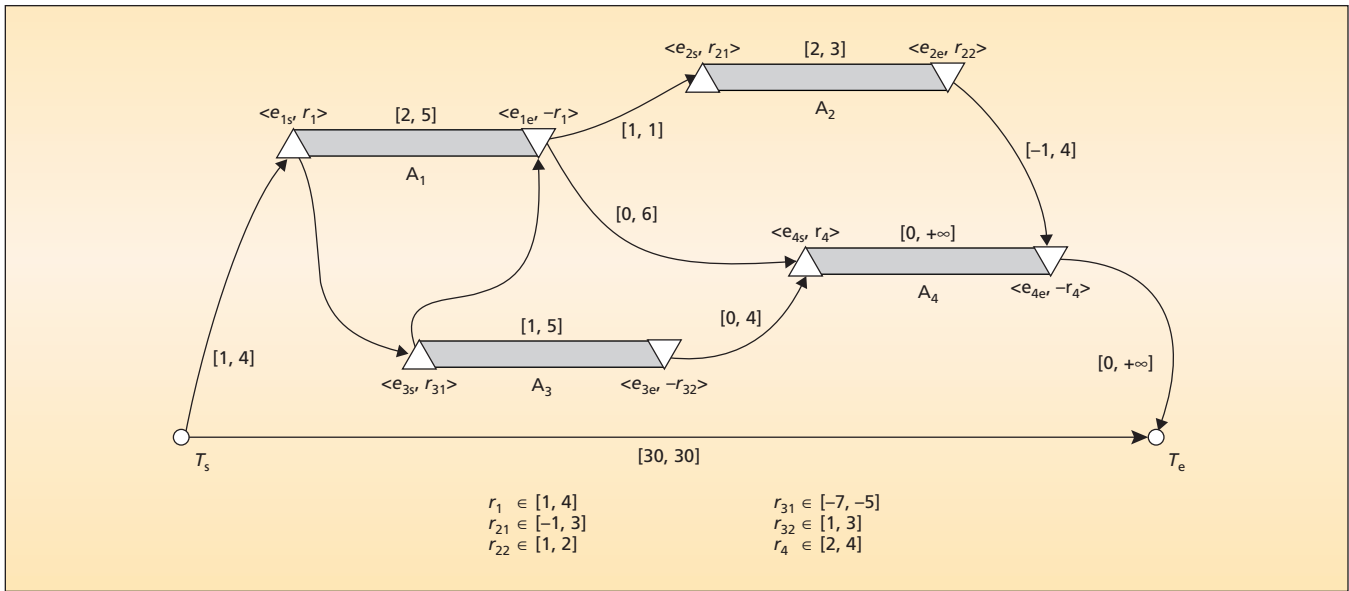
A new algorithm efficiently computes the tightest exact bound on the levels of resources induced by a flexible activity plan (see figure). Tightness of bounds is extremely important for computations involved in planning because tight bounds can save potentially exponential amounts of search (through early backtracking and detection of solutions), relative to looser bounds.

The bound computed by the new algorithm, denoted the resource-level envelope, constitutes the measure of maximum and minimum consumption of resources at any time for all fixed-time schedules in the flexible plan. At each time, the envelope guarantees that there

are two fixed-time instantiations — one that produces the minimum level and one that produces the maximum level. Therefore, the resource-level envelope is the tightest possible resource-level bound for a flexible plan because any tighter bound would exclude the contribution of at least one fixed-time schedule. If the resource-level envelope can be computed efficiently, one could substitute looser bounds that are currently used in the inner cores of constraint-posting scheduling algorithms, with the potential for great improvements in performance.

What is needed to reduce the cost of computation is an algorithm, the measure of complexity of which is no greater

than a low-degree polynomial in N (where N is the number of activities). The new algorithm satisfies this need. In this algorithm, the computation of resource-level envelopes is based on a novel combination of (1) the theory of shortest paths in the temporal-constraint network for the flexible plan and (2) the theory of maximum flows for a flow network derived from the temporal and resource constraints. The measure of asymptotic complexity of the algorithm is $O(N \cdot O(\maxflow(N)))$, where $O(x)$ denotes an amount of computing time or a number of arithmetic operations proportional to a number of the order of x and $O(\maxflow(N))$ is the measure of com-



An **Activity Network With Resource Allocations** constitutes a graphical representation of a flexible activity plan to which the instant algorithm applies. Each activity time interval (A_i) is characterized by (1) time variables e_{is} and e_{ie} for start and end events, respectively; (2) a non negative flexible activity-duration link (e.g., [2,5] for activity A_1); and flexible separation links between events (e.g., [0,4] from e_{3e} to e_{4s}). Associated with each event is a resource-allocation variable (e.g., r_{31} with event e_{3s}). It is assumed that all events occur after starting time T_s and before an ending event time T_e rigidly connected to T_s . The interval $[T_s, T_e]$ is denoted the time horizon of the network.

plexity (and thus of cost) of a maximum-flow algorithm applied to an auxiliary flow network of $2N$ nodes. The algorithm is believed to be efficient in practice; experimental analysis shows the practical cost of maxflow to be as low as $O(N^{1.5})$.

The algorithm could be enhanced following at least two approaches. In the first approach, incremental subalgorithms for the computation of the envelope could be developed. By use of tem-

poral scanning of the events in the temporal network, it may be possible to significantly reduce the size of the networks on which it is necessary to run the maximum-flow subalgorithm, thereby significantly reducing the time required for envelope calculation. In the second approach, the practical effectiveness of resource envelopes in the inner loops of search algorithms could be tested for multi-capacity resource scheduling. This

testing would include inner-loop backtracking and termination tests and variable and value-ordering heuristics that exploit the properties of resource envelopes more directly.

This work was done by Nicola Muscivtola of Ames Research Center and David Rijsman of Mission Critical Technologies Inc. For further information contact the Technology Partnerships Division, Ames Research Center, (650) 604-2954. ARC-14948-1

MSLICE Science Activity Planner for the Mars Science Laboratory Mission

NASA's Jet Propulsion Laboratory, Pasadena, California

MSLICE (Mars Science Laboratory InterfaCE) is the tool used by scientists and engineers on the Mars Science Laboratory rover mission to visualize the data returned by the rover and collaboratively plan its activities. It enables users to efficiently and effectively search all mission data to find applicable products (e.g., images, targets, activity plans, sequences, etc.), view and plan the traverse of the rover in HiRISE (High Resolution Imaging Science Experiment) images, visualize data acquired by the rover, and develop, model, and validate the activities the rover will perform. MSLICE enables users to securely contribute to the mission's activity planning process

from their home institutions using off-the-shelf laptop computers.

This software has made use of several plug-ins (software components) developed for previous missions [e.g., Mars Exploration Rover (MER), Phoenix Mars Lander (PHX)] and other technology tasks. It has a simple, intuitive, and powerful search capability. For any given mission, there is a huge amount of data and associated metadata that is generated. To help users sort through this information, MSLICE's search interface is provided in a similar fashion as major Internet search engines.

With regard to the HiRISE visualization of the rover's traverse, this view is a map of the mission that allows scientists

to easily gauge where the rover has been and where it is likely to go. The map also provides the ability to correct or adjust the known position of the rover through the overlaying of images acquired from the rover on top of the HiRISE image. A user can then correct the rover's position by collocating the visible features in the overlays with the same features in the underlying HiRISE image. MSLICE users can also rapidly search all mission data for images that contain a point specified by the user in another image or panoramic mosaic.

MSLICE allows the creation of targets, which provides a way for scientists to collaboratively name features on the surface of Mars. These targets can also be

used to convey instrument-pointing information to the activity plan. The software allows users to develop a plan of what they would like the rover to accomplish for a given time period. When developing the plan, the user can input constraints between activities or groups of activities. MSLICE will enforce said

constraints and ensure that all mission flight rules are satisfied.

This work was done by Mark W. Powell, Khawaja S. Shams, Michael N. Wallick, Jeffrey S. Norris, Joseph C. Joswig, Thomas M. Crockett, Jason M. Fox, Recaredo J. Torres of Caltech; James A. Kurien, Michael P. McCurdy, and Guy Pyrzak of NASA Ames Re-

search Center; and Arash Agheoli and Andrew G. Bachmann of Stinger Ghaffarian Technologies, Inc. for NASA's Jet Propulsion Laboratory.

This software is available for commercial licensing. Please contact Karina Edmonds of the California Institute of Technology at (626) 395-2322. Refer to NPO-45908.

Telemetry-Enhancing Scripts

NASA's Jet Propulsion Laboratory, Pasadena, California

Scripts Providing a Cool Kit of Telemetry Enhancing Tools (SPACKLE) is a set of software tools that fill gaps in capabilities of other software used in processing downlinked data in the Mars Exploration Rovers' (MER) flight and test-bed operations. SPACKLE tools have helped to accelerate the automatic processing and interpretation of MER mission data, enabling non-experts to understand and/or use MER query and data product command simulation software tools more effectively. SPACKLE has greatly accelerated some operations and provides new capabilities.

The tools of SPACKLE are written, variously, in Perl or the C or C++ language. They perform a variety of search and shortcut functions that include the following:

- Generating text-only, Event Report-annotated, and Web-enhanced views of command sequences;
- Labeling integer enumerations with their symbolic meanings in text messages and engineering channels;
- Systematic detecting of corruption within data products;
- Generating text-only displays of data-product catalogs including downlink status;
- Validating and labeling of commands related to data products;

- Performing of convenient searches of detailed engineering data spanning multiple Martian solar days;
- Generating tables of initial conditions pertaining to engineering, health, and accountability data;
- Simplified construction and simulation of command sequences; and
- Fast time format conversions and sorting.

This program was written by Mark W. Maimone of Caltech for NASA's Jet Propulsion Laboratory.

This software is available for commercial licensing. Please contact Karina Edmonds of the California Institute of Technology at (626) 395-2322. Refer to NPO-45700.

Analog Input Data Acquisition Software

John F. Kennedy Space Center, Florida

DAQ Master Software allows users to easily set up a system to monitor up to five analog input channels and save the data after acquisition. This program was written in LabVIEW 8.0, and requires the LabVIEW runtime engine 8.0 (free download from National Instruments; ni.com) to run the executable. A DAQ card must be installed in the computer for this program to work correctly, and it must have

up to five analog input channels. The user can set the channel configuration, and other channel details, from the setup tab after the program has begun.

A Setup tab holds all information for the channels that will be used for data acquisition, and allows the user to save or upload the settings for future use by writing or reading a configuration file. The Data Acquisition tab is where the

commands to acquire, stop, and save data are located, and where the data will be displayed. The user can choose to display scaled or un-scaled data while acquisition is taking place.

This work was done by Ellen Arens of Kennedy Space Center. For more information, visit http://www.openchannelsoftware.com/projects/Analog_Input_Data_Acquisition for a free download. KSC-13203

Relay Sequence Generation Software

NASA's Jet Propulsion Laboratory, Pasadena, California

Due to thermal and electromagnetic interactivity between the UHF (ultra-high frequency) radio onboard the Mars Reconnaissance Orbiter (MRO), which performs relay sessions with the Martian landers, and the remainder of the MRO payloads, it is required to integrate and

de-conflict relay sessions with the MRO science plan. The MRO relay SASE/PTF (spacecraft activity sequence file/ payload target file) generation software facilitates this process by generating a PTF that is needed to integrate the periods of time during which MRO supports relay

activities with the rest of the MRO science plans. The software also generates the needed command products that initiate the relay sessions, some features of which are provided by the lander team, some are managed by MRO internally, and some being derived.

By utilizing an input file provided by the lander team, along with a managed configuration file, the MRO relay SASF/PTF generation software runs MRO's MTT (Mars Target Tool) software recursively to construct the Relay PTF. It also references these same input products to generate the SASFs needed to support the overflight. Each SASF has

all of the parameters and commanding required to instruct MRO to initiate the relay session and to configure the on-board radio to transfer data to and from the landed asset. In addition, the software performs version checking on the current input file and determines any modifications to the file from any previous version. If instructed, it will output

only that information which is relevant to the changed entries.

This work was done by Roy E. Gladden and Teerapat Khanampornpan of Caltech for NASA's Jet Propulsion Laboratory.

This software is available for commercial licensing. Please contact Karina Edmonds of the California Institute of Technology at (626) 395-2322. Refer to NPO-46512.

GlastCam: A Telemetry-Driven Spacecraft Visualization Tool

Goddard Space Flight Center, Greenbelt, Maryland

Developed for the GLAST project, which is now the Fermi Gamma-ray Space Telescope, GlastCam software ingests telemetry from the Integrated Test and Operations System (ITOS) and generates four graphical displays of geometric properties in real time, allowing visual assessment of the attitude, configuration, position, and various cross-checks. Four windows are displayed: a "cam" window shows a 3D view of the satellite; a second window shows the standard position plot of the

satellite on a Mercator map of the Earth; a third window displays star tracker fields of view, showing which stars are visible from the spacecraft in order to verify star tracking; and the fourth window depicts Sun sensor measurements, enabling verification of the solar array deployment state. Each of these windows has telltales showing useful information applicable to each window, such as spacecraft axes, magnetic field vectors, the Sun-pointing direction, and the like. These can be tog-

gled on or off as desired. By breaking up the data into applicable windows, it is easier to monitor specific data of interest. Because the displays operate in real time and visually, any changes to the spacecraft's configuration or attitude are seen immediately. This allows for fast and intuitive spacecraft geometry assessment.

This work was done by Eric T. Stoneking and Dean Tsai of Goddard Space Flight Center. Further information is contained in a TSP (see page 1). GSC-15572-1

Robot Vision Library

NASA's Jet Propulsion Laboratory, Pasadena, California

The JPL Robot Vision Library (JPLV) provides real-time robot vision algorithms for developers who are not vision specialists. The package includes algorithms for stereo ranging, visual odometry and unsurveyed camera calibration, and has unique support for very wide-angle lenses (as used on the Mars Exploration Rover HazCams). JPLV gathers these algorithms into one uniform, documented, and tested package with a con-

sistent C API (application programming interface). The software is designed for real-time execution (10–20 Hz) on COTS (commercial, off-the-shelf) workstations and embedded processors.

This package incorporates algorithms developed over more than ten years of research in ground and planetary robotics for NASA, DARPA (Defense Advanced Research Projects Agency) and the Army Research Labs, and is cur-

rently being used in applications as diverse as legged vehicle navigation and large-scale urban modeling.

This work was done by Andrew B. Howard, Adnan I. Ansari, and Todd E. Litwin of Caltech and Steven B. Goldberg of Indelible Systems for NASA's Jet Propulsion Laboratory.

This software is available for commercial licensing. Please contact Karina Edmonds of the California Institute of Technology at (626) 395-2322. Refer to NPO-46532.

Mission Operations and Navigation Toolkit Environment

NASA's Jet Propulsion Laboratory, Pasadena, California

MONTE (Mission Operations and Navigation Toolkit Environment) Release 7.3 is an extensible software system designed to support trajectory and navigation analysis/design for space missions. MONTE is intended to replace the current navigation and trajectory analysis

software systems, which, at the time of this reporting, are used by JPL's Navigation and Mission Design section. The software provides an integrated, simplified, and flexible system that can be easily maintained to serve the needs of future missions in need of navigation services.

MONTE has an integrated case management system that allows users to create taxonomies to describe and categorize runs. It has the ability to plot and display multiple cases and scenarios simultaneously, using color to differentiate, allowing for side-by-side analysis. Users can define

their own plots with minimal effort, and can gain access to all of the features of the case management system. Users can also define their own models (including gravitational and non-gravitational force models), types of measurement, and optimizers, using software hooks that are made available in the scripting layer of the tool. This enables users to extend the functionality of MONTE without restriction.

MONTE provides maneuver optimization as well as re-optimization capability that includes support for particular constraints, such as cones and directions. The software has integrated support to help satisfy planetary quarantine requirements.

This work was done by Richard F. Sunseri, Hsi-Cheng Wu, Robert A. Hanna, Michael P. Mossey, Courtney B. Duncan, Scott E. Evans,

James R. Evans, Theodore R. Drain, Michelle M. Guevara, Tomas J. Martin Mur, and Ahlam A. Attiyah of Caltech for NASA's Jet Propulsion Laboratory.

This software is available for commercial licensing. Please contact Karina Edmonds of the California Institute of Technology at (626) 395-2322. Refer to NPO-46083.

Extensible Infrastructure for Browsing and Searching Abstracted Spacecraft Data

NASA's Jet Propulsion Laboratory, Pasadena, California

A computer program has been developed to provide a common interface for all space mission data, and allows different types of data to be displayed in the same context. This software provides an infrastructure for representing any type of mission data. Existing software requires that each type of mission data be treated separately. The new program's representations provide identifying information, and provide a means

of opening the data for further inspection. This is useful for searching and browsing large quantities of data across multiple databases.

The software is written in Java as part of the MSLICE program, and can be run on any Windows, Mac OS, or Linux computer. The software may be adapted to other mission operation software.

This work was done by Michael N. Wallick, Thomas M. Crockett, Joseph C. Joswig,

Recaredo J. Torres, Jeffrey S. Norris, Jason M. Fox, Mark W. Powell, David S. Mittman, Lucy Abramyan, Khawaja S. Shams, and Michael B. Vaughn of Caltech and Guy Pyrzak and Melissa Ludowise of Ames Research Center for NASA's Jet Propulsion Laboratory.

This software is available for commercial licensing. Please contact Karina Edmonds of the California Institute of Technology at (626) 395-2322. Refer to NPO-46397.

Lossless Compression of Data Into Fixed-Length Packets

NASA's Jet Propulsion Laboratory, Pasadena, California

A computer program effects lossless compression of data samples from a one-dimensional source into fixed-length data packets. The software makes use of adaptive prediction: it exploits the data structure in such a way as to increase the efficiency of compression beyond that otherwise achievable.

Adaptive linear filtering is used to predict each sample value based on past sample values. The difference between predicted and actual sample values is encoded using a Golomb code. The particular Golomb code used is selected using a

method described in "Simpler Adaptive Selection of Golomb Power-of-Two Codes" (NPO-41336), *NASA Tech Briefs*, Vol. 31, No. 11 (November 2007), page 71. As noted therein, the method is somewhat suboptimal (suboptimality $\leq 1/2$ bit per sample) but offers the advantage that it involves significantly less computation than does a prior method of adaptive selection of optimum codes through "brute force" application of all code options to every block of samples. Hence, the computer program is relatively simple and produces packets relatively rapidly.

The method and, hence, the program are robust to loss of packets: All parameters needed to decompress a packet are encoded in the packet. Therefore, the loss of one or more packets does not diminish the ability to reconstruct samples in remaining packets.

This work was done by Aaron B. Kieley and Matthew A. Klimesh of Caltech for NASA's Jet Propulsion Laboratory.

This software is available for commercial licensing. Please contact Karina Edmonds of the California Institute of Technology at (626) 395-2322. Refer to NPO-45942.

Video-Game-Like Engine for Depicting Spacecraft Trajectories

NASA's Jet Propulsion Laboratory, Pasadena, California

GoView is a video-game-like software engine, written in the C and C++ computing languages, that enables real-time, three-dimensional (3D)-appearing visual representation of spacecraft and trajectories (1)

from any perspective; (2) at any spatial scale from spacecraft to Solar-system dimensions; (3) in user-selectable time scales; (4) in the past, present, and/or future; (5) with varying speeds; and (6) for-

ward or backward in time. GoView constructs an interactive 3D world by use of spacecraft-mission data from pre-existing engineering software tools. GoView can also be used to produce distributable ap-

plication programs for depicting NASA orbital missions on personal computers running the Windows XP, Mac OS X, and Linux operating systems.

GoView enables seamless rendering of Cartesian coordinate spaces with programmable graphics hardware, whereas prior programs for depicting spacecraft trajectories variously require non-Cartesian coordinates and/or are not compatible with programmable hardware. GoView incorporates an algorithm for

nonlinear interpolation between arbitrary reference frames, whereas the prior programs are restricted to special classes of inertial and non-inertial reference frames. Finally, whereas the prior programs present complex user interfaces requiring hours of training, the GoView interface provides guidance, enabling use without any training.

This work was done by Paul R. Upchurch of Caltech for NASA's Jet Propulsion Laboratory. In accordance with Public Law 96-517,

the contractor has elected to retain title to this invention. Inquiries concerning rights for its commercial use should be addressed to:

*Innovative Technology Assets Management
JPL*

*Mail Stop 202-233
4800 Oak Grove Drive
Pasadena, CA 91109-8099*

E-mail: iaoffice@jpl.nasa.gov

Refer to NPO-45274, volume and number of this NASA Tech Briefs issue, and the page number.

Alert Notification System Router

Goddard Space Flight Center, Greenbelt, Maryland

The Alert Notification System Router (ANSR) software provides satellite operators with notifications of key events through pagers, cell phones, and e-mail. Written in Java, this application is specifically designed to meet the mission-critical standards for mission operations while operating on a variety of hardware environments.

ANSR is a software component that runs inside the Mission Operations Center (MOC). It connects to the mission's message bus using the GMSEC [God-

dard Space Flight Center (GSFC) Mission Services Evolution Center (GMSEC)] standard. Other components, such as automation and monitoring components, can use ANSR to send directives to notify users or groups. The ANSR system, in addition to notifying users, can check for message acknowledgements from a user and escalate the notification to another user if there is no acknowledgement.

When a firewall prevents ANSR from accessing the Internet directly, proxies

can be run on the other side of the wall. These proxies can be configured to access the Internet, notify users, and poll for their responses. Multiple ANSRs can be run in parallel, providing a seamless failover capability in the event that one ANSR system becomes incapacitated.

This work was done by Joseph Gurganus of Goddard Space Flight Center and Everett Cary, Robert Antonucci, and Peter Hitchener of Emergent Space Technologies, Inc. Further information is contained in a TSP (see page 1). GSC-15592-1

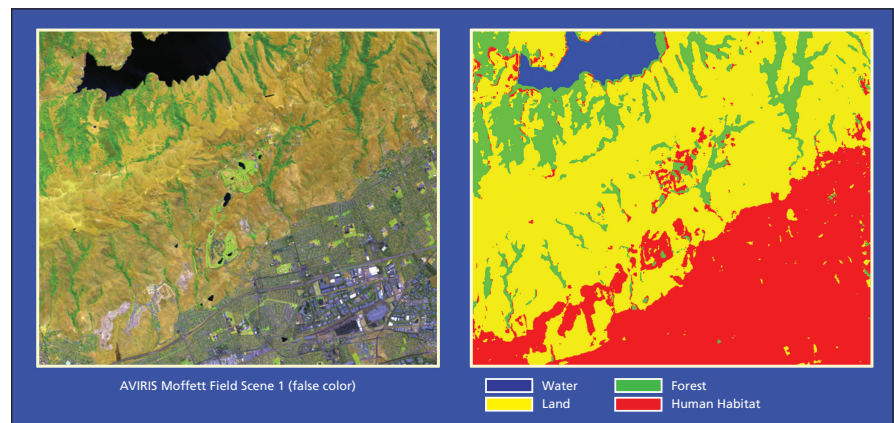
Lossless Compression of Classification-Map Data

This algorithm performs better than do general-purpose image-data compression algorithms.

NASA's Jet Propulsion Laboratory, Pasadena, California

A lossless image-data-compression algorithm intended specifically for application to classification-map data is based on prediction, context modeling, and entropy coding. The algorithm was formulated, in consideration of the differences between classification maps and ordinary images of natural scenes, so as to be capable of compressing classification-map data more effectively than do general-purpose image-data-compression algorithms.

Classification maps are typically generated from remote-sensing images acquired by instruments aboard aircraft (see figure) and spacecraft. A classification map is a synthetic image that summarizes information derived from one or more original remote-sensing image(s) of a scene. The value assigned to each pixel in such a map is the index of a class that represents some type of content deduced from the original image data — for exam-



This **False-Color Image and Classification Map** were derived from image data acquired by an airborne visible/infrared imaging spectrometer (AVIRIS) over Moffett Field, California. The classification map is typical of images meant to be processed by use of the present algorithm.

ple, a type of vegetation, a mineral, or a body of water — at the corresponding location in the scene. When classification maps are generated onboard the aircraft

or spacecraft, it is desirable to compress the classification-map data in order to reduce the volume of data that must be transmitted to a ground station.

Unlike ordinary (continuous-tone) images, a classification map typically contains a relatively small number of pixel values. Also, unlike in continuous-tone images, numerically close pixel values do not necessarily represent similar content. These properties make the problem of compressing classification-map-data differ from the problem of compressing data from ordinary images.

Prediction is commonly used in loss-less-compression schemes. In predictive compression, pixels or other samples are encoded sequentially on the basis of a probability distribution estimated from previously encoded samples. Context modeling is often used in conjunction with predictive compression. In context modeling, each pixel or other sample to be encoded is classified into one of several contexts based on previously en-

coded samples. A context-modeling algorithm maintains separate statistics for each context and uses these statistics to estimate and encode samples more effectively. Ideally, contexts are defined so that different contexts contain sets of pixels or other samples characterized by substantially different statistics.

The present algorithm incorporates a simple adaptive context modeler that feeds into a binary interleaved entropy coder. The algorithm operates on the pixels of a classification map or other image in raster scan order. A sequence of binary decision bits is produced for each pixel to indicate which, if any, neighboring pixel(s) it matches. The encoder maintains probability-of-zero estimates for these bits for each of the contexts. The interleaved entropy coder is bit-wise adaptable, enabling the context

modeler to quickly adapt to changing statistics in the image.

In tests, the present algorithm and three prior general-purpose image-data-compression algorithms were applied to five classification maps containing from 4 to 32 different classes. The four-class map is shown in the figure. The results of the tests showed that the volumes of data generated by the present algorithm ranged from 15 to 40 percent below those of the prior algorithms.

This work was done by Hua Xie and Matthew Klimesh of Caltech for NASA's Jet Propulsion Laboratory.

The software used in this innovation is available for commercial licensing. Please contact Karina Edmonds of the California Institute of Technology at (626) 395-2322. Refer to NPO-45103.

Framework for ReSTful Web Services in OSGi

NASA's Jet Propulsion Laboratory, Pasadena, California

Ensemble ReST is a software system that eases the development, deployment, and maintenance of server-side application programs to perform functions that would otherwise be performed by client software. Ensemble ReST takes advantage of the proven disciplines of ReST (Representational State Transfer — a style of software architecture for such distributed hypermedia systems as the World Wide Web) and OSGi (formerly, Open Services Gateway Initiative — an industry standard for software for connecting such devices as home appliances and security systems to the Internet). ReST leverages the standardized HTTP protocol to enable developers to offer services to a diverse variety of

clients: from shell scripts to sophisticated Java application suites.

Ensemble ReST abstracts away complexities associated with development of server-side application programs, enabling programmers to focus more on business logic than on server issues. It is robust, scalable, and secure; capable of serving dynamic as well as static content; and extensible to provide additional functionality. Services can be added, removed, or updated on a server, without restarting the server. Furthermore, the development environment for these services (Eclipse IDE) allows developers to debug the server-side applications side-by-side with the clients. The framework enables rapid prototyping and development of produc-

tion level ReSTlets that can be deployed to support mission critical applications. The rapid development cycle offered by this framework has enabled the Maestro team to develop and deploy many production server-side applications to MER, Phoenix, and MSL missions.

This program was written by Khawaja S. Shams, Jeffrey S. Norris, Mark W. Powell, Thomas M. Crockett, David S. Mittman, Jason M. Fox, Joseph C. Joswig, Michael N. Wallick, Recaredo J. Torres, and Kenneth Rabe of Caltech for NASA's Jet Propulsion Laboratory.

This software is available for commercial licensing. Please contact Karina Edmonds of the California Institute of Technology at (626) 395-2322. Refer to NPO-45848.

MAGIC: Model and Graphic Information Converter

John F. Kennedy Space Center, Florida

MAGIC is a software tool capable of converting highly detailed 3D models from an open, standard format, VRML 2.0/97, into the proprietary DTS file format used by the Torque Game Engine from GarageGames. MAGIC is used to convert 3D simulations from authoritative sources into the data needed to run the simulations in NASA's Distributed Observer Network.

The Distributed Observer Network (DON) is a simulation presentation tool

built by NASA to facilitate the simulation sharing requirements of the Data Presentation and Visualization effort within the Constellation Program. DON is built on top of the Torque Game Engine (TGE) and has chosen TGE's Dynamix Three Space (DTS) file format to represent 3D objects within simulations.

The DTS file structure is generally intended to contain common game objects, with less than ten thousand polygons

each, and if built using the standard methods will break (fail to load or contain corrupted geometry) after that amount.

MAGIC employs techniques to work around the DTS limitations, allowing for much more information to be successfully represented with the DTS file structure (millions of polygons). This ability opens up the Torque Game Engine to be used in applications where such detail is needed.

MAGIC can handle models of nearly limitless complexity (millions of polygons with complex scene structures) and save the information into a single DTS file to be used within a DON simulation. MAGIC also handles every other aspect of simulation conversion (texture map conversion/creation, support file generation,

mission folder, and hierarchy creation, etc.) and can create all the files needed for DON to successfully recreate simulations.

MAGIC is a freely distributable, stand-alone executable that runs on Windows XP (or later) operating systems. All that is required is to provide MAGIC with the simulation data (models, images,

telemetry, etc.) and a configuration file instructing MAGIC what it needs to do, then press "Go!".

This work was done by W.C. Herbert of Kennedy Space Center. For further information, contact the Kennedy Innovative Partnerships Program Office at (321) 861-7158. KSC-13201

Data Management Applications for the Service Preparation Subsystem

NASA's Jet Propulsion Laboratory, Pasadena, California

These software applications provide intuitive User Interfaces (UIs) with a consistent look and feel for interaction with, and control of, the Service Preparation Subsystem (SPS). The elements of the UIs described here are the File Manager, Mission Manager, and Log Monitor applications. All UIs provide access to add/delete/update data entities in a complex database schema without requiring technical expertise on the part of the end users. These applications allow for safe, validated, catalogued input of data. Also, the software has been designed in multiple, coherent layers to promote ease of code maintenance and reuse in addition to reducing testing and accelerating maturity.

The File Manager provides an interface for interactively publishing data

input files to a relational SQL-compliant database. It extracts/captures metadata automatically for use in building and maintaining the catalog of available data. Also, File Manager visualizes the data catalog in a tree format for easy use.

Mission Manager provides a single interface to define critical parameters describing both flight-and ground-based projects. Log Monitor provides access to system events recorded in execution of automatic generation of support data. This interface is critical in identifying events requiring attention/intervention to meet mission requirements.

The applications comprising the SPS User Interface Portal run on any platform that supports Java Runtime Environment 1.4.2. The UIs can interact with any suitably configured, SQL-compliant database,

and the content-driven nature of the UIs allows them to be easily adapted to present custom data. These applications are highly portable, and were designed for automatic deployment as WebStart applications, which reduces the effort involved in installing and updating these programs across dozens of user workstations at various physical locations.

This work was done by Ivy P. Luong, George W. Chang, Tung Bui, Christopher Allen, Shantanu Malhotra, Fannie C. Chen, Bach X. Bui, Sandy C. Gutheinz, Rachel Y. Kim, Silvino C. Zendejas, Dan Yu, Richard M. Kim, and Syed Sadaqathulla of Caltech for NASA's Jet Propulsion Laboratory.

This software is available for commercial licensing. Please contact Karina Edmonds of the California Institute of Technology at (626) 395-2322. Refer to NPO-45021.

Policy-Based Management Natural Language Parser

NASA's Jet Propulsion Laboratory, Pasadena, California

The Policy-Based Management Natural Language Parser (PBEM) is a rules-based approach to enterprise management that can be used to automate certain management tasks. This parser simplifies the management of a given endeavor by establishing policies to deal with situations that are likely to occur. Policies are operating rules that can be referred to as a means of maintaining order, security, consistency, or other ways of successfully furthering a goal or mission. PBEM provides a way of managing configuration of network elements, applications, and processes via a set of high-level rules or business

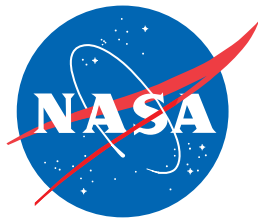
policies rather than managing individual elements, thus switching the control to a higher level. This software allows unique management rules (or commands) to be specified and applied to a cross-section of the Global Information Grid (GIG).

This software embodies a parser that is capable of recognizing and understanding conversational English. Because all possible dialect variants cannot be anticipated, a unique capability was developed that parses passed on conversation intent rather than the exact way the words are used. This software can increase productivity by enabling a user to

converse with the system in conversational English to define network policies. PBEM can be used in both manned and unmanned science-gathering programs. Because policy statements can be domain-independent, this software can be applied equally to a wide variety of applications.

This work was done by Mark James of Caltech for NASA's Jet Propulsion Laboratory. Further information is contained in a TSP (see page 1).

This software is available for commercial licensing. Please contact Karina Edmonds of the California Institute of Technology at (626) 395-2322. Refer to NPO-45816.



National Aeronautics and
Space Administration